Spring 2010

Roles for TRAIL in the immune response to influenza virus infection

Erik L. Brincks
University of Iowa

ROLES FOR TRAIL IN THE IMMUNE RESPONSE TO INFLUENZA VIRUS INFECTION

by

Erik L. Brincks

An Abstract

Of a thesis submitted in partial fulfillment
of the requirements for the Doctor of
Philosophy degree in Immunology
in the Graduate College of
The University of Iowa

May 2010

Thesis Supervisor: Associate Professor Thomas S. Griffith

ABSTRACT

The increasing threat of epidemic and pandemic influenza underscore the need to better-understand the immune response to influenza virus infections and to better understand the factors that contribute to the clearance of virus without complications of immunopathology. A hallmark of the adaptive immune response to primary influenza virus infections is the induction of influenza-specific $CD8^+$ T cell responses. These T cells target and kill influenza-infected epithelial cells in the airway, thereby clearing the virus and allowing recovery of the infected host.

Recent reports demonstrated that $CD8^+$ T cells express TNF-related apoptosis-inducing ligand (TRAIL) after influenza virus infection. While roles for perforin/granzyme and Fas:FasL interactions in clearing influenza virus infections had been established, little was known about the role of TRAIL in the $CD8^+$ T cell responses to influenza virus infection. We hypothesized that influenza-specific $CD8^+$ T cells would express TRAIL after influenza infection and could utilize TRAIL to induce the apoptosis of virally-infected cells. We discovered that $CD8^+$ T cells do express TRAIL after influenza infection, and that this expression occurs in an influenza-specific fashion. Further, we demonstrated that these influenza-specific $CD8^+$ T cells utilize this TRAIL to kill virally infected cells and protect the host from death, while T cells lacking TRAIL were unable to kill targets as efficiently and provided reduced protection. These data supported our hypothesis that $CD8^+$ T cells utilize TRAIL to kill infected cells.

Unexpectedly, when we increased the initial viral inoculum, the pulmonary cytotoxicity of T cells in $TRAIL^{-/-}$ mice was increased compared to those in TRAIL+/+ mice. Investigation of this phenomenon revealed that changes in cytotoxicity correlated not with changes in effector molecule expression on the T cells, but with increased recruitment of T cells to the lung. T cell recruitment to the lungs of $TRAIL^{-/-}$ mice was dependent on CCR5 and CXCR3, and likely the result of aberrant expression of MIG and

MIP-1α in the lungs. Together, these data suggest that TRAIL expression contributes not only to T cell cytotoxicity, but also to the regulation of chemokine expression and associated cell recruitment after influenza virus infections.

To confirm the relevance of our animal model to the study of human disease, we examined the potential role for TRAIL in the human immune response to infection. We determined that *in vitro* influenza infection stimulates upregulation of functional TRAIL on the surface of $CD3^+$, $CD14^+$, $CD19^+$, and $CD56^+$ PBMC populations. This expression was not caused by infection of the cells, but by interferon produced as a result of the infection. Infected (TRAIL-expressing) PBMCs killed influenza-infected lung epithelial cells, revealing that influenza infection sensitizes epithelial cells to TRAIL-induced apoptosis. Surprisingly, blocking TRAIL signaling, but not FasL signaling, was able to abrogate this killing of infected epithelial cells. Together, these data support a role for TRAIL in the human immune response to influenza virus infections.

Considered as a whole, the data from these studies suggest an additional, previously-unappreciated mechanism by which $CD8^+$ T cells can kill virally infected cells, TRAIL. They also suggest additional, previously-unappreciated roles for TRAIL in immune responses: in helping clear virally infected cells after infection and in helping control cytokine/chemokine expression, and thus the immune response, after infection.

Abstract Approved: _____
Thesis Supervisor

_____
Title and Department

_____
Date

ROLES FOR TRAIL IN THE IMMUNE RESPONSE TO INFLUENZA VIRUS INFECTION

by

Erik L. Brincks

A thesis submitted in partial fulfillment
of the requirements for the Doctor of
Philosophy degree in Immunology
in the Graduate College of
The University of Iowa

May 2010

Thesis Supervisor: Associate Professor Thomas S. Griffith

Graduate College
The University of Iowa
Iowa City, Iowa

CERTIFICATE OF APPROVAL

_____

PH.D. THESIS

_____

This is to certify that the Ph.D. thesis of

Erik L. Brincks

has been approved by the Examining Committee
for the thesis requirement for the Doctor of Philosophy
degree in Immunology at the May 2010 graduation.

Thesis Committee: _____
Thomas S. Griffith, Thesis Supervisor

_____
Kevin L. Legge

_____
John Colgan

_____
John T. Harty

_____
Aloysius J. Klingelhutz

To Natalie: not just for who you are,
but for who I am when I'm with you.

The entire history of science is a progression of exploded fallacies, not of achievements.

Ayn Rand
Atlas Shrugged

ACKNOWLEDGMENTS

Having entered my graduate education from the somewhat nontraditional background of science education, the process of considering who I wished to acknowledge in this section made me perhaps overly-reflective of my own past and education. With this in mind, I would like to first express appreciation for my teachers over the years, who reinforced my conviction that the free public schools are the foundation of our country's greatness. Thank you Mrs. St. John, who dissected a cow eyeball for our 4th grade class; Mr. Reetsma, who coordinated the science fairs in Algona Middle School for 25+ years; Mr. Zear, who guided us through making our own batteries in Seventh Science Studies; Mr. Payne, who taught us the finer points of Punnett squares and plate tectonics; Mr. Nettleton, who traipsed through the ditches alongside an Iowa highway to get a red-winged blackbird to dive at him during a Advanced Biology field trip; and Mr. Warner, who taught me chemistry, physics, calculus, and the joy of pushing past established limits and expectations not for a grade, but just for the fun of it. Thank you to John Aboud, who helped me realize that innate talent must be paired with hard work for true achievement to be realized. I'd like to also express my gratitude to Dr. Sandy Jones, who helped me to learn the importance of consistent quality in what one does. I'd like to thank Dr. Cherin Lee for her time, philosophical conversations on science and educational theory, and insights on life—academic and otherwise.

I would like to thank the members of my thesis committee: Dr. Kevin Legge, Dr. John Colgan, Dr. John Harty, and Dr. Aloysius Klingelhutz; who communicated to me the importance of precision and attention to detail in all aspects of science. I would like to thank the members of the Urology Research Journal Club and Lab Meetings, where I was first offered opportunities to present my research and practice giving talks. I also appreciate the individuals who participated in the Virology Journal Club and Dr. Harty's Joint Lab Meeting, where I was allowed to gain additional exposure to meaningful

research and quality critique of data. I would also like to thank the past and present members of the Griffith lab, who have aided my thesis work and my development as a scientist in one way or another. My sincerest thanks go to Dr. Thomas Griffith—who was willing to take a chance on a graduate student with no lab experience and little-to-no immunology background. His guidance was essential to my development as a scientist—from technical training to packaging data into a publishable story, from grant preparation and writing to experimental design, the guidance and training I received was sincerely appreciated. Lastly, I would like to thank my family, who provided me with a stable environment in which to grow and learn, and who taught me the joy of reading at an early age…without this foundation, any successes I've had in life would have been much more difficult to come by.

ABSTRACT

The increasing threat of epidemic and pandemic influenza underscore the need to better-understand the immune response to influenza virus infections and to better understand the factors that contribute to the clearance of virus without complications of immunopathology. A hallmark of the adaptive immune response to primary influenza virus infections is the induction of influenza-specific $CD8^+$ T cell responses. These T cells target and kill influenza-infected epithelial cells in the airway, thereby clearing the virus and allowing recovery of the infected host.

Recent reports demonstrated that $CD8^+$ T cells express TNF-related apoptosis-inducing ligand (TRAIL) after influenza virus infection. While roles for perforin/granzyme and Fas:FasL interactions in clearing influenza virus infections had been established, little was known about the role of TRAIL in the $CD8^+$ T cell responses to influenza virus infection. We hypothesized that influenza-specific $CD8^+$ T cells would express TRAIL after influenza infection and could utilize TRAIL to induce the apoptosis of virally-infected cells. We discovered that $CD8^+$ T cells do express TRAIL after influenza infection, and that this expression occurs in an influenza-specific fashion. Further, we demonstrated that these influenza-specific $CD8^+$ T cells utilize this TRAIL to kill virally infected cells and protect the host from death, while T cells lacking TRAIL were unable to kill targets as efficiently and provided reduced protection. These data supported our hypothesis that $CD8^+$ T cells utilize TRAIL to kill infected cells.

Unexpectedly, when we increased the initial viral inoculum, the pulmonary cytotoxicity of T cells in $TRAIL^{-/-}$ mice was increased compared to those in TRAIL+/+ mice. Investigation of this phenomenon revealed that changes in cytotoxicity correlated not with changes in effector molecule expression on the T cells, but with increased recruitment of T cells to the lung. T cell recruitment to the lungs of $TRAIL^{-/-}$ mice was dependent on CCR5 and CXCR3, and likely the result of aberrant expression of MIG and MIP-1α in the lungs.

Together, these data suggest that TRAIL expression contributes not only to T cell cytotoxicity, but also to the regulation of chemokine expression and associated cell recruitment after influenza virus infections.

To confirm the relevance of our animal model to the study of human disease, we examined the potential role for TRAIL in the human immune response to infection. We determined that *in vitro* influenza infection stimulates upregulation of functional TRAIL on the surface of $CD3^+$, $CD14^+$, $CD19^+$, and $CD56^+$ PBMC populations. This expression was not caused by infection of the cells, but by interferon produced as a result of the infection. Infected (TRAIL-expressing) PBMCs killed influenza-infected lung epithelial cells, revealing that influenza infection sensitizes epithelial cells to TRAIL-induced apoptosis. Surprisingly, blocking TRAIL signaling, but not FasL signaling, was able to abrogate this killing of infected epithelial cells. Together, these data support a role for TRAIL in the human immune response to influenza virus infections.

Considered as a whole, the data from these studies suggest an additional, previously-unappreciated mechanism by which $CD8^+$ T cells can kill virally infected cells, TRAIL. They also suggest additional, previously-unappreciated roles for TRAIL in immune responses: in helping clear virally infected cells after infection and in helping control cytokine/chemokine expression, and thus the immune response, after infection.

TABLE OF CONTENTS

LIST OF FIGURES

Figure

CHAPTER I

INTRODUCTION

Influenza virus (a Biodefense Category C priority pathogen) is a respiratory pathogen that infects 10-20% of the United States population annually, resulting in ~36,000 deaths and 114,000 hospitalizations (1-3). Seasonal influenza infections represents a substantial challenge to the health of children and the elderly (4, 5). During the 2007-2008 flu season, influenza and its associated pneumonias and complications resulted in the deaths of >80 children in the U.S (3). For children <3 years of age, which have the highest rate of infection (179 cases/1000), influenza represents a substantial health burden and as many as 43% of influenza-infected children will develop secondary complications, such as acute otitus media or pneumonia (6).

Importantly, influenza can also undergo substantial changes (through recombination/antigenic shift) leaving humans with little to no protective immunity and increasing influenza's mortality rate even among healthy young adults (7-9). The influenza pandemics of 1918 (20-40 million deaths world wide), 1957 (70,000 U.S. deaths), 1968-69 (34,000 U.S. deaths), and the recent appearance of H5N1 Avian "bird" influenza in Asia (~63% mortality rate Jan04-Feb08 (3)) further demonstrate that influenza is a considerable global public health and constant bioterrorism concern (7-10). Estimates predict that the release/appearance of an influenza strain with a virulence similar to that of the 1918 influenza would result in >100 million deaths worldwide. Along with influenza's impact on public health, yearly epidemics represent a potential economic loss of $4-12B due to medical costs and lost productively (1).

While presenting a substantially lower mortality rate than the Avian flu strains, the emergence of the novel H1N1 influenza virus has served as a model for the spread of a novel virus through the worldwide population. Since its emergence in spring 2009, the novel H1N1 virus lead to a spike in pediatric deaths during the summer months similar to

those normally observed during the winter flu season. Between August 30th, 2009, and October 31st, 2009, the CDC reported the deaths of 85 children—in just 2 months surpassing the annual total for 2006-2007. When sub-typed, 73 of the 85 patients tested positively as H1N1 infections (11), underscoring the health impact this new strain is having. Further, the British firm Oxford Economics has estimated the economic cost of the current pandemic could be as high as 5 percent of the gross domestic product (GDP) of Great Britain—a considerable cost with obvious repercussions for the economy of Britain an the rest of the world dealing with the novel H1N1 virus (12). Despite the characterization of this pandemic influenza strain as having "mild pathogenicity", its impact—both on the health of the population and on the economics of the world—underscores the importance of understanding influenza virus infections and how the immune system combats these infections, as better understanding will lead to better treatment and prevention strategies.

Influenza A virus

Influenza virus structure

Influenza A virus is a segmented, negative-sense RNA virus belonging to the orthomyxoviridae family. The structure of the individual virions varies to some degree, but the individual virions are typically spherical or ovoid in shape with a diameter of 80-120 nm (13); its structure is modeled in Figure 1. Influenza is an enveloped virus with the outer layer consisting of plasma membrane obtained from infected cells (14, 15). Within this envelope is the nucleocapsid protein of the influenza virus, and protruding from the envelope are two other glycoproteins of influenza origin—the rod-shaped hemagglutin (HA), and the more mushroom-shaped neuraminidase (NA) (16). Just

Figure 1. A schematic of the structure of influenza A virus and the virus genome. The mature influenza virus virion is composed of eight genomic segments, each of which encodes one or two proteins. Three segments encode proteins that form the virus polymerase complex: basic polymerase 2 (PB2), basic polymerase 1 (PB1), and the acidic protein (PA). Two segments encode surface envelope glycoproteins that function as viral antigens: haemagglutinin (HA; which is involved in binding to target cells as well as fusion of viral and endosomal membranes) and neuraminidase (NA; which is a protease responsible for virion release from the infected cell). A single segment encodes a nucleoprotein (NP). The seventh segment encodes two proteins that share a short overlapping region: the matrix protein M1 encodes the main component of the viral capsid, and M2, which is an integral membrane protein. The last segment encodes two proteins, NS1, which inhibits the interferon response, and NS2, which has roles in nucleocytoplasmic export of viral RNPs and in regulating influenza RNA levels.

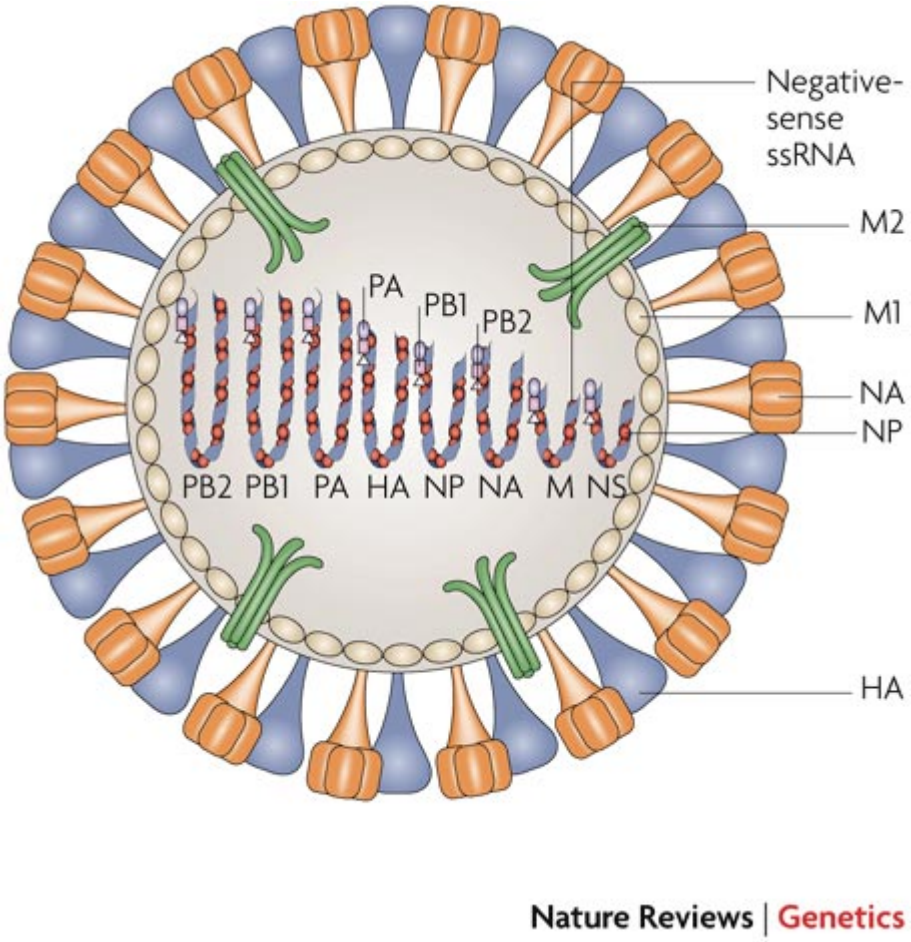

Source: Nelson, MI, and Holmes, EC. (2007) The evolution of epidemic influenza. *Nature Reviews Genetics* **8**, 196-205.

below the envelope is a layer composed of the viral membrane protein 1 (M_1). The other major component of the membrane is membrane protein 2 (M_2), which is an ion-channel with the role of acidifying the interior of the virus (17). Inside the M_1 layer reside the genome ribonucleoprotein segments. Each of the eight genome RNA segments is bound to nucleoprotein (NP) as well as PA, PB1, and PB2—all of which play roles in viral transcription (13). Upon infection of a host cell, the virus is also produces several non-structural proteins, which include NS_1, NS_2, and PB1-F2. NS_1 is has helps the virus evade immune responses by blocking interferon production (18). NS_2 serves to facilitate viral RNP export during the assembly of new virions (19) and helps to regulate the levels of viral RNA (20). Recently-discovered PB1-F2 is a mitochondrial protein that triggers cell death; current speculation is that PB1-F2 helps the virus survive by killing immune cells responding to infection (21).

Influenza virus infection

Upon inhalation of an aerosolized droplet containing influenza virions by an uninfected individual, the process of infection and viral replication takes place as modeled in Figure 2. Individual influenza virions bind to the surface of cells through interactions of influenza HA with sialic acid residues on the surface of epithelial cells in the airway (22). Upon binding, the virus is endocytosed, the endocytic compartment containing the virus is acidified, and the viral HA facilitates fusion of the viral and endosomal membranes (22). The acidification of the endosome activates the influenza M2 protein, which acidifies the viral interior and facilitates the release the viral ribonucleoprotein segments into the cytoplasm (17). After their unpacking and release into the cytoplasm, the genome segments traffic to the nucleus, where the RNA replication takes place. In the nucleus, replication of positive-sense mRNA and negative-sense genome RNA is produced (23). The influenza mRNA are synthesized using a unique “cap snatching” mechanism that utilizes the 5’cap of host pre-mRNAs and

Figure 2. Life cycle of the influenza virus. Individual influenza virions bind to the surface of cells when influenza haemagglutinin adheres to sialic acid residues on the surface of epithelial cells. Upon binding, the virus is endocytosed, the endocytic compartment containing the virus is acidified, and the virus fuses with the wall of the endocytic vesicle. This fusion releases the ribonucleoprotein segments into they cytoplasm, after which they traffic to the nucleus. In the nucleus, replication of positive-sense mRNA and negative-sense genome RNA is produced. The mRNA are exported to the cytoplasm where they use cell machinery to make influenza proteins. The influenza proteins then assemble at the cell surface, where the progeny virions bud from the cell surface. Detachment from the cell takes place when influenza neuraminidase cleaves the sialic acid residues connecting the virion to the cell surface.

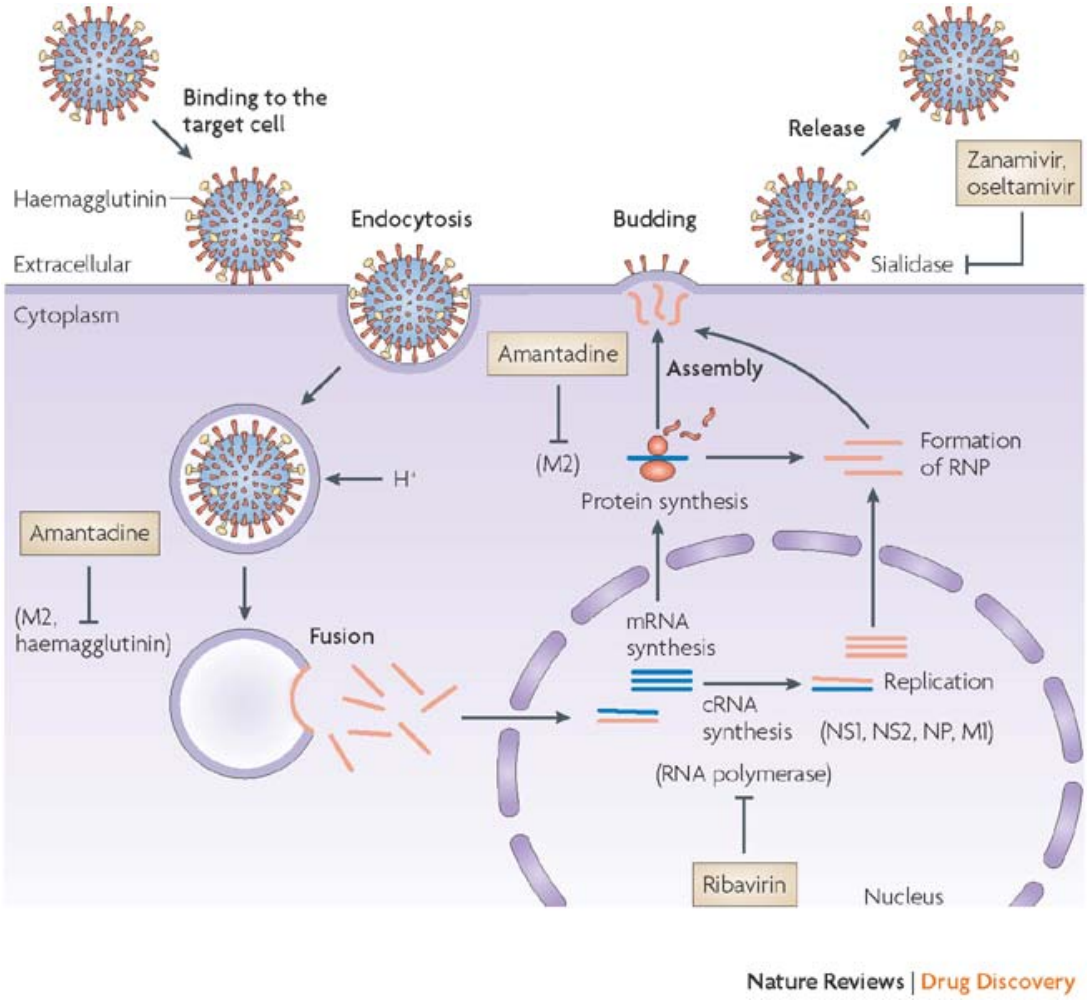

Source: von Itzstein, M. The war against influenza: discovery and development of sialidase inhibitors. *Nature Reviews Drug Discovery* **6**, 967-974.

subsequently cleaves the host nucleotides from the influenza segment (24). The viral mRNA are exported to the cytoplasm where they use cell machinery to make influenza proteins. Concomitantly, the negative-sense RNA genome segments are replicated for eventual packaging into new virions. After their production in the cytoplasm, influenza proteins then assemble at the cell surface where the progeny virions bud from the cell surface (25). Detachment from the cell takes place when influenza neuraminidase cleaves the sialic acid residues connecting the virion to the cell surface (26). This newly-released virion then travels through the airway until it encounters another cell expressing a sialic acid residue to which it can bind and start the process over again.

Immune response to influenza virus infections

Innate response

Within hours after initial infection with influenza virus, the infected host initiates a series of events to limit viral replication and eliminate the virus. The immune system has multiple pathways by which the virus itself or the products of viral replication are detected and initiate an immune response initiated. Double-stranded RNA (dsRNA) molecules are produced during viral replication; these dsRNA intermediates activate the serine/threonine kinase PKR, which leads to the production of IFN by the infected cell and results in the inhibition of viral replication (27, 28). Toll-like receptor 3 (TLR3) can also detect dsRNA in the cytoplasm of an infected cell, resulting in the production proinflammatory cytokines IL-8, IL-6, and IFN-β (29). Further, ssRNA in endosomes activates TLR7, which also stimulates the production of type-one interferons (28). Additionally, the RNA helicase retinoic acid-inducible gene-I (RIG-I) is activated by viral genomic RNA bearing a 5'-triphosphate end (30, 31) and results in proinflammatory cytokine production and the activation of interferon-regulatory factor 3 (IRF3) (29). Recently, ssRNA and dsRNA were shown to activate the NLRP3 inflammasome, and $NLRP3^{-/-}$ mice were more susceptible to influenza-associated morbidity and mortality

(32, 33). These reports demonstrated that NLRP3 senses viral RNA and activates the inflammasome after influenza virus infection, which enhances cytokine production that is key to the early responses to influenza infection (32, 33).

Type-one interferon production and signaling results in the transcription of many antiviral products that mediate antiviral effects, antiproliferative effects, and immunoregulatory responses (34). Foremost among these responses is the upregulation of 2'-5'-oligoadenylate synthetase (OAS), RNaseL, Mx proteins, and IRFs. OAS and RNaseL are proteins that recognize dsRNA, and, upon activation they mediate RNA degradation in the infected cell (35, 36). Mx proteins are GTPases that block influenza virus replication at a number of steps, including inhibition of genome replication and influenza protein synthesis (37, 38). Activation of IRF3 leads to its transloction to the nucleus induces an antiviral state through the transcription of interferons and other antiviral gene products (39-42).

Under steady-state, uninfected conditions, the airway contains two major phagocyte populations, dendritic cells (DC) and macrophages (Mϕ). In the airway, Mϕ have a regulatory role—helping to maintain an anti-inflammatory environment and suppressing immune responses (43, 44). Upon viral infection, interferon production and TLR/NLR stimulation results in the activation of the resident Mϕ population; these signals activate the Mϕ, which subsequently become highly-phagocytic, cytokine-producing cells (45). Additionally, airway influenza infection drives the recruitment of additional monocytes/macrophages to the airway via CCR2 (46). Influx of these cells correlates with pathology and morbidity (47, 48); but interestingly, removal of alveolar Mϕ prior to infection resulted in uncontrolled viral replication, supporting a role for Mϕ in controlling early infection (49). In a complementary study, depletion of the alveolar Mϕ resulted in increased respiratory distress, decreased antibody titers, and decreased virus-specific T cell responses (50).

During influenza virus infections, lung- and airway-resident DC take up antigen through environmental sampling (51, 52) or direct infection (53). Both the direct infection of DC and the IFN signals caused by the innate responses to virus infection result in activation of the DC populations. DC activation results in their production of proinflammatory chemokines and cytokines, including IL-6, IL-12, TNF, IP-10, RANTES, MIP-1β, and type I interferons (54). Additionally, DC activation stimulates their maturation and migration to the regional dLN, where they present antigen to naïve CD8 T cells via MHC class I (55, 56). The DC priming of CD8 T cells starts as early as 1-2 days after infection and continues out as late as day 9 post-infection (56, 57). During this time, DC interact with influenza-specific $CD8^+$ T cells, stimulating their activation and proliferation. The T cells then migrate to the lung and kill infected cells (53, 57, 58). Upon arrival in the lung environment, newly-primed T cells interact with pulmonary DC that have been recruited to the lung environment after the initial infection (59). The interactions between pulmonary DC (particularly the plasmacytoid DC and $CD8\alpha^+$ DC subsets) and the T cells provide survival signals to the virus-specific $CD8^+$ T cells that enhance their accumulation in the lung environment (59, 60).

Role for chemokines in T cell recruitment to the lung

Recruitment of these cells to the lung environment after their initial priming in the lung-draining LN is dependent on chemokine expression in the lung as well as chemokine receptor expression on the activated, IAV-specific T cells (61). Chemokines produced at the sites of inflammation are among the chemoattractants that control the migration of leukocytes. Roles for number of chemokines have been implicated in T cell homing to the airway, including the CXCR3 ligands CXCL9/MIG, CXCL10/IP-10, and CXCL11 /ITAC, and the CCR5 ligands, CCL3/MIP-1α, CCL4/MIP-1β, and CCL5 (RANTES)—all of which are commonly expressed in the lungs of mice infected with influenza virus (61-63). CXCR3 is expressed on the surface of effector Th1 and CD8 T

cells, NK cells, and NKT cells, whereas CCR5 is expressed on the surface of DC, Mϕ, activated T cells, and NK cells (64). The interactions of these chemokines with their respective receptors enhance integrin expression, and subsequently enhance the attachment/rolling of these cells that is essential in their migration into the lung environment (61, 62, 64).

Cellular adaptive immune response

$CD8^+$ T cell effector functions in the lung

Protective immunity to primary influenza virus infection involves the clearance of infected epithelial cells (65, 66) by $CD8^+$ T cells through either Fas- or perforin-dependent direct killing mechanisms (67). This T cell-mediated killing of infected cells is thought to occur through either Fas- or perforin-dependent direct killing mechanisms (67). Influenza-specific $CD8^+$ T cells first appear in the lungs around day 4-post infection (57, 68, 69) where their continued expansion and accumulation corresponds with the early stages of viral clearance (68, 69). The importance of $CD8^+$ T cells in protection from influenza infections is further highlighted by the fact that $CD8^+$ T cells mediate resistance and protection from lethal influenza virus infections in the absence of B cells, $CD4^+$ T cells, and neutralizing antibody (70, 71). The idea that $CD8^+$ T cells utilize perforin and Fas ligand to mediate killing of influenza-virus infected targets is most strongly supported by the work of Topham *et al* (67), who showed that pulmonary influenza-virus titers were maintained for longer durations when either perforin$^{-/-}$ or Fas$^{-/-}$ hosts were examined. Furthermore, when chimeric mice were made that possessed perforin$^{-/-}$ $CD8^+$ T cells and Fas$^{-/-}$ respiratory epithelium substantial pulmonary titers were maintained even out to 14 days post infection. However, despite the loss of both perforin and Fas, some of these mice showed lower virus titers on day 14 than on day 10 post infection (67). This outcome suggested the existence of an additional mechanism that $CD8^+$ T cells can use to kill influenza infected target cells.

$CD4^+$ T cell responses to influenza virus

In addition to the action of $CD8^+$ T cells, the primary response to influenza virus infection also includes contributions from $CD4^+$ T cells. Among the multitude of roles that the $CD4^+$ T cells play, providing "help" to the priming of $CD8^+$ T cell responses is perhaps the most well-established; the help provided by the $CD4^+$ T cells include cytokine production. In the absence of $CD4^+$ T cells, both IL-2 and IFN-γ production in the lung-draining lymph node and the BAL were decreased during immune responses to influenza virus (72). While the presence of $CD4^+$ T cells and the chemokines they produce are not necessary for clearance of primary infections, in the absence of $CD4^+$ T cell help, $CD8^+$ T cells have diminished cytolytic function (72), B cells have decreased antibody production (73, 74), and stable memory formation of both B cells (75-77) and $CD8^+$ T cells (77, 78) is perturbed. Beyond their "helper" functions, $CD4^+$ T cells also provide effector functions and contribute to the clearance of virus during primary and memory responses (79). These $CD4^+$ effector cells utilize perforin-mediated cytotoxic pathways to promote host survival (79).

Humoral Response

The humoral branch of the adaptive immune system produces antibodies that recognize antigens on the surface of virions and neutralize the viral particles—rendering them unable to infect cells. This antibody production and block of infection is the goal of current seasonal influenza vaccine strategies as well as the potential vaccines for pandemic strains (80). When an individual receives a vaccination or becomes infected with influenza virus, the influenza antigens are recognized by naïve B cells specific for influenza virus in the lymph node. This recognition of antigen activates the B cells and, with the additional signals from proinflammatory cytokines, induces class-switching, affinity maturation, and differentiation into antibody-producing plasma cells or memory B cells. These antibodies help to limit viral replication and can promote survival of an

Figure 3. The adaptive immune response to influenza virus. The adaptive immune response to influenza virus infection involves two branches that act in concert to protect the host from current (cellular adaptive response) and future infection (humoral and cellular response). The humoral response consists of B cells that interact directly with influenza-associated antigens and differentiate into antibody-producing plasma cells; this branch is outlined in the left column. The cellular response consists of CD4 and CD8 T cells that respond to influenza virus infections after interactions with dendritic cells, which are the cell population responsible for taking up antigen and presenting it to T cells. Upon activation, these T cells proliferate and mature into CD4 helper T cells that secrete cytokines and CD8 effector T cells with cytolytic capabilities.

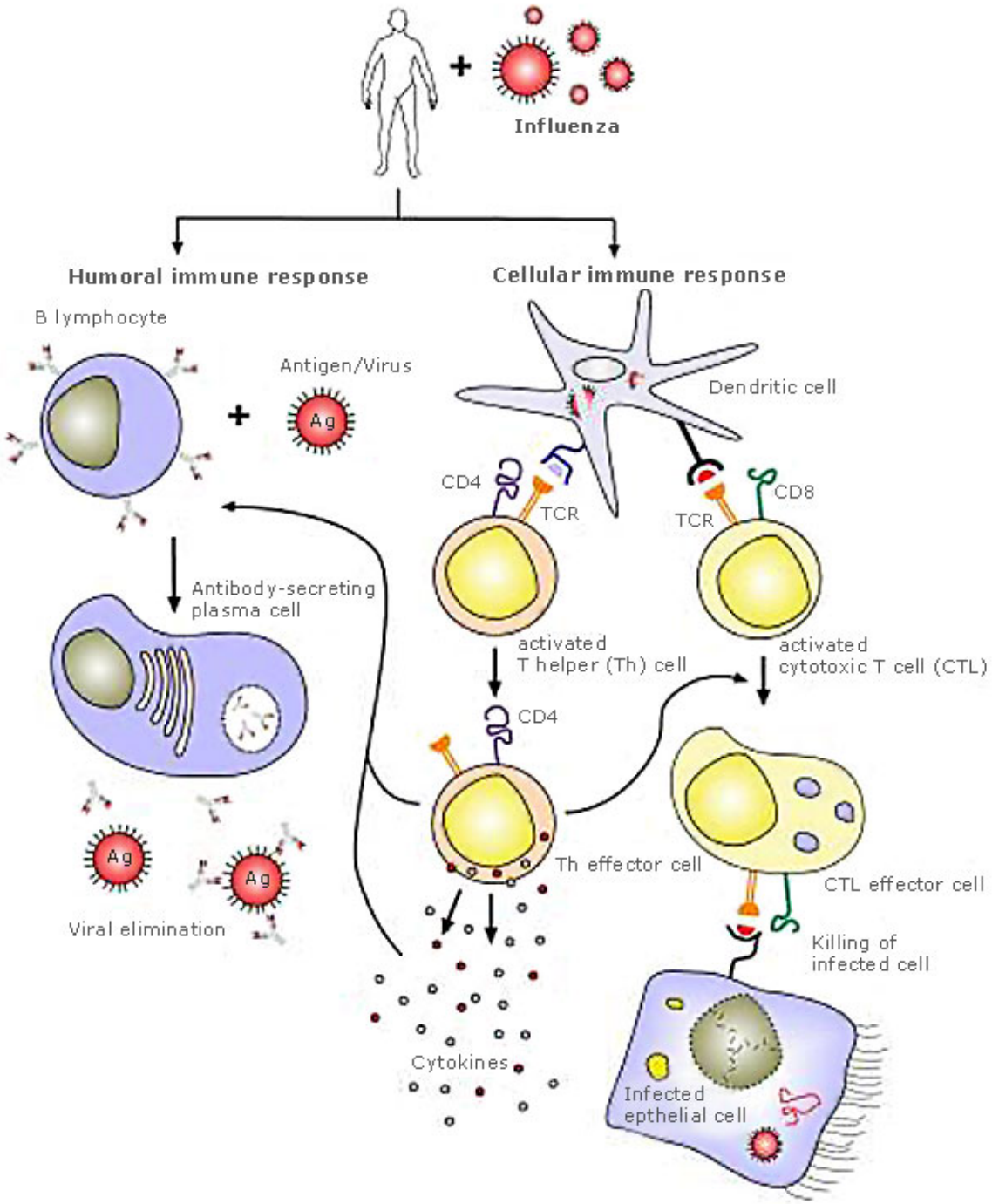

Immune response mechanisms
Courtesy: Influenza Report

Source: Behrens, G. and Stoll, M. (2009). Influenza Report: Pathogenesis and Immunology. http://www.influenzareport.com/ir/pathogen.htm

infected host upon secondary infection of a host, but they are not necessary for the clearance of virus from a host with an otherwise intact immune system (81, 82).

Influenza virus immunity and TRAIL

In addition to the Fas-FasL and perforin-Granzyme B pathways for killing, $CD8^+$ T cells have also been shown to utilize a TRAIL-DR5 dependent mechanism to eliminate infected cells during other types of virus infections. TRAIL induces apoptotic cell death (38, 83-85) by recruiting and aggregating caspase 8 upon binding to its receptor, DR5 (85-89). This aggregation in turn leads to a caspase cascade and eventually to apoptotic death of the $DR5^+$ cell (85-88, 90). Importantly, expression of TRAIL and DR5 are upregulated on $CD8^+$ T cells, NK cells, and infected cells following virus infection (91-93) or during increases of IFN-γ or TNF (93, 94). In turn, IFN-γ and TNF downregulate TRAIL receptor expression on uninfected cells (93). Overall, these results suggest that TRAIL/DR5 may play a role in the specific elimination of virus-infected cells.

Specifically regarding influenza virus infections, a recent report has suggested that TRAIL might play a role in the clearance of influenza virus from the lungs during influenza infection. In this study, Ishikawa and colleagues (91) show that TRAIL expression is increased on a fraction of $CD8^+$ and $CD4^+$ T cells, as well as NK cells, following influenza virus infections. Interestingly, the blockade of TRAIL with antibody delayed the clearance of influenza virus from the lungs. This suggests that TRAIL might be playing a substantial role as an effector molecule during the immune response to influenza virus infection.

Immunopathology during influenza virus infection

While several reports have underscored a role for alveolar Mϕ in controlling influenza virus infections, the chemokines and cytokines produced by activated Mϕ can have a deleterious effect on the infected host (95, 96). Part of the Mϕ response to influenza virus is the production of TNFα and nitric oxide species (NOS2), both of which

have been inculpated in influenza-associated immunopathology (50, 97, 98). While the production of NOS2 seems inherent in the Mϕ response to influenza (97, 99), the neutralization of these species revealed that they are unnecessary for clearing virus and actually contribute to immunopathology (97, 99, 100). Similarly, neutralization of TNFα ameliorated lung lesions and prolonged the survival an infected animals while having no effect on the viral titers in the lung, thus supporting a role for TNFα in immunopathology, but not viral clearance (98). Interestingly, a recent report has also implicated that Mϕ-expressed TRAIL contributes to immunopathology (101). This study demonstrated that inflammatory Mϕ recruited to the airway express TRAIL, and that TRAIL-induced apoptosis contributes to airway epithelial cell apoptosis, increased lung leakage, and decreased survival (101). Together, these studies demonstrate that while Mϕ contribute to early control of virus replication, their activation and associated effector functions contribute significantly to immunopathology.

Influenza infection can also trigger the death of infected alveolar macrophages by apoptosis and pulmonary epithelial by necrosis (102). These early death events contribute to localized inflammation and initiate signals, such as the release of chemokines (e.g. RANTES, MCP-1, MIP-1α/β) and cytokines (e.g. TNF, IL-1), which lead to an immune response (103, 104). Downstream from these initial signals, T cells are primed in the draining LN and eventually recruited to the lungs, where they are necessary for clearing virus (57, 67-69). In addition to contact-based effector functions, influenza-specific T cells responding to the infection also produce IFNγ and TNFα. While both of these cytokines contribute to tissue damage in pulmonary systems (96, 104-110), expression of IFNγ is associated with improved viral clearance and limiting tissue injury by T cells (111, 112). In contrast, TNFα expression by influenza-specific $CD8^+$ T cells is strongly associated with increased immunopathology (106, 108, 109), as measured by tissue damage, even after viral clearance. TNF is considered the primary cytokine responsible for immunopathology during influenza infection, doing so by direct tissue damage (lysis

of infected cells), as well as via the continued recruitment and activation of other effector cell populations (e.g. macrophages). Interestingly, the expression of these molecules, as well as other effector functions, on the T cells is regulated by both of costimulatory molecules present during priming (including CD28 and OX-40) (113, 114) and inhibitory signals received through NK cell receptors (109).

TNF-related Apoptosis-inducing Ligand (TRAIL)

TRAIL and its receptors

TRAIL is a TNF superfamily member that was first discovered when searching a cDNA library for sequences similar to TNF and FasL (83, 84). The extracellular domain of TRAIL is most homologous to Fas ligand (28% a.a. identity), but also has identity to TNF (23%), lymphotoxin (LT)-α (23%), and LT-β (22%) (115). Though the homology of TRAIL to other TNF family members may be considered low, the crystal structure of monomeric TRAIL is very similar to that of TNF-α and CD40 ligand (115). TRAIL monomers contain two antiparallel β-pleated sheets that form a β-sandwich core framework, and these monomers interact with other TRAIL monomers in a head-to-tail fashion to form a bell-shaped trimer (115). This oligomerization enhances TRAIL activity, as studies with recombinant soluble TRAIL found that the most biologically active form was multimeric rather than monomeric (84). Early studies of TRAIL indicated that it induced apoptosis of tumor or transformed cells, but not normal cells (84). In contrast, other TNF superfamily members were similarly cytotoxic to both tumor and normal cells.

Consistent with apoptosis induced by other TNF family members (i.e. FasL and TNF), cells undergoing TRAIL-induced death exhibit many of the hallmarks of apoptosis, including expression of pro-phagocytic signals (i.e. phosphatidylserine) on the cell membrane, cleavage of multiple intracellular proteins by caspases, and DNA fragmentation (83, 84, 116). Soluble TRAIL induces apoptosis in over 75% of the more

than sixty hematopoietic and non-hematopoietic tumor cell lines tested *in vitro*, suggesting that TRAIL could be used as a broad-spectrum, anti-tumor molecule *in vivo* (83, 84, 116, 117). Peripheral blood human T cells express TRAIL after CD3 crosslinking and type I IFN stimulation, perhaps contributing to T cell AICD (118). Human NK, Mϕ, and dendritic cells also express TRAIL following cytokine stimulation, transforming them into potent killers of tumor cells (116, 119, 120).

Apoptotic cell death can be triggered by a variety of agents acting on different cellular receptors, most notably by the death receptors of the TNF receptor superfamily. Unlike Fas-ligand and TNF, which interact with a single or pair of receptors, respectively, TRAIL specifically binds to four distinct human receptors: DR4 (88), DR5/TRAIL-R2 (86, 87, 117), TRID/DcR1/TRAIL-R3 (86, 87, 117), TRAIL-R4/DcR2 (86, 117) (hereafter referred to as TRAIL-R1, -R2, -R3, and -R4, respectively, Fig. 1). Both TRAIL-R1 and TRAIL-R2 contain a cytoplasmic death domain, and crosslinking by TRAIL or receptor-specific mAb activates the apoptosis signaling pathway in sensitive cells (86-88, 117, 121). In contrast, neither TRAIL-R3 (which is GPI linked) nor TRAIL-R4 (which is a type I membrane protein) contain a complete cytoplasmic death domain, and neither can mediate apoptosis upon ligation (86, 87, 117). Interestingly, only one murine death-inducing TRAIL receptor, Killer/DR5 (MK) (89), which is homologous to hTRAIL-R2/DR5 and contains a death domain motif and induces apoptosis when overexpressed or engaged by TRAIL, has been identified.

TRAIL/TRAIL-receptor signaling

Upon engagement of a non-decoy, apoptosis-inducing receptor (i.e. TRAIL-R1 or TRAIL-R2), the induction of apoptosis via TRAIL is similar to that induced by Fas; the red arrows in Figure 4 highlight this pathway. As noted above, induction of apoptosis occurs when a homotrimer of TRAIL molecules engage TRAIL-receptor. This ligation induces trimerization of the receptor and induces the formation of the Death-Inducing

Signaling Complex (DISC). First, the Fas-associated Death Domain (FADD) binds to the death domain (DD) on the cytoplasmic tail of the trimerized TRAIL receptors. Subsequently, pro-caspase 8 is recruited and activated—leading to the activation of the effector caspases 3, 6, and 7. Activation of these caspases involves the proteolytic cleavage of a constitutively-expressed proform of the caspase protein. The activation of these caspases is a cascade that leads to the proteolytic cleavage and activation of downstream caspases that lead to the apoptosis of the cell.

TRAIL/TRAIL-receptor signaling also leads to the induction of apoptosis by signaling through mitochondria-associated proteins; the purple arrows of figure 4 highlight this pathway. The activation of caspase 8 not only initiates the caspase cascade, but also activates the pro-apoptotic protein Bid. The activation of Bid leads to the subsequent activation of Bax and Bak, which in turn stimulate the release of cytochrome C from the mitochondria. Cytochrome C release initiates the formation of a complex of cytochrome C, APAF-1, and procaspase 9. The formation of this complex results in the cleavage and activation of caspase 9, which in turn facilitates caspase 3 activation and the induction of apoptosis.

Because TRAIL-R3 and -R4 bind to TRAIL without directly signaling for cell death, it was initially proposed that these receptors inhibit TRAIL-induced apoptosis by acting either as membrane-bound or soluble antagonistic receptors (86, 87, 117, 122) or via transduction of an anti-apoptotic signal (117). Therefore, the presence or absence of TRAIL-R3 and/or TRAIL-R4 was thought to determine whether a cell is resistant or sensitive, respectively, to TRAIL-induced apoptosis (86, 87, 122). Further investigation, however, disproved this theory as the sole mechanism regulating TRAIL-sensitivity and resistance (121, 123). The current thought in the field is that TRAIL-sensitivity or resistance is mediated by the balance of pro- and anti-apoptotic proteins inside the cell receiving signals through TRAIL-receptor (124). The relative levels of expression of Flice-like inhibitor protein (FLIP), Smac/DIABLO, Bcl-2 family members, and cIAP

Figure 4. TRAIL apoptotic signaling cascade. The intrinsic, apoptosis-inducing pathway initiated by ligation of TRAIL-R1 or TRAIL-R2 is depicted with red arrows. The mitochondrial-associated pathway is indicated with purple arrows. TRAIL-R3 is GPI anchored and does not induce apoptosis. TRAIL-R4 induces NF-κB activation and promotes anti-apoptotic signals.

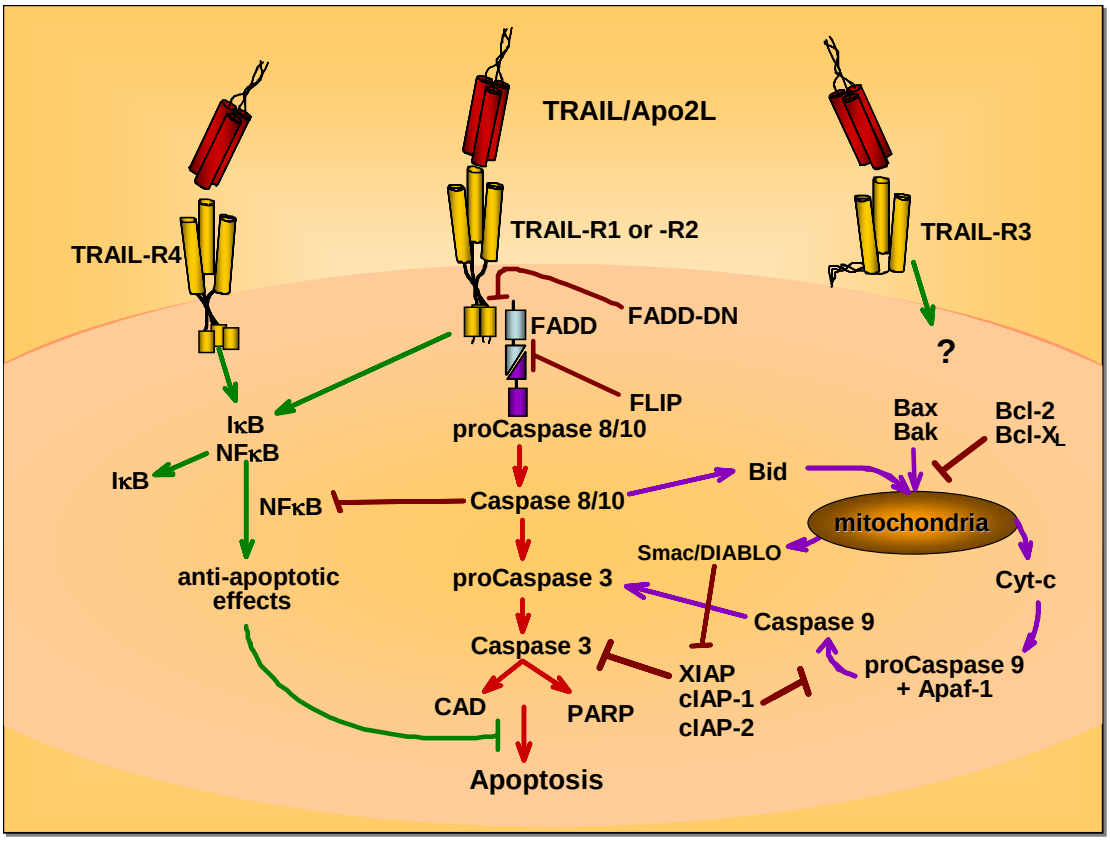

Source: Dr. Thomas S. Griffith, University of Iowa

family members can alter a cell's sensitivity to TRAIL-induced apoptosis by inhibiting FADD-initiated caspase activation or mitochondria-associated pathways (112, 124-128).

Non-apoptotic signaling though TRAIL/TRAIL-receptor interactions

Interactions of TRAIL with its death-inducing receptors inducing signaling pathways most similar to Fas/FasL interactions, yet evidence exists for the activation of non-apoptosis-inducing pathways upon ligation of TRAIL-R1, TRAIL-R2, or TRAIL-R4 (129). This alternative, non-apoptotic pathway utilizes TRADD, TRAF2, and RIP—proteins typically associated with TNF signaling—to activate NF-κB (130-132). NF-κB activation lead to the activation of multiple anti-apoptotic genes, including cellular inhibitor of apoptosis proteins 1 and 2 (cIAP 1 and cIAP2), FLIP, and Bcl-X_L (133-137). Beyond regulation of anti-apoptotic protein expression through NF-κB, TRAIL signals also regulate innate immune signals to toll-like receptors (TLR)-2, -3, and -4 (138). This regulation occurs through the NF-κB pathway and is associated with aberrant expression of IL-12, IFN-α, and IFNγ when TRAIL/DR5 signaling is absent in macrophages (138).

Regarding TRAIL deficiency

The numerous *in vitro* studies verified that TRAIL was a potent inducer of tumor cell apoptosis, but there was nothing known regarding the normal physiological activities of TRAIL *in vivo*. To address this question, Sedger *et al.* (139) generated TRAIL-gene targeted (-/-) mice. These mice develop normally and display no defects in lymphoid or myeloid cell homeostasis or function. The one abnormality observed in these mice, however, was that they were more susceptible to tumor burden. Interestingly, while the TRAIL deficiency resulted in a significant biological disadvantage for controlling the growth of TRAIL-sensitive tumors *in vivo,* the mice did not have an increased tendency to spontaneously develop tumors compared to normal mice. Soon thereafter, a series of studies were published clearly and elegantly demonstrating the importance of TRAIL-

expressing NK cells in the elimination of tumors *in vivo* in natural tumor immunosurveillance (94, 140-142). Subsequent reports have provided a glimpse into additional physiological roles for TRAIL. First, TRAIL appears to be important in controlling susceptibility to certain autoimmune diseases. Chronic blockade of TRAIL, by using TRAIL$^{-/-}$ mice or soluble TRAIL-R2:Fc in mice, exacerbated the development and severity of symptoms present in models of experimental autoimmune encephalomyelitis, collagen-induced arthritis, and diabetes compared to wild-type mice (143-146). Based on the observations in the collagen-induced arthritis model, it was also proposed that TRAIL was also important in proper thymocyte development (144). This conclusion has been met with some controversy, though, as conflicting results have been reported (94).

TRAIL and viral immunity

Complex cellular mechanisms operate during host defense against viral infections, during which the innate immune response cooperates with the adaptive immune response to eradicate the pathogen. Inducing apoptosis of virus-infected cells and viral resistance to apoptosis-inducing ligands are important factors that can determine the outcome of virus infection *in vivo*. In fact, many viruses have incorporated open reading frames encoding potent regulators of cell death (147, 148), and viruses with targeted disruptions or naturally occurring mutations in these genes often exhibit replication defects *in vitro* as well as reduced virulence *in vivo* (149-151). In the context of viral immunity, reovirus, measles virus, Newcastle disease virus, respiratory syncytial virus (RSV), human cytomegalovirus (hCMV), and encephalomyocarditis virus all induce TRAIL expression on immune effector cells. While the specific roles for TRAIL in clearing virus have not been elucidated, the induction of TRAIL is thought to occur primarily through the induction of type I and II IFN (92, 93, 152-156). The events that are required for TRAIL-resistant cells to become susceptible to TRAIL are complicated and not well understood.

Many viruses have a substantial impact on host cell metabolism; hence, it might be predicted that cells infected with viruses acquire sensitivity to TRAIL. Indeed, normal cells infected with respiratory syncytial virus, human cytomegalovirus, or encephalomyocarditis virus become susceptible to TRAIL-mediated killing (93, 152-154). While the specific mechanisms for TRAIL sensitization in the viral infections have not been determined, the evidence for increased sensitization to TRAIL suggest that TRAIL-mediated killing might be important in the immune response to these infections.

CHAPTER II. CD8 T CELLS UTILIZE TNF-RELATED APOPTOSIS-INDUCING LIGAND (TRAIL) TO CONTROL INFLUENZA VIRUS INFECTION

Abstract

Elimination of influenza virus infected cells during primary influenza virus infections is thought to be mediated by $CD8^+$ T cells though perforin- and FasL-mediated mechanisms. However, recent studies suggest that $CD8^+$ T cells can also utilize TNF-related apoptosis-inducing ligand (TRAIL) to kill virally-infected cells. Therefore, we herein examined the importance of TRAIL to influenza-specific $CD8^+$ T cell immunity and to the control of influenza virus infections. Our results show that TRAIL deficiency increases influenza-associated morbidity and influenza virus titers, and that these changes in disease severity are coupled to decreased influenza-specific $CD8^+$ T cell cytotoxicity in $TRAIL^{-/-}$ mice—a decrease that occurs despite equivalent numbers of pulmonary influenza-specific $CD8^+$ T cells. Further, TRAIL expression occurs selectively on influenza-specific $CD8^+$ T cells, and high TRAIL receptor (DR5) expression occurs selectively on influenza-virus-infected pulmonary epithelial cells. Finally, we show that adoptive transfer of $TRAIL^{+/+}$ but not $TRAIL^{-/-}$ $CD8^+$ effector T cells alters the mortality associated with lethal dose influenza virus infections. Collectively, the results suggest that TRAIL is an important component of immunity to influenza infections, and TRAIL deficiency decreases $CD8^+$ T cell-mediated cytotoxicity leading to more severe influenza infections.

Introduction

Primary infection with influenza virus results in a localized pulmonary infection and inflammation, and elicits an influenza-specific $CD8^+$ T cell immune response that is necessary for viral clearance (65-67, 70, 74, 157, 158). These $CD8^+$ T cells are thought to control virus infections by killing influenza-infected pulmonary cells using perforin- and Fas-dependent mechanisms (67). When $Fas^{-/-}$ or $perforin^{-/-}$ mice were infected with influenza virus in the absence of $CD4^+$ T cells, viral titers persisted for an additional 3 days beyond controls but virus was eventually cleared (67). This result suggests that in the absence of one death-inducing pathway influenza-specific $CD8^+$ T cells will compensate and utilize other cytotoxic mechanisms to eliminate influenza virus infected cells. In contrast, when $perforin^{-/-}$ bone marrow reconstituted $Fas^{-/-}$ mice were likewise infected with influenza virus, ~70% of the mice had sustained long term (i.e. 14 days p.i.) high viral titers (67) suggesting that influenza-specific $CD8^+$ T cell cytotoxicity requires access to either the perforin or Fas cytotoxic pathways to effectively control influenza virus infections. Interestingly however, ~30% of the above $perforin^{-/-}Fas^{-/-}$ mice were able to reduce pulmonary influenza virus titers leading to the idea that another cytotoxicity pathway could be involved in viral elimination (67).

$CD8^+$ T cells have recently be described to use the TNF-related apoptosis-inducing ligand (TRAIL) pathway, in addition to the Fas:FasL and perforin/granzyme (lytic granule) pathways, to kill target cells (159). TRAIL has classically been studied in tumor immunology settings, where it selectively induces apoptosis in transformed cells while leaving non-transformed cells unaffected (83, 84). Beyond a role in tumor surveillance, TRAIL-based immunity is also a component of the immune response during viral infections, including responses to CMV, HIV, and RSV (93, 152, 160). Moreover, a previous study has shown that the expression of mRNA for TRAIL and its receptor DR5 (TRAIL-R2) are increased in the lungs during influenza virus infections, that TRAIL is expressed by T cells in the lungs of influenza virus-infected mice, and that clearance of

influenza virus is delayed by administering a blocking anti-TRAIL mAb during primary infections (161). While these results suggest a role for TRAIL in immunity to influenza virus infections, it remains unknown if the expression of TRAIL by T cells during influenza infections is limited to just influenza-specific T cells, if influenza-specific $CD8^+$ T cells utilize TRAIL to kill influenza-infected cells and control virus infection, and how TRAIL deficiency alters the course and magnitude of influenza virus infections. Therefore, we utilized $TRAIL^{+/+}$ and $TRAIL^{-/-}$ mice to determine the contribution of TRAIL to the influenza-specific $CD8^+$ T cell immune response during primary influenza virus infections. Our results confirm a role for TRAIL in the primary immune response to influenza virus infection, and demonstrate that TRAIL-mediated apoptosis is a third mechanism which influenza-specific $CD8^+$ T cells can use to eliminate influenza-infected cells and drive recovery from influenza.

Materials and Methods

Mice, virus, peptides, and infections

C57Bl/6 ($TRAIL^{+/+}$; H-2^b) mice were purchased from the National Cancer Institute (Frederick, MD). C57Bl/6 TRAIL-deficient mice ($TRAIL^{-/-}$; H-2^b) were obtained from Amgen (Seattle, WA) (139) and C57BL/6 DR5-deficient mice ($DR5^{-/-}$, H-2b) were obtained from WS El-Deiry (162). DUC-18 TCR transgenic mice on the BALB/c background (TCR specific for tERK-I, QYIHSANVL; described previously (163)) were provided by Dr. Lyse Norian (University of Iowa, Iowa City, IA). Clone-4 TCR transgenic mice on the BALB/c background (TCR specific for HA_{518}, IYSTVASSL; described previously (164)) were obtained from Dr. Linda Sherman (The Scripps Research Institute, La Jolla, CA). Knockout mice were bred in our own facility at the University of Iowa, according to UI IACUC guidelines. They are >10 generations backcrossed to C57Bl/6. All mice were used at 12–20 weeks of age, and all animal experiments followed approved IACUC protocols. The mouse-adapted influenza A virus

A/PuertoRico/8/34 (PR8; H1N1) was grown in the allantoic fluid of 10 d old embryonated chicken eggs for 2 d at 37°C, as previously described (55, 69). Allantoic fluid was harvested and stored at -80°C. Groups of 24.5-27.5 g $TRAIL^{+/+}$ and $TRAIL^{-/-}$ mice were given a 500EIU dose of mouse-adapted PR8 virus in Iscove's media intranasally (i.n.) following anesthesia with halothane. The peptides used in this study, NP_{366} (ASNENMETM) and PA_{224} (SSLENFRAYV) were purchased from Biosynthesis Inc. (Lewisville, TX), and are derived from the amino acid sequence of A/PR/8/34 nucleoprotein (NP) or acid polymerase (PA), respectively (103, 165, 166).

Lung Virus Titer

Pulmonary viral titers were determined via endpoint dilution assay and expressed as Tissue Culture Infections $Dose_{50}$ ($TCID_{50}$). Briefly, 10-fold dilutions of homogenized and clarified lung from influenza virus infected mice were mixed with 10^5 MDCK cells in DMEM. After 24 h incubation at 37°C, the inoculum was removed and DMEM media containing 0.0002% L-1-(tosylamido-2-phenyl)ethyl chloromethyl ketone (TPCK)-treated trypsin (Worthington Diagnostics, Freehold, NJ) and penicillin (100U/ml) /streptomycin (100mg/ml) was added to each well. After 3 d incubation at 37°C in a humidified atmosphere of 5% CO_2, supernatants were mixed with an equal volume of 0.5% chicken RBC, the agglutination pattern read, and the $TCID_{50}$ values calculated.

Quantitative RT-PCR

Total RNA was harvested from homogenized lungs with TRIzol reagent (Invitrogen, Carlsbad, CA). Total RNA (2 mg) was reverse-transcribed using Superscript II. The quantitative PCR primer/probe sets for mouse TRAIL, DR5, Fas, FasL, perforin, granzyme B, and rRNA were purchased from PE Applied Biosystems (Foster City, CA). 250 ng of cDNA was used as a template for TaqMan assays for all transcripts and the internal control. The TaqMan PCR reaction was completed as described previously (167).

In vitro peptide stimulation of transgenic T cells

Splenocyte antigen-presenting cells (APC) were harvested from BALB/c mice and pulsed for 2 hours at 37ºC with 10 μM $HA_{518-526}$ peptide (IYSTVASSL; from Biosynthesis Inc. of Lewisville, TX), or left unpulsed. Naïve Clone-4 T cells or naïve DUC-18 T cells were isolated using CD8 MicroBead Kit (Miltenyi Biotech, Auburn, CA) per the manufacturer's suggested protocol. The T cells were then labeled with 2 μM CFSE (Invitrogen; Eugene, OR), mixed with the APC at a 1:1 ratio, and cultured for 24 hours. After incubation, cells were harvested, stained with anti-CD8a and anti-TRAIL monoclonal antibodies, and analyzed by flow cytometry.

Cytotoxicity Assays

Splenocytes from $DR5^{+/+}$ and $DR5^{-/-}$ C57Bl/6 mice (162) were resuspended in NycoPrep 1.077A (Axis-Shield; Norton, MA) and then purified according to the manufacturer's instructions. NycoPrep-purified splenic mononuclear cells (10^7/ml) were labeled with either 2 μM CFSE (Invitrogen; Eugene, OR) at 37°C for 10 min or 2 μM PKH-26 (Sigma; St. Louis, MO) at room temperature for 5 min. After labeling, residual non-cell-associated CFSE and PKH-26 were neutralized by adding an equal volume of fetal calf serum to the cell suspension. CFSE-labeled splenic mononuclear cells (10^7/ml) were pulsed with 10 μM PA_{224} and NP_{366} peptide for 1 h at 37°C. $PKH\text{-}26^+$ splenic mononuclear cells (10^7/ml) were similarly incubated without peptide for 1 h at 37°C. The cells were then washed and mixed at a 1:1 ratio, and 10^7 cells (i.e., 5×10^6 $CFSE^+$, 5×10^6 $PKH\text{-}26^+$ cells) were adoptively transferred i.v. into influenza-virus-infected $TRAIL^{+/+}$ or $TRAIL^{-/-}$ mice. After 8 h, the lungs were removed, digested, and analyzed by flow cytometry as previously described (69).

Flow-Cytometry Analysis

Surface Labeling

Isolated lung cells (10^6) were stained with: PE, PerCP-CY5.5, or APC-conjugated anti-mouse CD8α (53-6.7; BD Biosciences, San Jose, CA); biotinylated anti-mouse CD178/FasL (MFL3; eBioscience, San Diego, CA); or biotinylated anti-mouse TRAIL (N2B2; eBioscience). Cells stained with biotinylated mAb were subsequently incubated with Strepavidin-PerCP, Strepavidin-PE, or Strepavidin-APC (BD Bioscience). Stained cells were fixed and erythrocytes lysed with FACS lysing solution (BD Biosciences), and subsequently analyzed on a FACSCalibur flow cytometer. NP_{366} and PA_{224} tetramers were obtained from the National Institute of Allergy and Infectious Disease MHC Tetramer Core Facility (Germantown, MD).

Pulmonary Epithelial Staining

Isolated lung cells (10^6) were stained with the FITC-conjugated anti-mouse T1α/Podoplanin (8F11; MBL, Woburn, MA) or isotype control, and PE-conjugated anti-mouse DR5 (MD5-1; eBioscience) or isotype control. Subsequently, the cells were fixed, permeabilized, and stained with biotinylated anti-NP (H16-L10-4R5; a kind gift from Walter Gerhard, Wistar Institute, University of Pennsylvania). Biotinylated antibody was subsequently revealed with PerCP-CY5.5.

Intracellular Staining

Granzyme B. Isolated lung cells (10^6) were surfaced stained with PerCP-CY5.5-conjugated anti-mouse CD8α. Subsequently, the cells were fixed, permeabilized, and stained with the PE-conjugated anti-human Granzyme B mAb (GB11; Invitrogen), or isotype control (57). *IFN-γ.* Cells from mice infected with influenza were cultured at 2×10^6 cells/well in the presence of 1 μM of influenza peptides or media control, FITC-conjugated anti-CD107a (1D45; eBioscience) or isotype control, 400 U/ml recombinant

human IL-2, and 1 μg/ml brefeldin A. After 6 h, cells were harvested, stained with PE-conjugated rat anti-mouse CD8α, fixed, permeabilized, and stained with APC-conjugated rat anti-mouse IFN-γ (XMG1.2; eBioscience) or isotype control (168).

$CD8^+$ T cell Adoptive Transfer

Groups of 24.5–27.5g $TRAIL^{+/+}$ (CD45.2) and $TRAIL^{-/-}$ (CD45.2) mice were given a 500EIU dose of mouse-adapted A/PR/8/34 virus in Iscove's media intranasally (i.n.) following anesthesia with halothane. On day 8 p.i., single-cell suspensions of pulmonary cells from the infected $TRAIL^{+/+}$ or $TRAIL^{-/-}$ mice were incubated with anti-CD8α microbeads and $CD8^+$ cells purified according to the manufacturer's instructions (Miltenyi Biotec, Auburn, CA). The purified $CD8^+$ cells ($1x10^6$ T cells per mouse) were then transferred intravenously into CD45.1 $TRAIL^{+/+}$ mice (obtained from Dr. Robert Cook, University of Iowa) that had previously been infected with a lethal dose (2200EIU) of mouse-adapted A/PR/8/34. Cell transfer into lethally infected mice occurred on d 5 p.i. For T cell homing control experiments, $2x10^6$ T cells were transferred. Overall morbidity and mortality of mice was monitored to 21 days after lethal infection.

Statistical analysis

For each analysis, normal distribution of data was first verified. To assess the difference between two sets of data with normal distribution, statistical significance was assessed using an unpaired, one-tailed t-test or a paired t-test for control and experimental data groups that could be paired. If normality test failed, Mann-Whitney Rank Sum tests were completed to compare data sets. To assess the differences among multiple sets of data with normal distribution, statistical significance was assessed using an ANOVA analysis of the data sets. If normality test failed, Kruskal-Wallis One Way Analysis of Variance on Ranks test was used to determine overall significance with subsequent pair wise comparisons completed using Dunn’s Method. To determine differences in survival and viral clearance, Kaplan-Meier Survival Analysis: Log-Rank tests were run to

determine significant differences between data sets. When appropriate, subsequent pair wise multiple comparisons were completed using the Holm-Sidak method. Differences were considered statistically significant at $p \leq 0.05$.

Results

TRAIL-deficient mice display increased morbidity and influenza loads during influenza infection

To rigorously investigate the role that TRAIL plays in the regulation of influenza virus infections, we initially determined the impact of TRAIL deficiency on the severity of influenza virus infections. As shown in Figure 5A, TRAIL $^{-/-}$ mice demonstrated significant ($p < 0.05$) weight loss (i.e. morbidity) relative to wildtype C57Bl/6 (TRAIL$^{+/+}$) controls following infection with a low dose of influenza virus. This increase in disease severity correlated with increased pulmonary viral titers (Figure 5B). Specifically, while the amount of virus in the lungs of TRAIL$^{+/+}$ animals was reduced by ~1 log between days 4–6 p.i., TRAIL$^{-/-}$ mice showed little change in the amount of infectious virus present in their lungs. Furthermore, while TRAIL$^{-/-}$ animals were able to eventually reduce pulmonary virus levels by day 8 post infection (p.i.), the number of TRAIL$^{-/-}$ mice that had cleared virus below the limit of detection remained significantly reduced relative to TRAIL$^{+/+}$ animals ($p = 0.036$). Together, these results suggest that the increased morbidity observed in TRAIL$^{-/-}$ mice might, in part, be tied to an increased and sustained pulmonary viral burden.

Influenza-induced TRAIL and DR5 expression

Since our above results suggested that TRAIL played a role in the control and resolution of influenza virus infections, we next examined TRAIL and DR5 mRNA expression in influenza-infected lungs. The amount of TRAIL mRNA was increased in total lung homogenates from TRAIL$^{+/+}$ mice following i.n. influenza virus infection (as

expected, no TRAIL mRNA was detected in the TRAIL$^{-/-}$ mice; Figure 6). Moreover, DR5 mRNA expression was similarly upregulated in the lungs of both TRAIL$^{+/+}$ and TRAIL$^{-/-}$ mice following i.n. influenza virus infection, indicating that the lack of TRAIL expression did not significantly affect DR5 mRNA expression in the TRAIL$^{-/-}$ mice. Given that the upregulation of TRAIL and DR5 mRNA (starting at 6–8 days p.i.) in TRAIL$^{+/+}$ mice corresponds with the timing of increased disease in TRAIL$^{-/-}$ mice (Figure 5A), these results further support the concept that TRAIL plays a major role in mediating the control and course of influenza virus infection. These results also largely confirm similar data recently described by Ishikawa and colleagues (161); however, unlike their results we do not observe increases in pulmonary TRAIL mRNA expression until 8 days p.i. (as opposed to 4 days p.i.). Furthermore, we observed a more rapid decrease in TRAIL and DR5 mRNA expression from their peak at 8–14 days p.i. These differences may be related to the difference in virus inoculum administered (500 EIU herein vs. 25 PFU), as well as the corresponding alterations in the inflammatory cytokines produced.

To verify that the above changes in DR5 mRNA expression were reflected in alterations of DR5 protein expression, we next determined DR5 expression on pulmonary epithelial cells prior to and during an influenza virus infection. While there was a low amount of DR5 expressed on the surface of alveolar epithelial type I cells (i.e. T1α^{+} cells) (169) from uninfected mice (Figure 7A), overall DR5 expression was significantly increased following influenza virus infection ($p = 0.004$). Moreover, the upregulation of DR5 by epithelial cells correlated with those cells that had been directly infected with influenza virus (i.e. NP^{+} cells), as NP^{+} epithelial cells expressed ~5x more DR5 relative to NP^{-} epithelial cells from the same lungs (Figure 7 A, B). These data suggest that influenza infection of pulmonary epithelial cells results in selective upregulation of DR5 on influenza-infected lung epithelial cells, potentially increasing their susceptibility to TRAIL-mediated lysis.

The greatest difference in morbidity between $TRAIL^{+/+}$ and $TRAIL^{-/-}$ mice was seen after 6 days p.i., paralleling the increase in TRAIL and DR5 expression. These kinetics are similar to the described kinetics of influenza-specific $CD8^+$ T cell recruitment into the lungs (57, 69). Since $CD8^+$ T cells mediate the clearance of influenza-infected cells (65-67, 70, 74), our results suggested that the increased disease severity and viral burden in $TRAIL^{-/-}$ mice might be linked to altered pulmonary influenza-specific $CD8^+$ T cells responses. Therefore, we next examined TRAIL expression on influenza-specific $CD8^+$ T cells in the lungs during influenza infections, and found that TRAIL was indeed expressed by influenza-specific $CD8^+$ T cells in the lungs of $TRAIL^{+/+}$ mice (Figure 7C). In contrast, the vast majority of non-influenza-specific $CD8^+$ T cells within the lungs at the same time did not appear to express TRAIL. The small residual $TRAIL^+$ shoulder in the NP_{366} or PA_{224} negative T cell populations is likely attributable to the remaining unstained immunodominant PA_{224} or NP_{366} specific cells, respectively, with potential minor contributions from the other 6 subdominant epitopes (165, 170). Similar to the correlation with influenza $CD8^+$ T cell epitope specificity observed in the lungs, TRAIL was also selectively expressed on influenza-specific $CD8^+$ T cells within the lung draining lymph nodes on day 6 p.i. (Figure 8). Consistent with a previous report demonstrating TCR stimulus driven upregulation of TRAIL on naïve and effector CD8 T cells (171), we also observed antigen-specific upregulation of TRAIL by naïve influenza-specific CD8 T cells after 24 hours of *in vitro* culture (Figure 9). Together the antigen-specific nature and location of TRAIL expression suggest that TRAIL expression by $CD8^+$ T cells likely relates to their initial programming within the draining lymph nodes (171-174) and could be amplified by interactions with viral-peptide MHC I complexes in the lungs (171).

Influenza-specific $CD8^+$ T cell response in $TRAIL^{-/-}$ mice

The observed difference in morbidity between $TRAIL^{+/+}$ and $TRAIL^{-/-}$ mice, combined with the selective expression of TRAIL on influenza-specific $CD8^+$ T cells, suggests vigorous resolution of the infection requires the participation of TRAIL-expressing $CD8^+$ T cells. The likely explanation for the increased morbidity in the $TRAIL^{-/-}$ mice is that the influenza-specific $CD8^+$ T cells are unable to kill influenza-infected cells, but it may also be possible that other factors contribute to the pathology, such as a reduction in the number of lung-infiltrating antigen-specific effector $CD8^+$ T cells. Thus, we examined the magnitude and phenotype of the pulmonary $CD8^+$ T cell response in influenza-infected $TRAIL^{+/+}$ and $TRAIL^{-/-}$ mice. Interestingly, TRAIL deficiency did not alter the magnitude of the NP_{366} or PA_{224} influenza-specific $CD8^+$ T cell response in the lungs (Figure 10A & B). The level of IFN-γ produced per cell was also similar between both influenza antigen-specific $TRAIL^{+/+}$ and $TRAIL^{-/-}$ $CD8^+$ T cells ($TRAIL^{+/+}$ NP_{366} MFI= 235; $TRAIL^{-/-}$ NP_{366} MFI= 303; $TRAIL^{+/+}$ PA_{224} MFI= 242 $TRAIL^{-/-}$ PA_{224} MFI=423; not significant as determined by Kruskal-Wallis One Way Analysis of Variance on Ranks). However, TRAIL deficiency did result in a significant reduction in influenza-specific $CD8^+$ T cell-mediated cytotoxicity *in vivo* (Figure 10C; $p = 0.029$). Indeed, while $TRAIL^{-/-}$ mice have an equal *in vivo* E:T ratio to that of $TRAIL^{+/+}$ mice, the influenza-specific $CD8^+$ T cells killed wildtype $DR5^{+/+}$ influenza peptide-pulsed targets with substantially reduced (~40%) efficiency. Further, when influenza peptide-pulsed $DR5^{-/-}$ targets were adoptively transferred into either influenza infected $TRAIL^{-/-}$ or $TRAIL^{+/+}$ hosts, killing was reduced ~60% relative to $DR5^{+/+}$ targets in $TRAIL^{+/+}$ animals.

The reduced cytotoxicity of $TRAIL^{-/-}$ $CD8^+$ T cells or during transfer of $DR5^{-/-}$ targets was intriguing given the increased viral load and disease severity observed in $TRAIL^{-/-}$ mice (Figure 5). Together our results suggest that between 40–60% of influenza-specific CD8 T cell mediated cytotoxicity within the lungs on day 8 p.i. may be

TRAIL:DR5 dependent. Yet disruption of a single cytotoxicity pathway was not expected to have major pathological consequences, based upon the redundant roles of the Fas/FasL and perforin/Granzyme pathways in mediating control of influenza virus infections (67). In those studies, mice deficient in either Fas or perforin showed only marginal changes in pulmonary viral load. It took a deficiency in both perforin^{+} T cells and Fas^{+} targets cells to sustain viral titers until day 14 post infection - a time point when virus has normally been eliminated from the lungs. Therefore, we next measured the expression of Fas, FasL, perforin, and Granzyme B mRNA in the lungs, as well as FasL and Granzyme B protein expression and degranulation potential in TRAIL$^{+/+}$ and TRAIL$^{-/-}$ influenza-specific CD8^{+} T cells found within the lungs. Fas, FasL, Granzyme B, and perforin mRNA were all upregulated to similar levels in both TRAIL$^{+/+}$ and TRAIL$^{-/-}$ mice peaking at day 8 p.i. (Figure 6). Further, neither NP_{366} nor PA_{224} specific TRAIL$^{-/-}$ CD8^{+} T cells had altered expression of FasL or Granzyme B or changes in the ability to degranulate (i.e. surface CD107a expression) relative to TRAIL$^{+/+}$ controls (Figure 11). Therefore, these results collectively suggest TRAIL:DR5 interactions may play more prominent roles in CD8^{+} T cell-mediated clearance of influenza virus infected cells than has previously been appreciated.

TRAIL$^{+/+}$ CD8 T cells protect from ongoing lethal influenza virus infections

Since our results suggested that influenza-specific CD8^{+} T cells utilize TRAIL to eliminate virally-infected pulmonary epithelial cells and therein control virus infections, we tested the ability of TRAIL$^{+/+}$ and TRAIL$^{-/-}$ influenza-specific effector CD8^{+} T cells to control and resolve an ongoing lethal-dose influenza virus infection in TRAIL$^{+/+}$ mice. During such infections, endogenous pulmonary influenza-specific CD8^{+} T cells and virus control are limited due to a previously described elimination of effector CD8^{+} T cells during their development in the lymph nodes (69). However, this lethality can be

overcome when normal T cell numbers are restored to the lungs (69). When we intravenously adoptively transferred TRAIL$^{+/+}$ pulmonary effector CD8^{+} T cells 5 days p.i into lethal dose influenza infected mice, 83.3% of the mice survived and recovered from the high dose influenza infection (Figure 12). In contrast, while the donor TRAIL$^{-/-}$ effector T cells migrated into the lungs at equivalent numbers to TRAIL$^{+/+}$ effector T cells (Figure 13), the TRAIL$^{-/-}$ effector T cells were only able to protect 33.3% of the lethally-infected mice, a percentage that was not statistically different from the non-T cell transferred controls. Since no differences in IFNγ, FasL, Granzyme B, or degranulation were observed in the NP_{366} and PA_{224} effector CD8 T cell populations (Figure 11) and these T cells arrived in the lungs in equivalent numbers upon adoptive transfer, our results suggest that the TRAIL expression or deficiency alone is responsible for the differential ability to protect these mice from lethal-dose influenza virus infections.

Discussion

TRAIL-expressing CD8^{+} T cells, NK cells, and plasmacytoid DC have all been implicated in cytotoxicity and control of viral infections (91, 113, 175). The results presented herein suggest that the differences observed during influenza virus infection of TRAIL$^{+/+}$ and TRAIL$^{-/-}$ mice are predominately due to altered CD8^{+} T cells responses. First, while some minor increases in morbidity were observed within the first 3 days following influenza virus infection (i.e. the window of time normally ascribed to innate [NK/pDC] control of infection), significant increases were not seen until after influenza-specific CD8^{+} T cells have arrived in the lungs (i.e. ~day 4+ p.i.) (57, 68, 69). Further, the kinetics of TRAIL and DR5 expression within the lungs correspond with the appearance of influenza-specific CD8^{+} T cells in the lungs, TRAIL expression by pulmonary CD8^{+} T cells appears to be directly linked to influenza-virus specificity, and adoptive transfer of TRAIL$^{+/+}$, but not TRAIL$^{-/-}$ T cells, can mediate protection from ongoing lethal dose influenza virus infections. Finally, our *in vivo* cytotoxicity

experiments directly show that TRAIL deficiency on T cells or DR5 deficiency on target cells results in significantly ($p < 0.029$) reduced $CD8^+$ T cell cytotoxicity of influenza peptide pulsed target cells despite the presence of equal numbers of pulmonary influenza-specific $CD8^+$ T cells and identical levels of IFNγ, FasL, Granzyme B, and degranulation by influenza-specific $TRAIL^{+/+}$ and $TRAIL^{-/-}$ CD8 effectors.

Of note, our results show that TRAIL expression appears to selectively correlate only with those pulmonary $CD8^+$ T cells that are specific for influenza. Further, upregulation of DR5, the receptor for TRAIL, to high levels on pulmonary epithelial cells is linked to direct infection of the cells with influenza virus. Together these results suggest that elimination of virus-infected cells by influenza-specific $CD8^+$ T cells could be specific not only at the level of recognition of virus peptide/MHC I complexes but also by the high level of DR5 expression. In this manner high expression of DR5 may permit T cell-mediated elimination of virally infected cells and allow survival of any surrounding non-infected epithelial cells or even pulmonary APC that carry viral peptide MHC complexes but have not upregulated DR5 due to direct infection - an idea that would be consistent with previously described selective TRAIL cytotoxicity within tumor systems (176). It is important to keep in mind that the amount of DR5 expressed on a cell's surface is not the only point that determines TRAIL susceptibility. The events that are required for TRAIL-resistant cells to become susceptible to TRAIL are complicated and not well understood. Many viruses substantially alter host cell metabolism, such that it might be predicted that cells infected with viruses acquire sensitivity to death-inducing ligands (including TRAIL). Normal cells infected with RSV, human cytomegalovirus, or encephalomyocarditis virus become susceptible to TRAIL-mediated killing (93, 152-154), and we have also found the TRAIL-resistant human lung adenocarcinoma cell line, A549, can be sensitized to TRAIL following influenza virus infection (figure 31). While it is beyond the scope of this report, we are actively investigating the mechanism(s) that regulate TRAIL susceptibility in influenza virus-infected cells.

In the current study, TRAIL expression by $CD8^+$ T cells correlates with reduced viral loads and disease severity; however, increased TRAIL expression may also lead to increased disease during some influenza virus infections (177). H5N1 influenza virus-infected human monocyte-derived macrophages express TRAIL at levels that are able to kill T cells - an outcome that could be inhibited by introduction of anti-TRAIL-R2 blocking antibodies (177). In this manner the TRAIL-expressing macrophages are thought to help drive the T cell lymphopenia observed with H5N1 influenza infections (177, 178). Influenza infection commonly induces the production of type I and II IFN as part of the innate immune response (179-181). Both types of IFN are potent inducers of TRAIL expression on many cells in the immune system (182, 183), and monocytes/Mϕ are exquisitely sensitive to IFN-induced TRAIL expression (184). Thus, while direct H5N1 influenza infection can induce TRAIL expression, the breadth and amount of TRAIL expressed by cells of the immune system may be further enhanced by IFN-mediated events. Therefore, our data and the results from the above studies would collectively suggest that TRAIL expression during influenza infections normally has a beneficial effect on viral control (i.e. $CD8^+$ T cell-mediated elimination of infected pulmonary epithelial cells, etc), but that TRAIL may also serve to enhance the virulence of some influenza virus infections. The factors that regulate the beneficial versus deleterious effects, and possibly distinct cellular expression patterns of TRAIL during influenza infections, await further study.

Our observation that $TRAIL^{-/-}$ mice do not significantly reduce viral titers as substantially from day 4 to 6 p.i. when compared to $TRAIL^{+/+}$ mice (Figure 5B) suggests that TRAIL-mediated cytotoxicity by $CD8^+$ T cells may be more important than the Fas and perforin pathways of cytotoxicity during the early stages of influenza infections. This increased dependence upon TRAIL at these early times might relate to the low numbers of influenza-specific $CD8^+$ T cells present (57, 68, 69), and hence low functional *in vivo* effector: target ratios in the lungs – an idea which would be consistent with TRAIL-

dependent killing of some target cell lines *in vitro* (185). However, at later the stages of infection (i.e. days 6-8 p.i.) when the number of effector $CD8^+$ T cells has expanded (57, 68, 69), the loss of TRAIL may be compensated for by the other cytotoxicity pathways resulting in redundant and overlapping mechanisms of viral control and the 1 log reduction in pulmonary virus levels. Regardless, our results show that a third pathway (i.e. TRAIL: DR5) of cytotoxicity is used along with the previously described Fas- and perforin-dependent killing pathways to eliminate and control influenza virus infection.

In conclusion, the results presented herein show that TRAIL plays a role in the regulation and control of influenza virus infections. Specifically, the early adaptive influenza-specific $CD8^+$ T cell response appears to utilize TRAIL-mediated lysis of $DR5^+$ (i.e. TRAIL receptor) influenza-infected cells in addition to FasL:Fas and perforin/granzyme dependent cytotoxicity pathways to control influenza virus infection. Further our results show that TRAIL and DR5 upregulation by $CD8^+$ T cells and pulmonary epithelial cells is closely linked to either the antigen specificity of the T cells or the infection status of the epithelial cells, respectively. This suggests that TRAIL:DR5 specific interactions may partner with TCR:viral peptide-MHCI interactions to allow the targeted elimination of only influenza virus infected cells.

Figure 5. TRAIL deficiency correlates with increased disease severity after influenza virus infection. *A*, C57BL/6 $TRAIL^{+/+}$ (○) or $TRAIL^{-/-}$ (▲) mice (n = 4 mice/group) were infected with influenza and weighed daily to assess morbidity. The values displayed represent the daily weight relative to the weight on day of infection (i.e. starting weight). *, $p < 0.05$, Mann-Whitney Rank Sum Test. No significant differences in mortality existed between the two groups. Data are representative of 2 separate experiments. *B*, Pulmonary virus titers were assessed by determining $TCID_{50}$ in MDCK cell cultures (as described in the Materials and Methods). *, $p = 0.002$, Mann-Whitney Rank Sum Test. Viral clearance was significantly different between the $TRAIL^{+/+}$ and $TRAIL^{-/-}$ with a p = 0.036 as analyzed by a Kaplan-Meier Survival Analysis: Log-Rank.

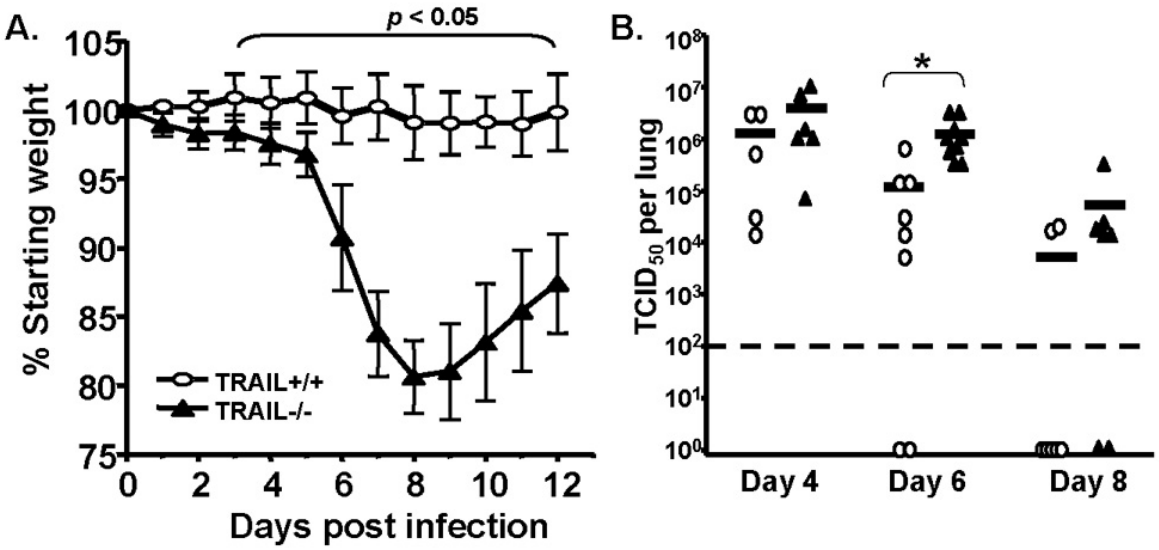
A.
p < 0.05
% Starting weight
105
100
95
90
85
80
75
0
2
4
6
8
10
12
Days post infection
TRAIL+/+
TRAIL-/-
B.
TCID50 per lung
Day 4
Day 6
Day 8
*

Figure 6. Expression of effector molecule and receptor mRNA is equivalent in the lungs of TRAIL$^{+/+}$ and TRAIL$^{-/-}$ mice during influenza virus infection. TRAIL, DR5, FasL, Fas, perforin, and Granzyme B mRNA expression in the lungs of TRAIL$^{+/+}$ (■) and TRAIL$^{-/-}$ (●) mice were determined by quantitative RT-PCR on d 4, 6, 8, 14, 18, and 21 after infection. 18s rRNA was used to normalize the gene expression. Data are representative of 2 independent experiments.

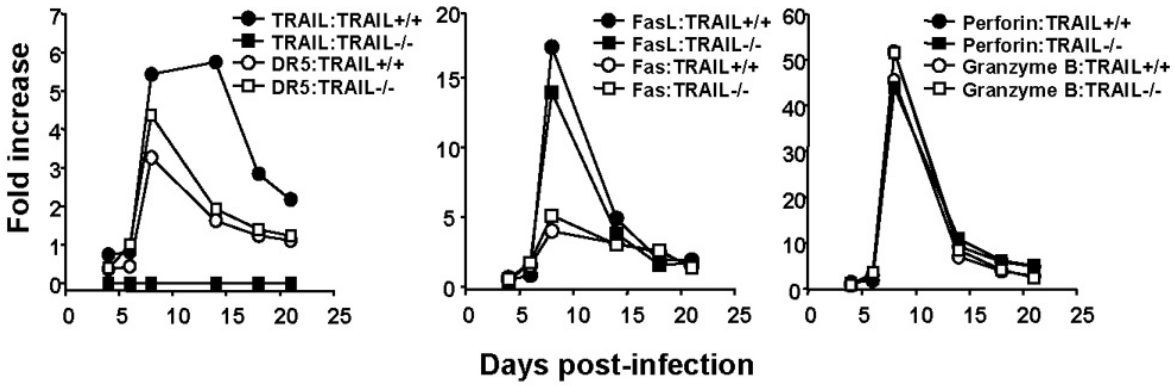
Fold increase
TRAIL:TRAIL+/+
TRAIL:TRAIL-/-
DR5:TRAIL+/+
DR5:TRAIL-/-
FasL:TRAIL+/+
FasL:TRAIL-/-
Fas:TRAIL+/+
Fas:TRAIL-/-
Perforin:TRAIL+/+
Perforin:TRAIL-/-
Granzyme B:TRAIL+/+
Granzyme B:TRAIL-/-
Days post-infection

Figure 7. Pulmonary expression of TRAIL-receptor (DR5) and TRAIL occurs in an influenza-specific fashion. At d 4 p.i., lungs were harvested from $TRAIL^{+/+}$ mice and prepared into a single cell suspension. *A*, Isolated cells were stained with anti-T1α, anti-DR5, and anti-NP or respective isotype controls. The top histogram represents the basal DR5 expression in uninfected T1α-positive pulmonary cells (dashed line) relative to the DR5-isotype control (shaded histogram). The bottom histogram shows DR5 expression on $T1\alpha^{+}/NP^{+}$ (solid line) and $T1\alpha^{+}/NP^{-}$ (dashed line) pulmonary cells relative to the isotype control (shaded histogram). *B*, DR5 mean fluorescence intensity (MFI) on NP^{+} and NP^{-} $T1\alpha^{+}$ cells from the lungs of infected mice (n = 5). Data are representative of 3 individual experiments. *C*, On day 8 p.i. cells isolated from $TRAIL^{+/+}$ mice were stained with anti-CD8α, anti-CD3ε, NP_{366} and PA_{224} tetramers, and anti-TRAIL (open histograms) or isotype controls (shaded histograms). Data are representative of 5 mice from 2 experiments.

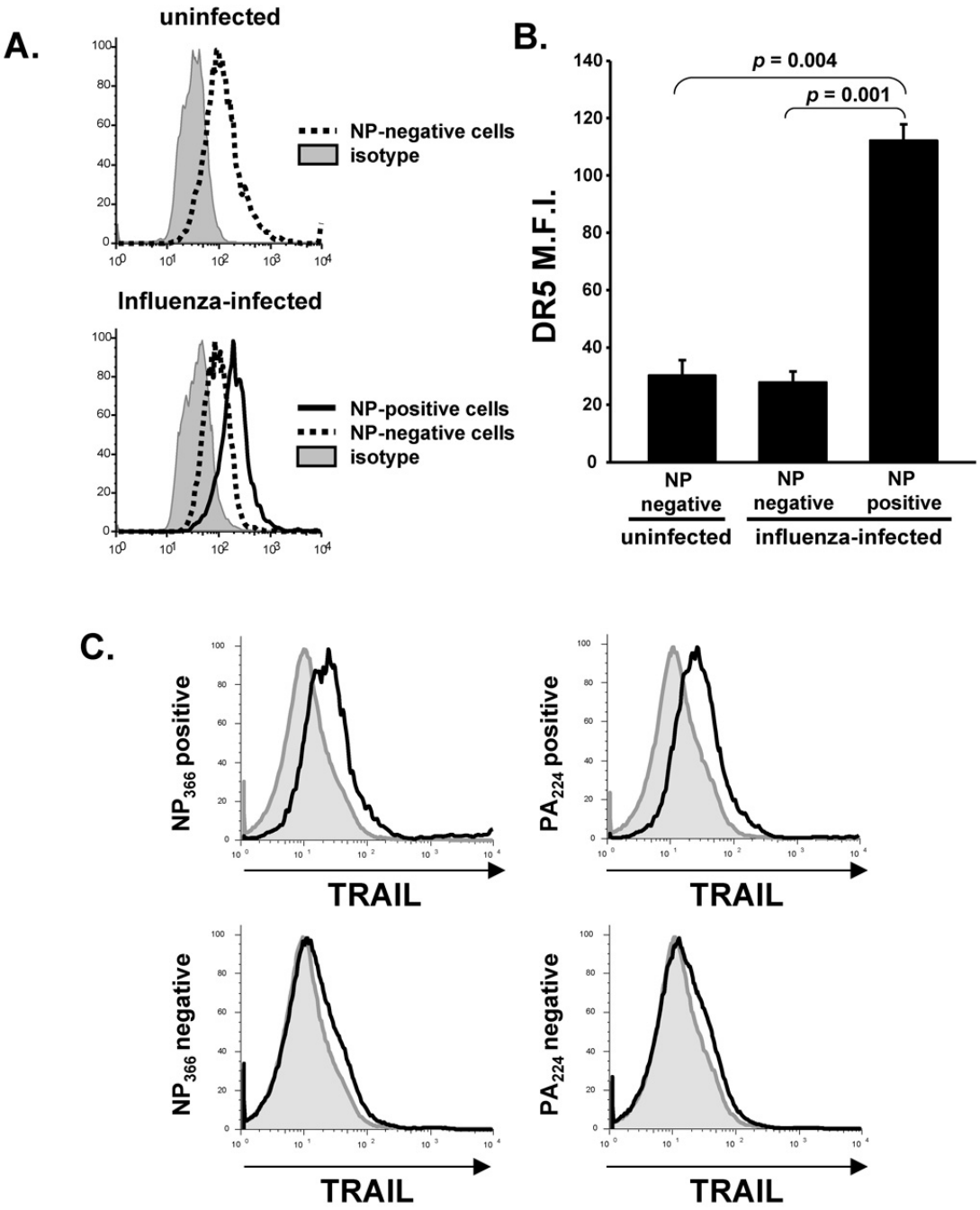
A.
uninfected
NP-negative cells
isotype
Influenza-infected
NP-positive cells
NP-negative cells
isotype
B.
p = 0.004
p = 0.001
DR5 M.F.I.
NP negative
NP negative
NP positive
uninfected
influenza-infected
C.
NP366 positive
PA224 positive
NP366 negative
PA224 negative
TRAIL

Figure 8. Expression of TRAIL in the lung-draining lymph nodes occurs in an influenza-specific fashion. At d 6 p.i., lung-draining lymph nodes were harvested from $TRAIL^{+/+}$ mice and prepared into a single cell suspension. The cells were then stained with anti-CD8α, anti-CD3ε, NP_{366} and PA_{224} tetramers, and anti-TRAIL (open histograms) or isotype controls (shaded histograms). No upregulation was observed on tetramer negative populations. Data are representative of 4-5 mice from 2 experiments.

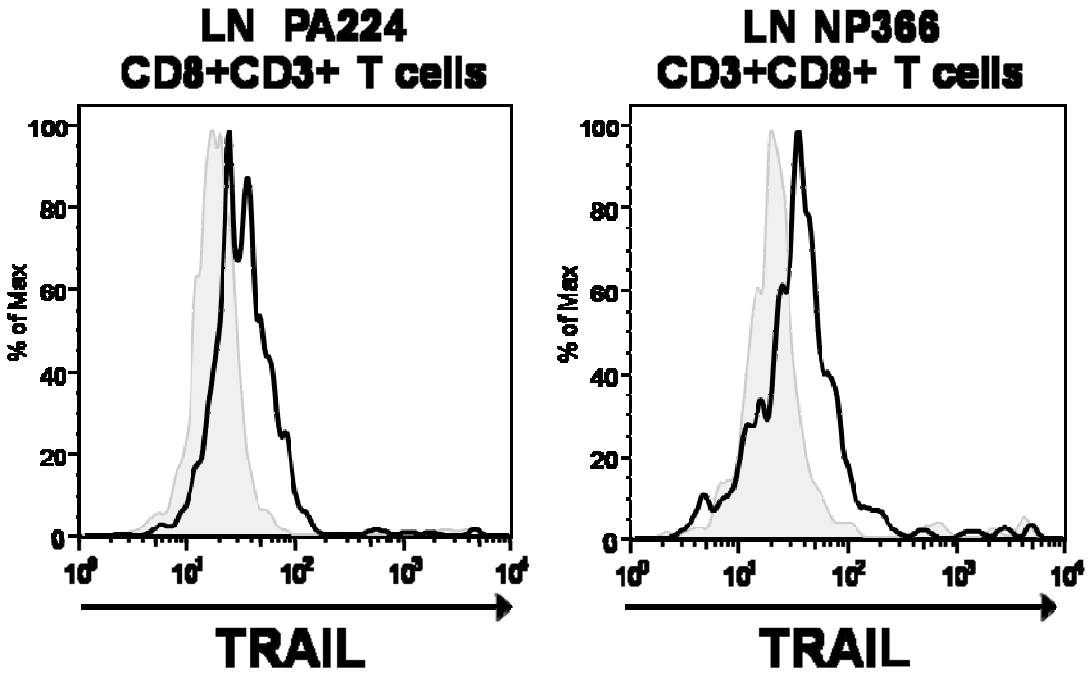
LN PA224
CD8+CD3+ T cells
% of Max
100
80
60
40
20
0
10^0
10^1
10^2
10^3
10^4
TRAIL
LN NP366
CD3+CD8+ T cells
% of Max
100
80
60
40
20
0
10^0
10^1
10^2
10^3
10^4
TRAIL

Figure 9. Antigen-specific stimulation through the T cell receptor results in TRAIL upregulation. Splenocyte antigen-presenting cells (APC) were harvested from BALB/c mice and pulsed with HA_{518} peptide or left unpulsed. Naïve Clone-4 T cells (transgenic T cells expressing a T cell receptor specific for the HA_{518} peptide) or naïve DUC-18 T cells (transgenic T cells expressing a T cell receptor specific for tERK-I_{136} peptide) were isolated, labeled with CFSE, mixed with the APC at a 1:1 ratio, and incubated for 24 hours. After incubation, cells were harvested, stained with anti-CD8a and anti-TRAIL monoclonal antibodies, and analyzed by flow cytometry. Histograms represent TRAIL expression on $CFSE^{+}CD8^{+}$ T cells from each group.

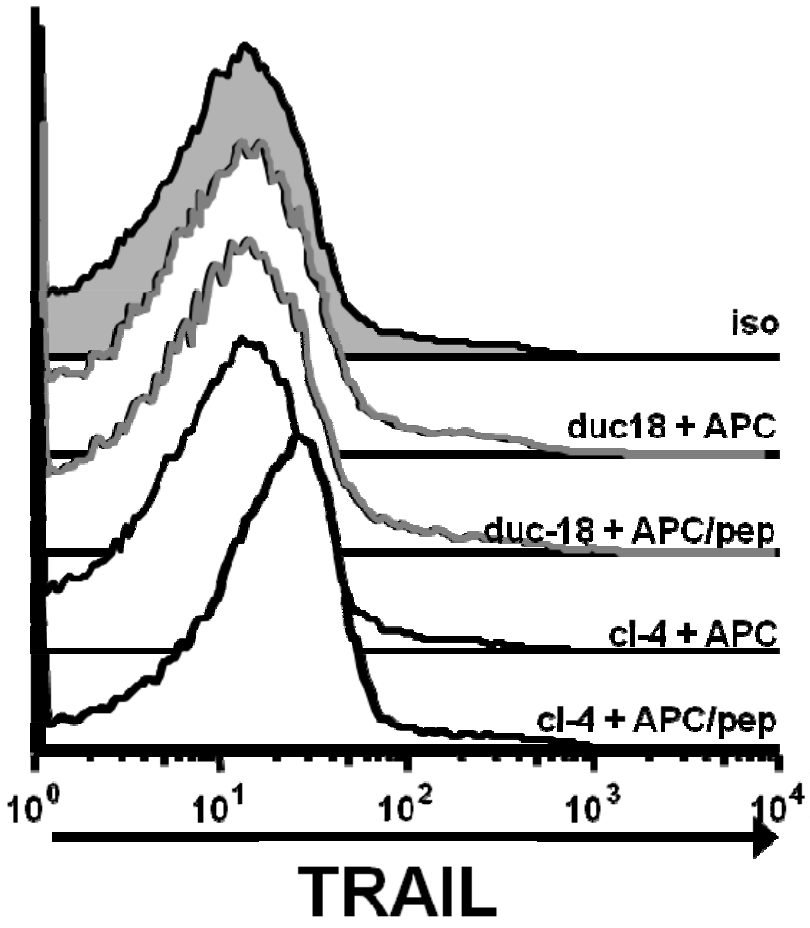
iso
duc18 + APC
duc-18 + APC/pep
cl-4 + APC
cl-4 + APC/pep
10^0
10^1
10^2
10^3
10^4
TRAIL

Figure 10. Despite similar $CD8^+$ T cell responses, cytotoxicity is decreased in influenza virus-infected $TRAIL^{-/-}$ animals. At d 8 p.i., lungs were harvested from C57BL/6 $TRAIL^{+/+}$ (□) or $TRAIL^{-/-}$ (■)mice. *A*, Isolated cells from $TRAIL^{+/+}$ or $TRAIL^{-/-}$ mice were stained with anti-CD8α, NP_{366} tetramer or PA_{224} tetramer, and anti-CD3ε and the number of $CD8^+tetramer^+$ T cells (mean ± SD) enumerated using total counts and flow cytometry. ANOVA analysis yielded no significant differences among the number of $TRAIL^{+/+}$ and $TRAIL^{-/-}$ $tetramer^+$ T cells or between the individual tetramers. Data are representative of 3 experiments. B, Pulmonary cells were incubated with NP_{366} and PA_{224} peptides (or control media); the frequency of antigen-specific T cells was measured by IFNγ ICS. Shown is the percentage of IFN-γ^+ of $CD8^+$ cells. ANOVA analysis yielded no significant differences between the number or percentage of $TRAIL^{+/+}$ and $TRAIL^{-/-}$ IFNγ^+ T cells or between the two epitopes. Data are representative of 2 experiments. *C*, The pulmonary influenza-specific $CD8^+$ T cell response in $TRAIL^{+/+}$ (○) or $TRAIL^{-/-}$ (●) mice was measured by *in vivo* cytotoxicity assay on d 8 p.i. Target cells were purified from $DR5^{+/+}$ and $DR5^{-/-}$ were used as indicated. Percent influenza-specific killing was calculated by comparing unpulsed target lysis to influenza-peptide pulsed target lysis. Target frequencies were normalized to ratios harvested from transfers into naïve mice. C insert, targets from $DR5^{+/+}$ were verified to be $DR5^+$ by flow cytometry. *, $p = 0.029$ determined using a 24 paired *t*-test.

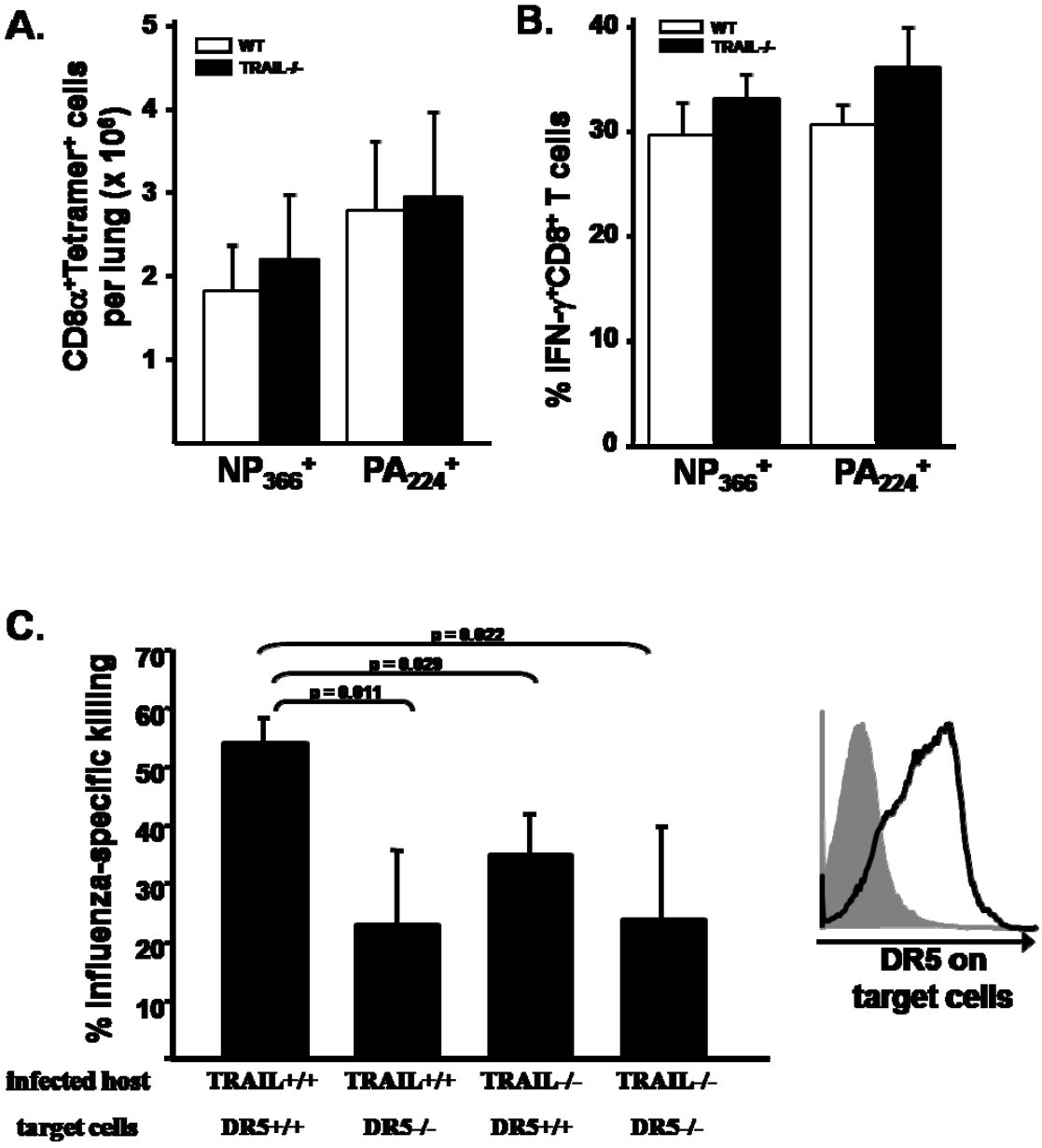
A.
WT
TRAIL-/-
CD8α+Tetramer+ cells per lung (x 10⁶)
5
4
3
2
1
NP366+
PA224+
B.
WT
TRAIL-/-
% IFN-γ+CD8+ T cells
40
30
20
10
0
NP366+
PA224+
C.
p=0.022
p=0.029
p=0.011
% Influenza-specific killing
70
60
50
40
30
20
10
infected host
target cells
TRAIL+/+
DR5+/+
TRAIL+/+
DR5-/-
TRAIL-/-
DR5+/+
TRAIL-/-
DR5-/-
DR5 on target cells

Figure 11. $TRAIL^{-/-}$ and $TRAIL^{+/+}$ influenza-specific $CD8^+$ T cells have similar granzyme B and FasL expression as well as similar degranulation. At d 8 p.i., lungs were harvested from C57BL/6 $TRAIL^{+/+}$ or $TRAIL^{-/-}$ mice. *A*, Isolated cells were stained with anti-CD8α, NP_{366} tetramer, PA_{224} tetramer, anti-granzyme B or isotype control, or anti-FasL or isotype control mAb. Upper panels show Granzyme B (left) or FasL expression (right) on $CD8^+NP_{366}{}^+$ cells from C57BL/6 $TRAIL^{+/+}$ or $TRAIL^{-/-}$ mice. Lower panels show Granzyme B (left) or FasL expression (right) on $CD8^+PA_{224}{}^+$ cells from $TRAIL^{+/+}$ or $TRAIL^{-/-}$ mice. Gray histograms represent isotype control staining. Histograms are representative of 5 mice and 2 separate experiments. *B*, Isolated cells were incubated with NP_{366} and PA_{224} (or control media), BFA, and anti-CD107a for 5 h. After incubation, the cells were stained with anti-CD8 and anti-IFN-γ. Histograms represent the CD107a expression on $CD8^+IFN\text{-}\gamma^+$ cells from $TRAIL^{+/+}$ or $TRAIL^{-/-}$ mice. Histograms are representative of 5 mice and 2 separate experiments.

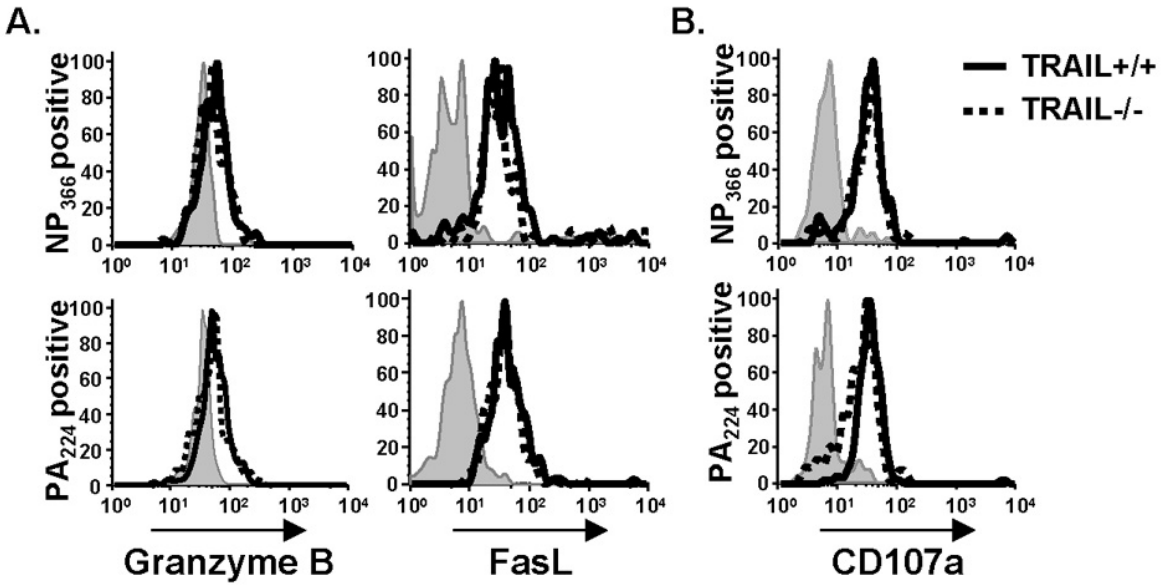
A.
B.
TRAIL+/+
TRAIL-/-
NP366 positive
PA224 positive
Granzyme B
FasL
CD107a

Figure 12. Transfer of pulmonary $CD8^+$ T cells from influenza-infected $TRAIL^{+/+}$ mice, but not $TRAIL^{-/-}$ mice, reduces the mortality of lethal dose influenza-infected mice. At d 8 p.i., lungs were harvested from C57BL/6 $TRAIL^{+/+}$ or $TRAIL^{-/-}$ mice. $CD8^+$ T cells were isolated and transferred i.v. into mice that had been previously infected with a lethal dose of influenza virus (transfer made at day 5 p.i.). The values displayed represent the current percentage of mice surviving after receiving $TRAIL^{+/+}$ T cells, $TRAIL^{-/-}$ T cells, or no transfer of cells. Data represent 2 pooled experiments (total mice no transfer n=9; total mice receiving $TRAIL^{-/-}$ T cells n=9; total receiving $TRAIL^{+/+}$ T cells n = 6). No transfer vs. $TRAIL^{+/+}$ transfer, $p = 0.00551$; $TRAIL^{+/+}$ transfer vs. $TRAIL^{-/-}$ transfer, $p = 0.05$; no transfer vs. $TRAIL^{-/-}$ transfer, $p = 0.517$.

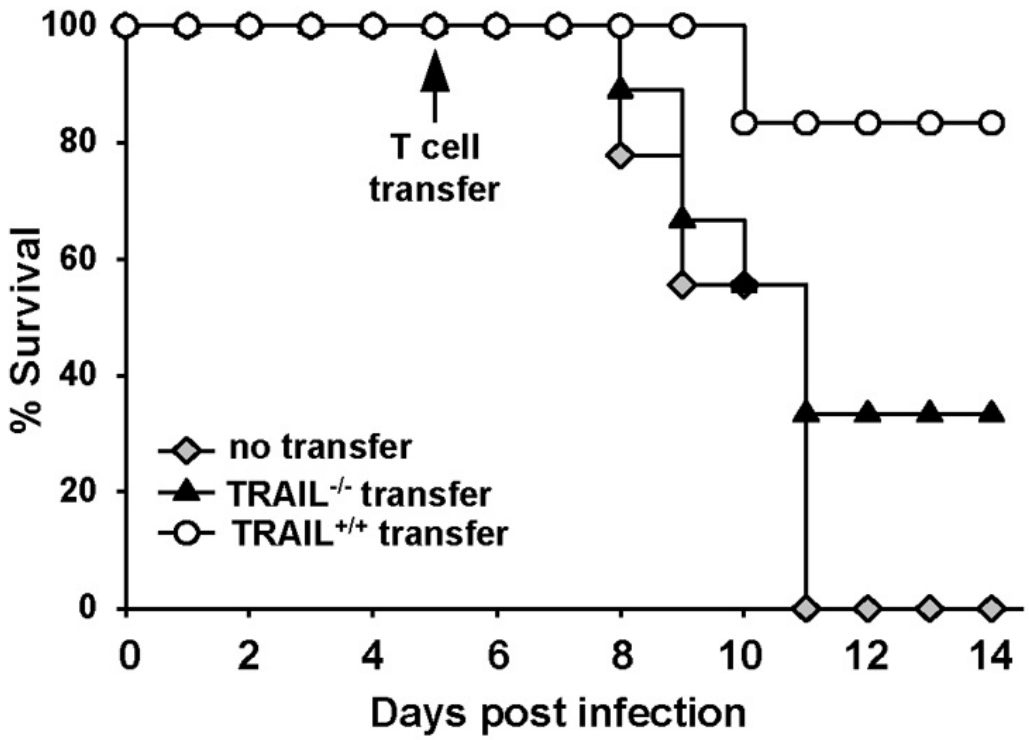
100
80
60
40
20
0
% Survival
T cell
transfer
no transfer
TRAIL-/- transfer
TRAIL+/+ transfer
0
2
4
6
8
10
12
14
Days post infection

Figure 13. Pulmonary $CD8^+$ T cells harvested from influenza-infected $TRAIL^{+/+}$ mice or $TRAIL^{-/-}$ mice migrate similarly to the lungs of lethally-infected mice. At d 8 p.i., lungs were harvested from C57BL/6 $TRAIL^{+/+}CD45.2^+$ or $TRAIL^{-/-}CD45.2^+$ mice. $CD8^+$ T cells were isolated and $2x10^6$ transferred i.v. into $CD45.1^+$ mice that had been previously infected with a lethal dose of influenza virus (transfer made at day 5 p.i.). The values displayed represent the number of $CD45.2^+$ cells present in the lung of recipient mice 24 hours after transfer. No significant differences were observed in numbers of cells migrating to the lung, as measured by paired *t*-test.

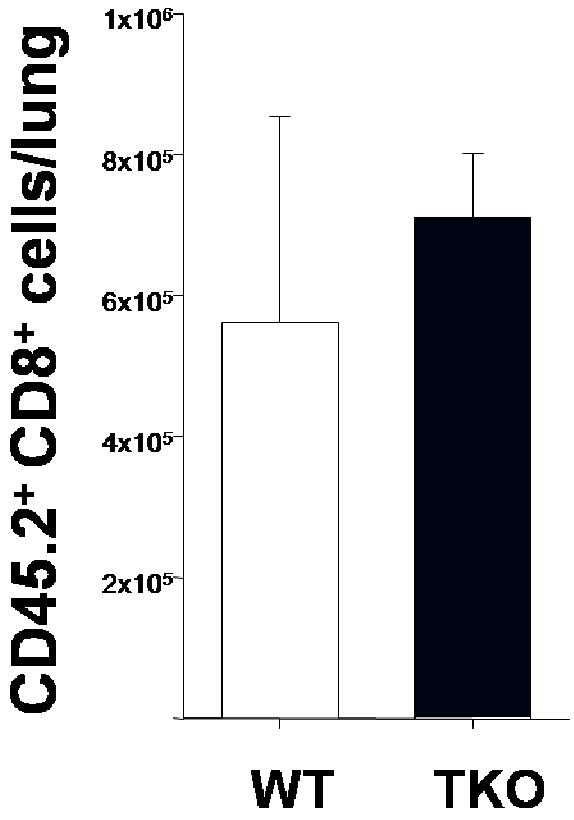
CD45.2+ CD8+ cells/lung
1x10^6
8x10^5
6x10^5
4x10^5
2x10^5
WT
TKO

CHAPTER III. THE MAGNITUDE OF T CELL-MEDIATED IMMUNE RESPONSES TO INFLUENZA VIRUS INFECTION IS REGULATED BY TNF-RELATED APOPTOSIS-INDUCING LIGAND (TRAIL)

Abstract

An immune response of appropriate magnitude controls pathogen spread while simultaneously limiting immune system-induced damage to the infected host. The objective of the present study was to determine the role of TNF-related apoptosis-inducing ligand (TRAIL) in shaping the magnitude of the pulmonary $CD8^+$ T cell response to primary influenza virus infection. Using $TRAIL^{+/+}$ and $TRAIL^{-/-}$ mice infected with a clinical dose of influenza virus, we tested the hypothesis that increased Ag-specific $CD8^+$ T cell responses observed in $TRAIL^{-/-}$ mice result from enhanced chemokine expression in the lung. Compared to $TRAIL^{+/+}$ mice, influenza-infected $TRAIL^{-/-}$ mice experienced increased morbidity and mortality, despite similar viral titers and rates of viral clearance. The increased disease correlated with increased pulmonary pathology, inflammation, and cellular infiltration in the $TRAIL^{-/-}$ mice. Analysis of the lung-infiltrating lymphocytes revealed increased numbers of Ag-specific $CD8^+$ T cells in the lungs of influenza-infected $TRAIL^{-/-}$ mice, which correlated with increased pulmonary cytotoxicity. Despite the difference in *in vivo* killing, the influenza-specific $CD8^+$ T cells from $TRAIL^{+/+}$ and $TRAIL^{-/-}$ mice killed similarly on a per-cell basis and expressed similar levels of Granzyme B, FasL, IFNγ, and TNF. While Ag-specific T cells from $TRAIL^{+/+}$ and $TRAIL^{-/-}$ mice also expressed similar levels of CXCR3 and CCR5, the $TRAIL^{-/-}$ mice had enhanced pulmonary MIG and MIP-1α expression. Blocking the receptors for these chemokines on primed T cells blocked their recruitment to the lung. Together, these data suggest that TRAIL regulates the magnitude of $CD8^+$ T cell responses to influenza virus infection by controlling the pulmonary expression of chemokines important for T cell recruitment.

Introduction

Primary infection with influenza virus results in a localized pulmonary infection and inflammation, and elicits an influenza-specific $CD8^+$ T cell immune response that is necessary for viral clearance (57, 68, 69). Recruitment of T cells to the lung environment after their initial priming in the lung-draining LN is dependent on chemokine expression in the lung as well as chemokine receptor expression on the activated, influenza-specific T cells. A plethora of chemokines have been inculpated in T cell homing to the airway, including MIP-1α, MIP-1β, MIP-3α, RANTES, and IP-10 (61). Similarly, expression of the corresponding chemokine receptors—including CCR2, CCR5, and CXCR3—has been detected on activated T cells after influenza virus infection. The interactions of these chemokines with their respective receptors enhance integrin expression, and subsequently enhance the attachment/rolling of these cells, which is essential in their migration into the lung environment (61).

During primary influenza virus infections, the resulting T cell response is initiated by DC in the lung-draining LN that present Ag and induce the expression of the aforementioned chemokine receptors necessary for homing to the site of infection, as well as the expression of effector molecules necessary for killing infected cells. During influenza virus infections, the influenza-specific $CD8^+$ T cells are primed in the lung-draining LN and subsequently migrate to the lung where they kill infected cells via Fas:FasL interactions and Granzyme B/Perforin secretion (67). In addition to these well-characterized killing pathways, previous work from our laboratory also identified a role for TNF-related apoptosis-inducing ligand (TRAIL)-expressing $CD8^+$ T cells in the primary immune response to influenza virus infection (65-67, 186, 187). TRAIL has classically been studied in tumor immunology settings, where it selectively induces apoptosis in transformed cells while leaving non-transformed cells unaffected (83, 84, 90). More recently, TRAIL-based immunity has become appreciated as a key component in the immune response during viral infections, including responses to cytomegalovirus,

human immunodeficiency virus, and respiratory syncytial virus (91-93, 152, 154-156, 188). Recent reports also demonstrate that TRAIL contributes to the immune response to influenza virus (91, 101, 186, 189). While TRAIL contributes to the killing of virally-infected cells by antigen-specific $CD8^+$ T cells (186), TRAIL expression on macrophages is associated with increased lung damage and susceptibility to pneumonia (101, 189).

Seasonal influenza virus infections affect 10-20% of the U.S. population each winter, resulting in substantial morbidity (~114,000 hospitalizations) and mortality (~36,000 deaths) (3). Utilizing models that recapitulate infection characteristics is imperative to understanding the characteristics of an immune response that result in virus clearance while limiting immunopathology. The infectious dose of influenza virus utilized in the previous investigation induced minimal morbidity in the $TRAIL^{+/+}$ mice (186); to better model human infections in the current study, we altered the infection protocol to examine the role of TRAIL in the $CD8^+$ T cell-mediated immunity induced in response to a dose of influenza virus that induces clinical symptoms in $TRAIL^{+/+}$ mice. The results show that $TRAIL^{-/-}$ animals given clinical-dose influenza virus infections are at greater risk for morbidity and mortality compared to $TRAIL^{+/+}$ mice. The increased disease severity correlated with increased lung damage, increased pulmonary inflammation, and increased pulmonary recruitment of influenza-specific $CD8^+$ T cells in the $TRAIL^{-/-}$ mice. Consistent with the increased number of T cells, $TRAIL^{-/-}$ mice had enhanced influenza-specific pulmonary cytotoxicity *in vivo*, despite similar *in vitro* killing capacity and similar expression of effector molecules. Interestingly, the enhanced T cell recruitment to the lung correlated with increased pulmonary MIG and MIP-1α expression in the lungs of $TRAIL^{-/-}$ mice compared with the lungs of $TRAIL^{+/+}$ mice. Blocking of the corresponding receptors for these chemokines on primed T cells blocked their recruitment to the lung. These data collectively suggest that TRAIL plays a role in limiting pulmonary inflammation and damage after clinical-dose influenza virus infection by regulating the expression of chemokines and the recruitment of Ag-specific T cells.

Materials and Methods

Mice, virus, peptides, and infections

C57Bl/6 ($TRAIL^{+/+}$) were purchased from the National Cancer Institute (Frederick, MD). C57Bl/6 TRAIL-deficient ($TRAIL^{-/-}$) mice were obtained from Amgen (Seattle, WA) (139). These mice have been backcrossed onto the C57Bl/6 background >10 generations. BALB/c ($TRAIL^{+/+}$) mice were purchased from the Jackson Laboratory. BALB/c TRAIL-deficient ($TRAIL^{-/-}$) mice were obtained from Tom Sayers (NCI, Frederick, MD). These mice have been backcrossed onto the BALB/c background >10 generations. All mice were used at 16–24 weeks of age, and all animal experiments followed approved University of Iowa IACUC protocols. The mouse-adapted influenza A virus A/PuertoRico/8/34 (PR8; H1N1) was grown in the allantoic fluid of 10 d old embryonated chicken eggs for 2 d at 37°C, as previously described (55, 69). Allantoic fluid was harvested and stored at -80°C. Groups of 20.5-22.5 g $TRAIL^{+/+}$ and $TRAIL^{-/-}$ mice were given 1500EIU of mouse-adapted PR8 virus in Iscove's media intranasally (i.n.) following anesthesia with isofluorane. The peptides NP_{366} (ASNENMETM), PA_{224} (SSLENFRAYV), HA_{533} (IYSTVASSLI), and NP_{147} (TYQRTRALV) were purchased from Biosynthesis Inc. (Lewisville, TX).

Histology

Whole lungs with the heart attached were harvested from $TRAIL^{+/+}$ or $TRAIL^{-/-}$ mice on various days after influenza virus infection. Lungs were placed in 10% formalin (Fisher Scientific). After ten days, fixed lungs were processed and embedded in paraffin at the University of Iowa Comparative Pathology Laboratory. Paraffin blocks were sectioned at 5-µm thickness. Sections were H&E stained at the University of Iowa Central Microscopy Core; alternatively, sections were stained with anti-influenzaNP and counter-stained with hematoxylin. Slides were blinded and scored by a board-certified veterinary pathologist (D. Meyerholz, University of Iowa, Iowa City, IA). H&E

stained slides were scored from 0 to 5 on a graded scale in which 0 represents undetectable inflammation and 5 represents severe cellular inflammation.

Scoring of cellular infiltration was defined as follows: 0 – none detected; 1 – rare to uncommon; 2 - detectable extravasated neutrophils in small aggregates in airway and or alveoli; 3 - multiple moderate foci/aggregates in airway and/or alveoli; 4 – Severe coalescing foci/aggregates that efface alveoli.

NP influenza scoring was defined by distinct airway epithelium staining: 1 – no distinct NP Ag detection; 2 – rare to uncommon aggregates of cellular NP Ag staining in airway epithelium (<1/3 affected); 3 - small aggregates of staining airway epithelium (1/3 to 2/3 affected), and 4 – NP antigen staining of most airway epithelia (>2/3 affected).

Determination of lung virus titer

Pulmonary influenza viral titers were determined via endpoint dilution assay and expressed as Tissue Culture Infections $Dose_{50}$ ($TCID_{50}$). Briefly, 10-fold dilutions of homogenized and clarified lung from influenza virus-infected mice were mixed with 10^5 MDCK cells in DMEM. After 24 h incubation at 37ºC, the inoculum was removed and DMEM media containing 0.0002% L-1-(tosylamido-2-phenyl) ethyl chloromethyl ketone (TPCK)-treated trypsin (Worthington Diagnostics, Freehold, NJ) and penicillin (100U/ml)/streptomycin (100 μg/ml) was added to each well. After 3 d incubation at 37°C, supernatants were mixed with an equal volume of 0.5% chicken RBC, the agglutination pattern read, and the $TCID_{50}$ values calculated.

In Vivo Cytotoxicity Assays

Splenocytes were resuspended in NycoPrep 1.077A (Axis-Shield; Norton, MA) and then purified according to the manufacturer's instructions. NycoPrep-purified splenic mononuclear cells (10^7/ml) were labeled with either 2 μM CFSE (Invitrogen; Eugene, OR) at 37°C for 10 min or 2 μM PKH-26 (Sigma; St. Louis, MO) at room temperature for 5 min. After labeling, residual non-cell-associated CFSE and PKH-26 were

neutralized by adding an equal volume of fetal calf serum to the cell suspension. CFSE-labeled splenic mononuclear cells (10^7/ml) were pulsed with 10 μM PA_{224} and NP_{366} peptide for 1 h at 37°C. PKH-26^+ splenic mononuclear cells (10^7/ml) were similarly incubated without peptide for 1 h at 37°C. The cells were then washed and mixed at a 1:1 ratio, and 10^7 cells were adoptively transferred i.v. into influenza virus-infected $TRAIL^{+/+}$ or $TRAIL^{-/-}$ mice. After 8 h, the lungs were removed, digested, and analyzed by flow cytometry, as previously described (69), to enumerate the number of remaining target cells. Uninfected mice were used as controls. The percent reduction in the number of recovered peptide-pulsed target cells in the uninfected versus infected mice was considered the percent killing.

In Vitro Cytotoxicity Assays

On day 8 post-infection, lungs were harvested from $TRAIL^{+/+}$ and $TRAIL^{-/-}$ mice. Lungs were homogenized, and $CD8^+$ T cells purified by CD8 MicroBead Kit (Miltenyi Biotech, Auburn, CA) per manufacturer's protocol. A portion of the T cells was then stained with anti-CD8α, NP_{366} tetramer, and PA_{224} tetramer. The percentage of tetramer-positive $CD8^+$ cells was used to calculate the number of influenza-specific effectors. Splenocytes were harvested from C57BL/6 mice and were pulsed with 10 μM PA_{224} and NP_{366} peptide for 1 h at 37°C or left unpulsed. After peptide pulse, cells were labeled with 100 μCi of ^{51}Cr for 1 h at 37°C, washed three times, and resuspended in complete medium. To determine T cell-induced death, ^{51}Cr-labeled tumor cells (10^4/well) were incubated with 3 x 10^5 T cells for 18 hours. Assay was performed in 96-well round-bottom plates, and the percent specific lysis was calculated as: 100 X (experimental c.p.m. - spontaneous c.p.m.)/(total c.p.m. - spontaneous c.p.m.). Spontaneous and total ^{51}Cr release were determined in the presence of either medium alone or 1% NP-40, respectively.

T cell migration assay

TRAIL$^{-/-}$ recipient mice and WT or CXCR3$^{-/-}$ donor mice were infected with A/PR/8/34. At day 6 post-infection, lung dLN from donor mice were harvested and homogenized. CD8^{+} cells were purified using Miltenyi CD8 Microbeads. The CD8+ populations were then blocked with anti-CCR5 at 50μg/ml (or isotype) and stained with 4μM PKH-26 (experimental groups) or 4μM PKH-67 (control groups). The blocked/knockout cells (PKH-26 labeled) were then mixed with an unblocked/WT reference population (PKH-67 labeled) at a 1:1 ratio; 3.5 x 10^5 of the mixed cells were transferred to recipient mice. 20 hours later, the lungs were harvested from the recipient mice, homogenized, and collected on a FACS DiVa. T cell trafficking was assessed by comparing migration of the blocked/knockout populations (PKH-26^{+} cells) to the cotransferred WT population (PKH-67^{+} cells). All values were adjusted to account for variability in input ratios. Bars are normalized to the migration observed in the unblocked/WT population group and the data represent pooled lungs from 3-4 mice/group.

Flow-Cytometry Analysis.

Surface Labeling

Isolated lung cells (10^6) were stained with the following mAb: PE, PerCP-CY5.5, or APC-conjugated anti-mouse CD8α (53-6.7; BD Biosciences, San Jose, CA); biotinylated anti-mouse CD178/FasL (MFL3; eBioscience, San Diego, CA); or biotinylated anti-mouse TRAIL (N2B2; eBioscience). Cells stained with biotinylated mAb were subsequently incubated with Strepavidin-PerCP, Strepavidin-PE, or Strepavidin-APC (BD Bioscience). Stained cells were fixed and erythrocytes lysed with FACS lysing solution (BD Biosciences), and subsequently analyzed on a FACSCalibur flow cytometer. NP_{366} and PA_{224} tetramers (for C57BL/6 studies) as well as HA_{533} and

NP_{147} tetramers (for BALB/c studies) were obtained from the National Institute of Allergy and Infectious Disease MHC Tetramer Core Facility (Germantown, MD).

Pulmonary Epithelial Staining

Isolated lung cells (10^6) were stained with the FITC-conjugated anti-mouse T1α/Podoplanin (8F11; MBL, Woburn, MA) or isotype control, and PE-conjugated anti-mouse DR5 (MD5-1; eBioscience) or isotype control. Subsequently, the cells were fixed, permeabilized, and stained with biotinylated anti-NP (H16-L10-4R5; obtained from Walter Gerhard, Wistar Institute, University of Pennsylvania). Biotinylated antibody was subsequently revealed with PerCP-CY5.5.

Intracellular Staining

Granzyme B. Isolated lung cells (10^6) were surfaced stained with PerCP-CY5.5-conjugated anti-mouse CD8α. Subsequently, the cells were fixed, permeabilized, and stained with the PE-conjugated anti-human Granzyme B mAb (GB11; Invitrogen), or isotype control (57). *IFN-γ.* Splenocytes from influenza-infected mice were cultured at 2 × 10^6 cells/well in the presence of 1 μM of influenza peptides or media control, FITC-conjugated anti-CD107a (1D45; eBioscience) or isotype control, 400 U/ml recombinant human IL-2, and 1 μg/ml brefeldin A. After 6 h, cells were harvested, stained with PE-conjugated rat anti-mouse CD8α, fixed, permeabilized, and stained with APC-conjugated rat anti-mouse IFN-γ (XMG1.2; eBioscience) or isotype control (eBioscience).

Statistical analysis

For each analysis, normal distribution of data was first verified. To assess the difference between two sets of data with normal distribution, statistical significance was assessed using an unpaired, one-tailed t-test or a paired t-test for control and experimental data groups that could be paired. If normality test failed, Mann-Whitney Rank Sum tests were completed to compare data sets. To assess the differences among multiple sets of

data with normal distribution, statistical significance was assessed using an ANOVA analysis of the data sets. If normality test failed, Kruskal-Wallis One Way Analysis of Variance on Ranks test was used to determine overall significance with subsequent pair wise comparisons completed using Dunn's Method. To determine differences in viral clearance, Kaplan-Meier Survival Analysis: Log-Rank tests were run to determine significant differences between data sets. When appropriate, subsequent pair-wise multiple comparisons were completed using the Holm-Sidak method. Differences were considered to be statistically significant at $p < 0.05$.

Results

$TRAIL^{-/-}$ mice have increased morbidity and mortality compared to $TRAIL^{+/+}$ mice

In the previous report examining the role of TRAIL in the immune response to influenza virus infections, we utilized a dose of influenza that induced minimal morbidity and no mortality in $TRAIL^{+/+}$ mice. While it is possible for humans to experience asymptomatic influenza virus infections, substantial public health interest exists in better understanding immune responses to influenza virus infections that induce clinical symptoms. To better model the host reaction and immune response to an infection with clinical symptoms, we altered the infectious inoculum to induce observable morbidity in $TRAIL^{+/+}$ mice. Consistent with previous findings, $TRAIL^{-/-}$ mice showed increased weight loss relative to $TRAIL^{+/+}$ mice following clinical-dose influenza infection (Figure 14A). This morbidity increase in the $TRAIL^{-/-}$ mice also correlated with increased mortality compared to $TRAIL^{+/+}$ mice (Figure 14B). Reinforcing the importance for TRAIL in the immune response to influenza virus infection, increased mortality was also observed in $TRAIL^{-/-}$ BALB/c mice infected with influenza virus compared to $TRAIL^{+/+}$ BALB/c mice (Figure 15).

Despite similar clearance of influenza virus from the lungs, TRAIL$^{-/-}$ mice have enhanced pulmonary cellular infiltrates, increased inflammation, and increased tissue damage compared to TRAIL$^{+/+}$ mice

Our previous investigation of TRAIL$^{+/+}$ and TRAIL$^{-/-}$ mice infected with a subclinical dose of influenza virus found a significant increase in lung viral titers and a significant delay in viral clearance in TRAIL$^{-/-}$ mice (Figure 5). With this in mind, we examined viral titers from the lungs of TRAIL$^{+/+}$ and TRAIL$^{-/-}$ mice infected with a clinical dose of influenza virus. Despite the differences in morbidity and mortality, the influenza viral titers and rate of viral clearance from the lungs of TRAIL$^{+/+}$ and TRAIL$^{-/-}$ mice were surprisingly similar (Figure 14C). These titers were consistent with influenza NP localization, as immunohistochemistry revealed similar NP distribution in the lungs of influenza-infected TRAIL$^{+/+}$ and TRAIL$^{-/-}$ mice (Figure 16). Thus, pathology mediated directly by viral infection and subsequent lysis of infected cells does not appear to be the mechanism behind the enhanced disease severity observed in TRAIL$^{-/-}$ mice.

The efficiency with which TRAIL$^{-/-}$ mice cleared a clinical-dose influenza virus infection combined with the increased morbidity/mortality of these mice prompted us to histologically examine the pulmonary inflammation. Consistent with the increased morbidity/mortality in the TRAIL$^{-/-}$ mice, evaluation of lung sections revealed increased interstitial and perivascular inflammation in the TRAIL$^{-/-}$ mice after influenza virus infection. This increase in inflammation correlated with an increase in pulmonary tissue damage and loss of organized tissue architecture (Figure 17). Further, the lungs of TRAIL$^{-/-}$ mice had increased numbers of cellular foci after influenza virus infection (Figure 18). These data suggest that the enhanced immune response to clinical dose influenza virus infection in TRAIL$^{-/-}$ mice leads to increased inflammation and tissue damage compared to TRAIL$^{+/+}$ mice.

$TRAIL^{-/-}$ mice have increased antigen-specific pulmonary T cell numbers, which correlates with increased influenza-specific pulmonary cytotoxicity

The kinetics of viral clearance from the lung, as well as the increased mortality of $TRAIL^{-/-}$ mice, is consistent with the kinetics of T cells arriving into the lungs after influenza virus infection. Further, immunopathology associated with influenza virus infections has been attributed to $CD8^+$ T cells (108, 109, 111). In the previous investigation of sub-clinical influenza virus infection, Ag-specific $CD8^+$ T cell responses were of similar magnitude in $TRAIL^{+/+}$ and $TRAIL^{-/-}$ mice (Chapter 2, (186). To determine the extent to which altered T cell recruitment enhances pulmonary T cell cytotoxicity in $TRAIL^{-/-}$ mice, we examined the pulmonary, influenza-specific $CD8^+$ T cell response. By utilizing NP_{366} and PA_{224} tetramers, the two D^b-restricted immunodominant epitopes from the A/PR/8/34 strain of influenza virus, we observed a significant increase in the number of NP_{366}^+ ($p = 0.041$) and PA_{224}^+ ($p < 0.001$) $CD8^+$ T cells infiltrating the lungs of $TRAIL^{-/-}$ mice compared to $TRAIL^{+/+}$ mice (Figure 19). Consistent with these findings, tetramer analysis in BALB/c $TRAIL^{+/+}$ and $TRAIL^{-/-}$ mice showed significant increases in pulmonary NP_{147}–specific ($p = 0.022$) and HA_{533}-specific ($p = 0.029$) $CD8^+$ T cells in the lungs of $TRAIL^{-/-}$ mice compared to $TRAIL^{+/+}$ mice (Figure 20). Interestingly, this enhanced recruitment of antigen-specific $CD8^+$ T cells in $TRAIL^{-/-}$ mice appears to be specific to the lung, as decreased numbers of antigen-specific $CD8^+$ T cells were observed in the spleens of $TRAIL^{-/-}$ mice compared to the numbers of antigen-specific $CD8^+$ T cells in the spleens of $TRAIL^{+/+}$ mice after clinical-dose influenza virus infection (Figure 19).

During primary influenza virus infections, $CD8^+$ T cells are the cell population responsible for clearing virus (65, 66). After their initial priming in the regional-draining lymph node, influenza-specific $CD8^+$ T cells migrate to the lung, where they recognize infected cells utilizing MHC:TCR interactions (53, 58). Subsequent to this recognition,

the T cells trigger apoptosis in the infected cells through FasL:Fas interactions, Granzyme B/perforin secretion (67), and TRAIL:DR5 interactions (186). In the previous examination of sub-clinical dose infections, pulmonary T cells in $TRAIL^{-/-}$ mice had decreased cytotoxic function, which correlated with delayed viral clearance compared to that observed in $TRAIL^{+/+}$ mice. The efficiency with which the $TRAIL^{-/-}$ mice cleared a clinical-dose infection prompted us to examine $CD8^+$ T cell function. Consistent with the enhanced pulmonary T cell response and efficient clearance of virus in the $TRAIL^{-/-}$ mice, the *in vivo* influenza-specific killing by pulmonary $CD8^+$ T cells was significantly higher ($p = 0.031$) in the $TRAIL^{-/-}$ mice compared to the killing in WT mice (Figure 21). However, when the cytotoxic function of the pulmonary T cells from $TRAIL^{+/+}$ and $TRAIL^{-/-}$ mice was assessed *in vitro*, the T cells killed the target cells similarly, indicating that the per-cell killing capacity by the pulmonary $CD8^+$ T cells was similar (Figure 22). Together, these results suggest that pulmonary $CD8^+$ T cells in $TRAIL^{-/-}$ and $TRAIL^{+/+}$ animals have similar inherent killing ability following a clinical-dose influenza virus infection, but different *in vivo* killing capacity. Considering the increased antigen-specific T cell responses in the lung environment of the $TRAIL^{-/-}$ mice, the increased *in vivo* killing in the $TRAIL^{-/-}$ mice is likely a result of their increased pulmonary T cell numbers compared to the $TRAIL^{+/+}$ host. Further, these data suggest that the observed increase in illness in the $TRAIL^{-/-}$ mice might result from an aberrant immune response to the influenza virus infection—which help clear the virus efficiently, but could also negatively enhance inflammation and pulmonary damage during the immune response.

Influenza-specific $CD8^+$ T cells in $TRAIL^{+/+}$ and $TRAIL^{-/-}$ mice express effector molecules similarly

In addition to the magnitude of the T cell response, other factors can contribute to alterations in T cell cytotoxicity. Specifically, changes in the effector phenotype (i.e. effector molecule expression, activation state, anergy/exhaustion, etc.) of the influenza-

specific $CD8^+$ T cells responding to the infection could contribute to the observed differences in cytotoxicity. Subsequent phenotypic analysis of these influenza-specific $CD8^+$ T cells (Figure 23) showed that they had similar expression of granzyme B ($TRAIL^{+/+}$ MFI = 59.4±14.9; $TRAIL^{-/-}$ MFI = 37.9±12.2), FasL ($TRAIL^{+/+}$ MFI = 351±134; $TRAIL^{-/-}$ MFI = 333±106), TNF ($TRAIL^{+/+}$ MFI = 20.1±4.6; $TRAIL^{-/-}$ MFI = 32.1±21.3), as well as similar ability to degranulate, as measured by CD107a staining. Thus, these data indicate that the differences in pulmonary cytotoxicity between the $TRAIL^{+/+}$ and $TRAIL^{-/-}$ $CD8^+$ T cells responding to the influenza virus infection could not be explained by the "effector" phenotypic parameters measured. Further, the data support the idea that the differential *in vivo* cytotoxicity was simply the result of increased numbers of influenza-specific $CD8^+$ T cells responding to a clinical dose influenza infection in $TRAIL^{-/-}$ mice.

$TRAIL^{-/-}$ mice have increased pulmonary chemokine expression after influenza virus infection

To determine the possible cause of the differential T cell recruitment to the lungs of $TRAIL^{-/-}$ mice compared to $TRAIL^{+/+}$ mice, we measured the pulmonary expression of chemokines known to be associated with T cell recruitment (61-63). Interestingly, significant increases in MIG expression ($p < 0.001$) and MIP-1α expression ($p = 0.027$) were observed in the lungs of $TRAIL^{-/-}$ mice compared to $TRAIL^{+/+}$ mice, while expression of other chemokines associated with T cell recruitment (IP-10, MCP-1, and RANTES) was similar between the two groups (Figure 24A). For chemokines to effectively act on T cells and enhance their migration into the lungs, the T cells need to express the corresponding receptor for the chemokine. Examination of the Ag-specific $CD8^+$ T cells responding to the influenza infection revealed that CXCR3 (receptor for MIG) and CCR5 (receptor for MIP-1α) had similar levels of expression on pulmonary T cells from $TRAIL^{+/+}$ and $TRAIL^{-/-}$ mice (Figures 24B). Because of the established

importance for these chemokine receptors in recruiting T cells to the lungs during influenza infection (61), and to determine if other chemokine receptors were playing a major role in T cell recruitment, we examined the importance of the CXCR3 and CCR5 on migration to the lung from the lung-draining LN. T cells were isolated from the lung-draining lymph nodes of $CXCR3^{-/-}$ and $CXCR3^{+/+}$ mice. After treatment with chemokine receptor blocking antibody or isotpye control, these T cells were then transferred into an infected $TRAIL^{-/-}$ host. The T cells lacking CXCR3 on their surface migrated to the lungs of $TRAIL^{-/-}$ mice 50% less efficiently compared $CXCR3^{+/+}$ T cells (Figure 25). Similarly, T cells with CCR5 blocked migrated to the lungs 50% less efficiently than their unblocked counterparts (Figure 25). Loss of signal through both chemokine receptors (CCR5 block on $CXCR3^{-/-}$ T cells) further inhibited the efficient migration of transferred cells to the lung compared with unblocked, $CXCR3^{+/+}$ T cells. These data reinforce the important role these receptors play in T cell migration to the lung after influenza virus infection. Importantly, these blocking experiments demonstrate that no heretofore undescribed chemokine/chemokine-receptor pairs are responsible for the increased pulmonary T cell recruitment observed in $TRAIL^{-/-}$ mice. Together, these data suggest that the $TRAIL^{-/-}$ environment might enhance the number of Ag-specific $CD8^+$ T cells that respond to influenza virus infections by enhancing the pulmonary expression of chemokines important for their recruitment to the lung.

Discussion

Classically, TRAIL has been described as a potent inducer of apoptosis in tumor systems, where TRAIL selectively induces the death of transformed cells. More recently, TRAIL-expressing $CD8^+$ T cells, NK cells, macrophages, and plasmacytoid DC have all been implicated in the cytotoxicity and control of virus infections. Previously, we demonstrated that $CD8^+$ T cells utilize TRAIL as a means of killing influenza virus-infected cells, and that influenza virus-infected epithelial cells are sensitized to TRAIL-

receptor-induced apoptosis (186, 187). The results presented herein examined the role of TRAIL in the immune response to a clinical dose of influenza virus infection. These results demonstrate some striking differences to the sub-clinical dose infection model, and suggest an additional role for TRAIL in shaping the magnitude of the $CD8^+$ T cell response to influenza virus infections. Consistent with the previous study, $TRAIL^{-/-}$ mice showed increased morbidity after infection; not surprisingly, this increased morbidity correlated with increased mortality at the clinical infectious dose. Unexpectedly, however, this increase in morbidity/mortality in the $TRAIL^{-/-}$ mice did not result from a delay in viral clearance or an increase in viral load, as was observed in the sub-clinical influenza virus infection model (186). Instead, the increased morbidity/mortality in the $TRAIL^{-/-}$ mice appears to result from increased immunopathology.

Primary influenza virus infections are thought to be cleared by $CD8^+$ T cells that eliminate virally-infected cells via FasL, cytolytic granule secretion (perforin/granzyme), and TRAIL-mediated mechanisms (67, 186). Despite the loss of one of these three pathways, $CD8^+$ T cells from $TRAIL^{-/-}$ mice given a clinical-dose influenza virus infection were still able to control viral loads and clear virus similarly to $TRAIL^{+/+}$ counterparts. In fact, T cells from $TRAIL^{+/+}$ and $TRAIL^{-/-}$ mice exhibit similar *in vitro* killing capacity. In contrast, examination of the *in vivo* cytotoxicity mediated by influenza-specific $CD8^+$ T cells revealed enhanced killing by T cells from $TRAIL^{-/-}$ mice after clinical-dose influenza virus infection (186). Interestingly, these results are in opposition to those observed during responses to sub-clinical influenza virus infections. The T cell cytotoxicity observed in the clinical dose infection of $TRAIL^{-/-}$ mice did not result from compensatory increases in FasL expression or granzyme B production; rather, the increases in T cell killing correlated with an increased number of antigen-specific T cells. These data suggest differential functions for TRAIL during the immune response to influenza virus that depend on the initial infection conditions. That is, during the immune response to sub-clinical dose infections, TRAIL is expressed on antigen-specific

$CD8^+$ T cells which induce the apoptosis of infected cells, and during the immune response to clinical dose infections, TRAIL limits pulmonary chemokine expression and the recruitment of antigen specific T cells.

The model system we chose for this investigation utilized a higher infectious dose of influenza virus with the aim of better modeling the clinical symptoms observed in human patients infected with influenza virus. In particular, the clinical dose infection model increased morbidity and mortality, symptoms that were not observed in sub-clinically infected $TRAIL^{+/+}$ mice. While this infectious dose resulted in similar peak viral titers, the clinical dose infection presumably delivered a relatively higher load of immunostimulatory signaling molecules, or pathogen-associated molecular patterns (PAMPs). The danger signals associated by an influenza virus infection can be detected by both TLR and NLR, which initiate signaling cascades that lead to immune responses. Diehl et.al. have reported that DR5-deficienct DC and macrophages are hyper-responsive to TLR stimuli; specifically, TLR2, TLR3, and TLR4 signals simulate increased production of IL-12, IFNα, and IFNγ in $DR5^{-/-}$ mice compared to wildtype mice (138). This previous report suggests a regulatory role for TRAIL:DR5 interactions that is consistent with the increased pulmonary expression of MIG and MIP-1α that was observed the $TRAIL^{-/-}$ mice infected with influenza virus.

The absence of TRAIL signals resulted in loss of regulation of the chemokine production. Presumably, the viral stimuli responsible for activating TLR/NLR pathways was similar in the $TRAIL^{+/+}$ and $TRAIL^{-/-}$ mice, the similar viral loads were observed in the two strains. However, influenza virus infection of $TRAIL^{-/-}$ mice still resulted in increased chemokine production compared to their $TRAIL^{+/+}$ counterparts. Future studies should examine the extent to which TRAIL:DR5 interactions regulate the cytokine and chemokine production stimulated by TLRs that detect influenza virus—e.g. TLR3 and TLR7/8 (28, 29). Given the recent reports that influenza virus triggers the inflammasome (32, 33, 190, 191) as well as reports that IL-1R-deficiency shifted a low-

lethality virus to a high-lethality phenotype (192), it would also be interesting to examine the extent to which TRAIL:DR5 interactions also help to regulate the cytokine production induced by influenza virus activation of the inflammasome. In addition to the TLR and NLR proteins, other virus-detecting molecules, such as PKR and RIG-I, could also have their downstream products regulated by TRAIL:DR5 signaling; hence, examining the extent to which TRAIL signals regulate the other influenza-sensing cytoplasmic proteins—e.g. RIG-I and PKR (28, 29).

In addition to determining the specificity of TLR/NLR regulation by TRAIL, future studies should also aim to determine the mechanism by which this regulation occurs. A primary mechanism by which TRAIL could regulate cytokine and chemokine production resulting from TLR/NLR signals is via direct apoptosis of cells producing the cytokines and chemokines. To determine if apoptosis induction is the means by which TRAIL is controlling the chemokine production, future studies will aim to determine the specific cells producing the chemokines after influenza virus infection. Utilizing a combination of intracellular staining and ex vivo tissue cultures, the cell type(s) responsible for chemokine production will be determined and, the induction of apoptosis of these cells in $TRAIL^{-/-}$ and $TRAIL^{+/+}$ systems would be assessed.

While the induction of apoptosis of chemokine-producing cells is a likely mechanism by which TRAIL regulates chemokine expression during influenza virus infections, differences in non-apoptotic TRAIL signaling in $TRAIL^{-/-}$ and $TRAIL^{+/+}$ mice could also explain their different expression of chemokines. Additional studies could determine the extent to which TRAIL expression and non-apoptotic TRAIL signaling influences the chemokine production after influenza virus infection. Utilizing agonistic anti-DR5 antibodies in the $TRAIL^{-/-}$ system, TRAIL signals could be added back and the effect of these signals on chemokine expression determined. If a non-apoptotic regulatory effect was observed after stimulation of the TRAIL receptor, subsequent studies would determine the non-apoptotic signal proximal to the TRAIL receptor that

might influence chemokine production. Based on previous study of non-apoptotic signals through DR5 in the regulation of TLR signaling (138), such signals could include the activation of NF-κB and jnk.

Of obvious public heath interest are the ongoing studies examining the immune response to the pandemic H1N1 influenza virus (i.e. swine-origin H1N1 influenza virus) and immune responses to emerging highly-pathogenic H5N1 influenza virus (i.e. "bird flu" strains). Studies of the H1N1 pandemic strains revealed increased viral titers, increased morbidity, and increased pulmonary pathologic lesions compared with seasonal influenza virus infections (193, 194); interestingly, these symptoms are consistent with phenotype we have observed in TRAIL$^{-/-}$ mice infected with a clinical dose of influenza virus. Similarly, studies of the immune response to highly-pathogenic H5N1 influenza strains have demonstrated increased chemokines (e.g. MIP-1α, MIG, RANTES) and cytokines (e.g. IFNγ, IL-6) compared to low-pathogenic infections (192). These increased cytokine/chemokine responses that are also consistent with the phenotype observed in TRAIL$^{-/-}$ mice infected with a clinical dose of influenza virus. Interestingly, the increased morbidity and mortality seen following H5N1 infection has been correlated with attenuated type I interferon responses (195), and influenza virus infection of IFNα receptor-deficient mice results in increased morbidity/mortality (196). TRAIL upregulation after type I and II interferon signals is well-established (116, 118-120), so future lines of investigation would determine if the attenuated interferon responses after H5N1 infections result in aberrant TRAIL expression on lymphocytes responding to virus infection. Further, studies examining H5N1 infections in TRAIL$^{+/+}$, TRAIL$^{-/-}$, and DR5$^{-/-}$ mice would determine the extent to which TRAIL:DR5 interactions contribute to the phenotypes observed in the above H5N1 infections. Specifically, treatment with agonistic anti-DR5 antibody could recapitulate TRAIL signals in the TRAIL$^{-/-}$ mice while having no effect in the DR5$^{-/-}$ mice. Together, these studies would help define the role for TRAIL in regulating the immune response to influenza virus infections and offer

insight about how aberrant TRAIL expression and function could contribute to the pathology of new influenza virus strains. On a related note, a recent report demonstrated that TRAIL-expressing macrophages contribute to influenza-virus-induced pneumonia by inducing apoptosis of airway epithelial cells (101). Together, the data from this macrophage report, the data presented in chapter 2, and the data presented here suggest that TRAIL can have both positive roles (i.e. roles in clearing virus efficiently and limiting immunopathology) and negative roles (i.e. roles contributing to immunopathology) in the immune response to influenza virus. Improving the understating of these various roles will aid in improving the treatment of influenza virus infections and the symptoms associated with influenza virus infection.

In conclusion, the results presented herein demonstrate that TRAIL plays a vital role in regulating the cellular immune response to influenza virus infections. Specifically, TRAIL-deficiency results in an increase in the magnitude of the T cell response, which allows for viral clearance similar to that observed in $TRAIL^{+/+}$ hosts, despite the absence of a major apoptosis-inducing pathway. The enhanced recruitment and pulmonary killing correlate with increased pulmonary chemokine expression in $TRAIL^{-/-}$ mice. Together, these data suggest that in addition to its previously-established role in the killing of virally-infected cells by antigen-specific $CD8^+$ T cells, TRAIL regulates the magnitude of the antigen-specific $CD8^+$ T cell responses by controlling the pulmonary expression of chemokines important for T cell recruitment. These results offer insight to the mechanisms that control the immune responses to pulmonary pathogens that control the infectious pathogen while limiting immunopathology.

Figure 14. TRAIL deficiency correlates with increased disease severity after clinical dose influenza virus infection. $TRAIL^{+/+}$ (●) or $TRAIL^{-/-}$ (▲) C57BL/6 mice (n = 6 mice/group) were infected with 1500 EIU of A/PR/8/34 and weighed daily to assess morbidity **(A)** and mortality **(B)**. **In A,** the values displayed represent the daily weight relative to the weight on day of infection. *, $p < 0.05$; Mann-Whitney Rank Sum Test. **In B,** data represent the percentage of mice surviving on the given day after infection; significant increases in mortality were observed in the $TRAIL^{-/-}$ mice. *, $p = 0.007$; Kaplan-Meier Survival Analysis: Log-Rank. Data are representative of 2 separate experiments. **For C,** $TRAIL^{+/+}$ (black bars) or $TRAIL^{-/-}$ (gray bars) C57BL/6 mice were infected with 1500 EIU of A/PR/8/34. At indicated days after infection, lungs were harvested, and pulmonary viral titers were assessed by determining the $TCID_{50}$ in Madin-Darby canine kidney cell cultures (as described in the *Materials and Methods*). No significant difference was observed in the viral titers or the rate of viral clearance at the clinical dose of infection. Data are representative of 2 separate experiments with 3-5 mice per group

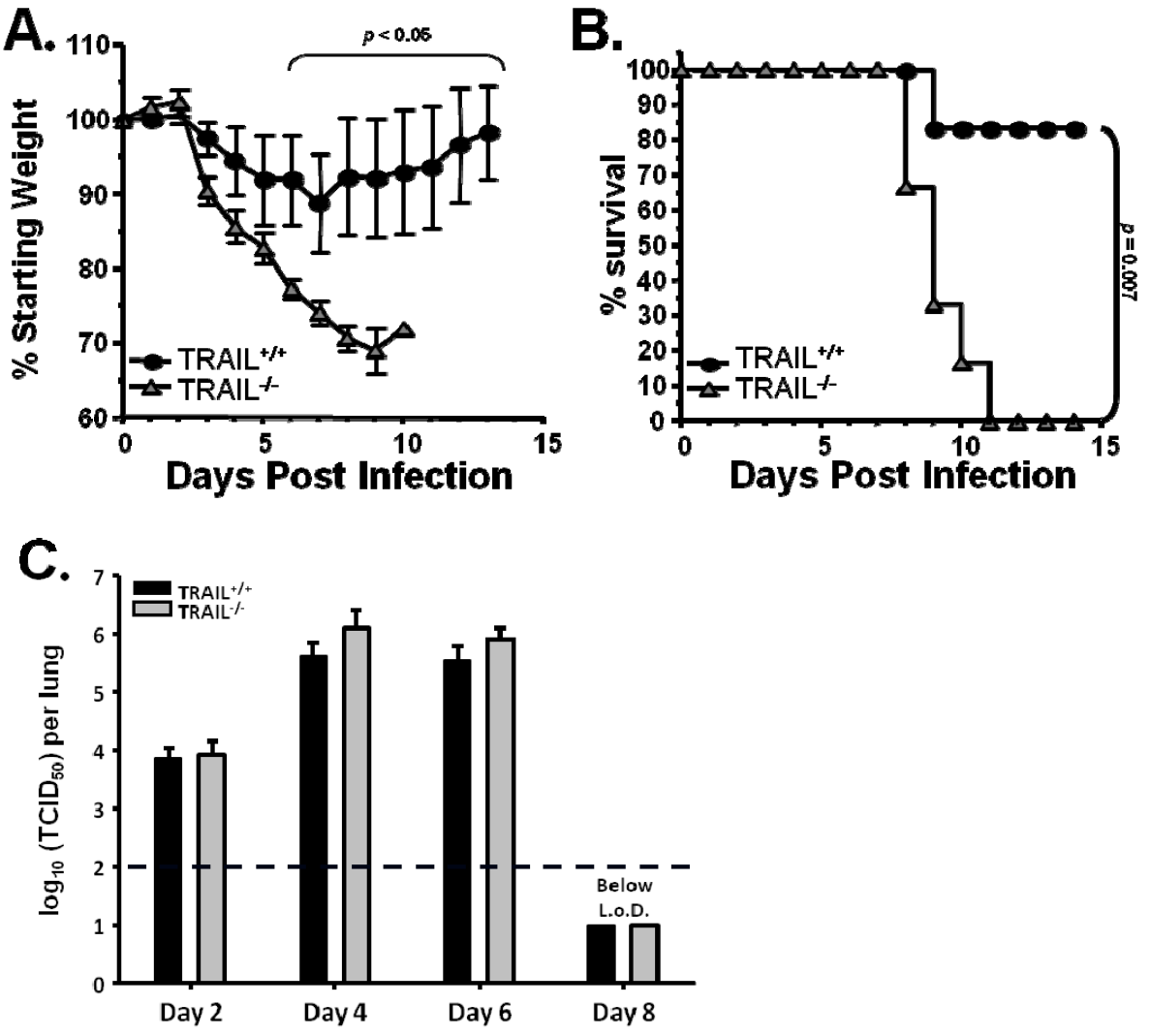
A.
p < 0.05
% Starting Weight
Days Post Infection
TRAIL+/+
TRAIL-/-
B.
% survival
Days Post Infection
p = 0.007
TRAIL+/+
TRAIL-/-
C.
log10 (TCID50) per lung
TRAIL+/+
TRAIL-/-
Below L.o.D.
Day 2
Day 4
Day 6
Day 8

Figure 15. TRAIL$^{-/-}$ BALB/c mice show enhanced mortality after clinical dose influenza virus infection compared to TRAIL$^{+/+}$ BALB/c mice. TRAIL$^{+/+}$ or TRAIL$^{-/-}$ BALB/c mice were infected with 500 EIU of A/PR/8/34. After infection, mice were monitored for mortality induced by infection. p=0.047 Survival differences assessed by Kaplan-Meier Survival Analysis: Log-Rank.

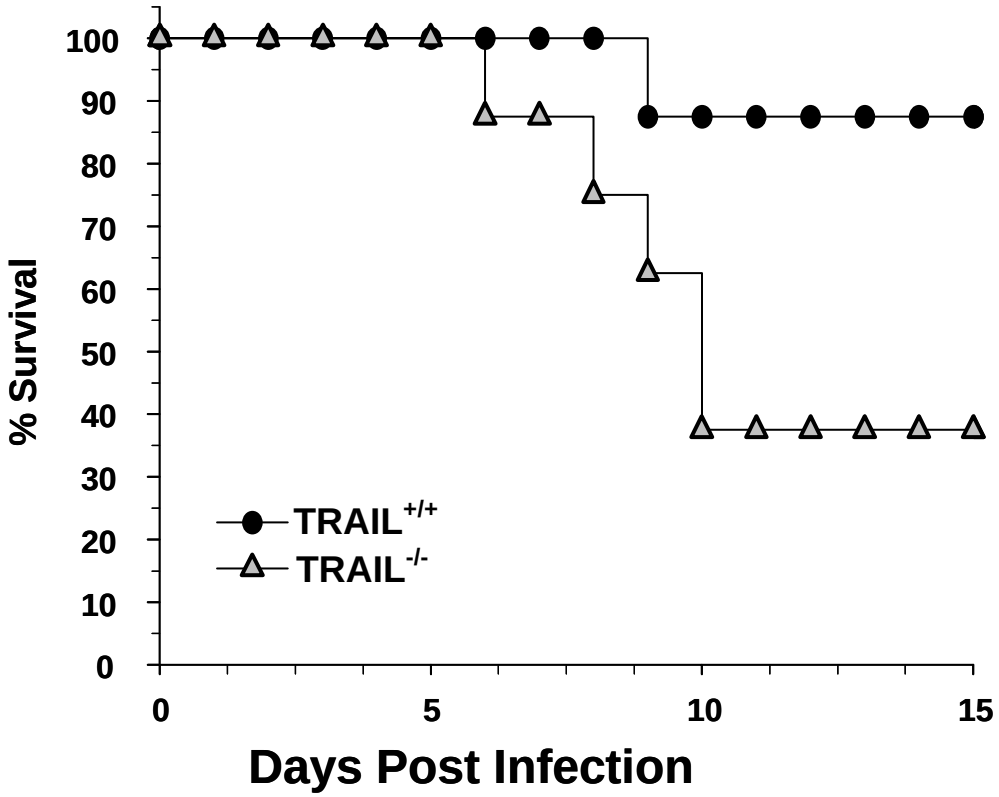
100
90
80
70
60
50
40
30
20
10
0
% Survival
TRAIL+/+
TRAIL-/-
0
5
10
15
Days Post Infection

Figure 16. TRAIL$^{+/+}$ and TRAIL$^{-/-}$ mice express similar levels of NP in their lungs after influenza virus infection. C57BL/6 TRAIL+/+ (●) or TRAIL-/- (▲) mice (n = 6 mice/group) were infected with 1500 E.I.U. of A/PR/8/34. On day 6 after infection, lungs were harvested and insufflated with 10% buffered formalin. Subsequently, the lung tissue was sectioned, mounted, and stained for influenza-NP and Hematoxylin counterstain. Slides were blinded and evaluated for positive influenza NP staining; scoring for distinct epithelial staining of influenza-NP revealed no significant difference between sections from TRAIL$^{+/+}$ mice (NP score = 2.35) and those from TRAIL-/- mice (NP score = 2.5). Images displayed are at 20x magnification.

TRAIL$^{+/+}$

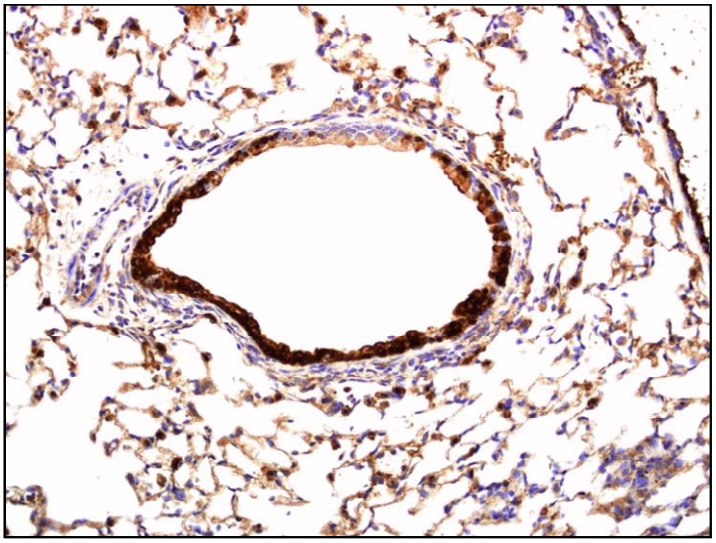

TRAIL$^{-/-}$

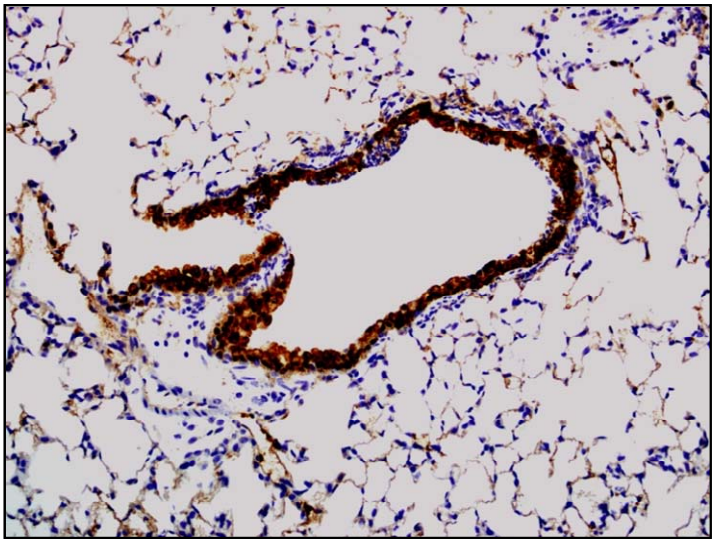

Figure 17. $TRAIL^{-/-}$ mice have increased pulmonary cellular infiltration and increased inflammation after clinical dose influenza virus infection. $TRAIL^{+/+}$ (●) or $TRAIL^{-/-}$ (▲) C57BL/6 mice (n = 6 mice/group) were infected with 1500 EIU of A/PR/8/34. On various days after infection, lungs were harvested and insufflated with 10% buffered formalin. Subsequently, the lung tissue was sectioned, mounted, and stained with Hematoxylin and Eosin (H&E). Slides were blinded and evaluated for cellular infiltration; scores for each time point are indicated in the insert. No significant differences between $TRAIL^{+/+}$ and $TRAIL^{-/-}$ were observed in edema. Images displayed are at 10x magnification.

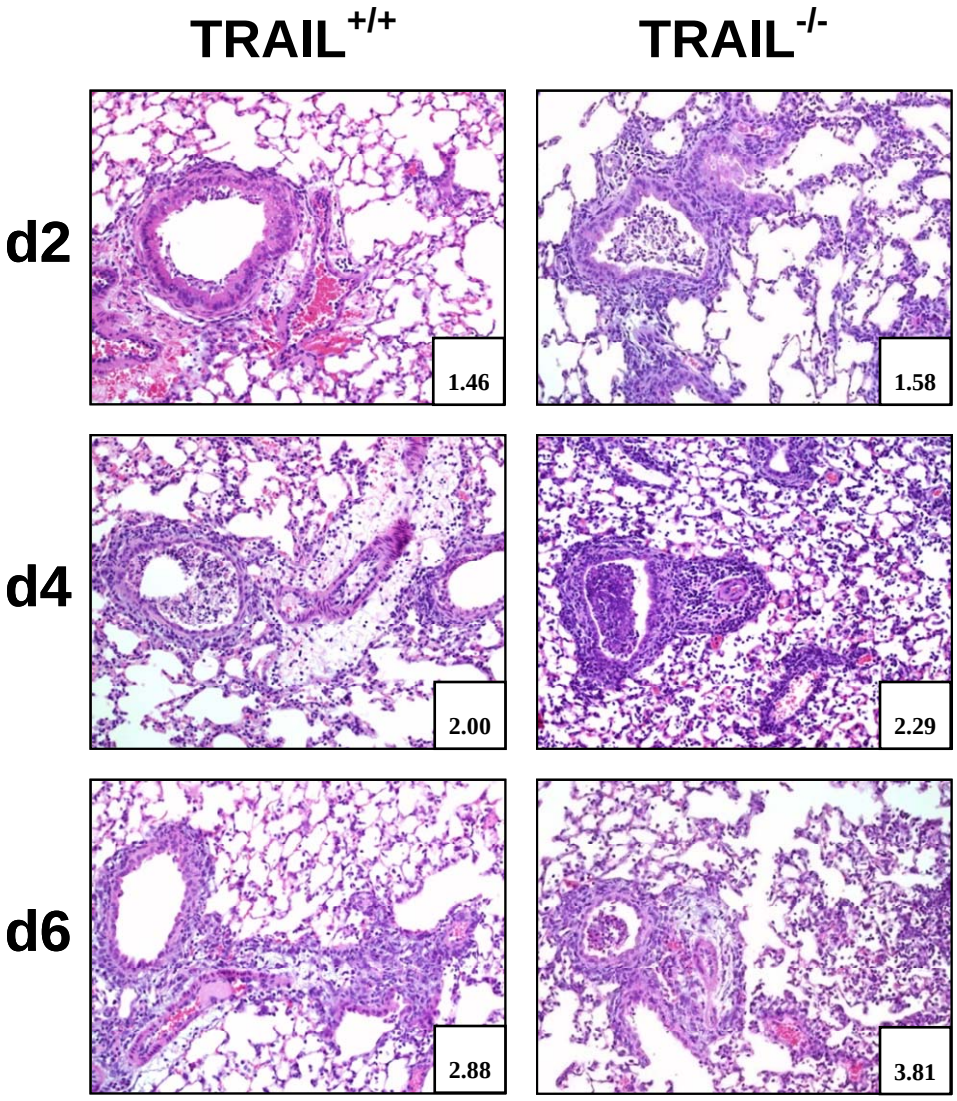
TRAIL+/+
TRAIL-/-
d2
d4
d6
1.46
1.58
2.00
2.29
2.88
3.81

Figure 18. TRAIL$^{-/-}$ mice have enhanced cellular foci in their lungs after influenza virus infection compared to TRAIL$^{+/+}$ mice. C57BL/6 TRAIL$^{+/+}$ or TRAIL$^{-/-}$ mice were infected with 1500 EIU of A/PR/8/34. After 6 days, lungs were harvested and insufflated with 10% buffered formalin. Subsequently, the lung tissue was sectioned, mounted, and stained with Hematoxylin and Eosin. Slides were blinded and evaluated for cellular infiltrates and parameters of inflammation. Left panels show a representative lobe of lung (2x magnification); right panels show a focused view (40x magnification) on one of the cellular foci from the TRAIL$^{+/+}$ (top row) or TRAIL$^{-/-}$ (bottom row) mice.

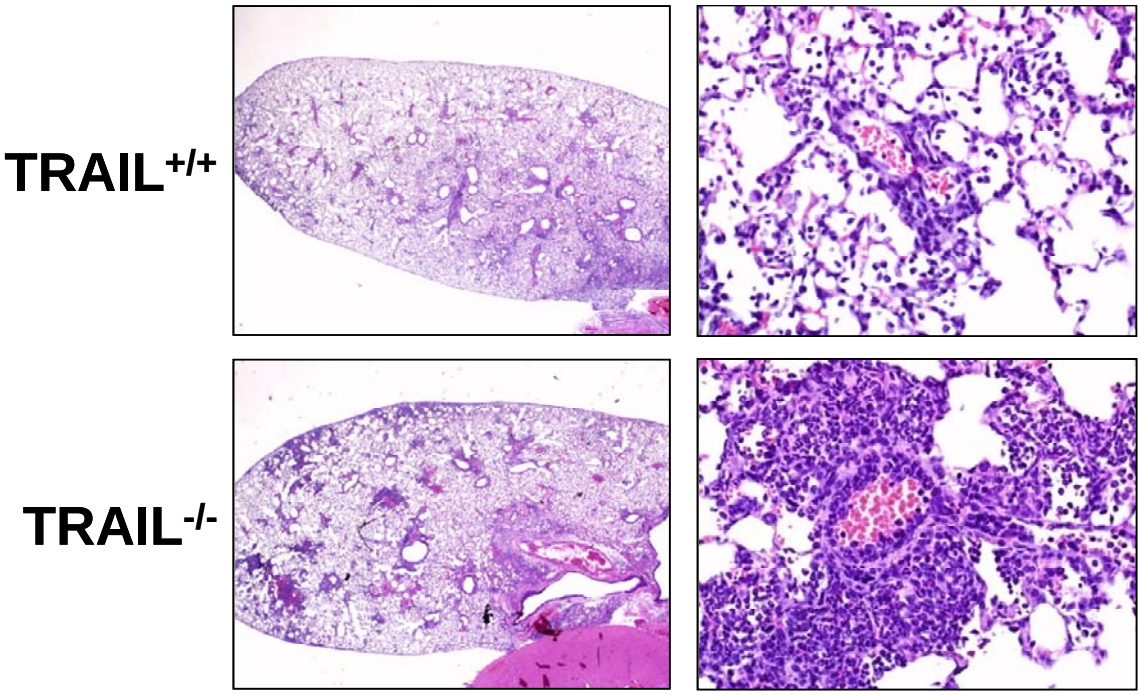
TRAIL+/+
TRAIL-/-

Figure 19. $TRAIL^{-/-}$ mice infected with a clinical dose of influenza virus show enhanced pulmonary T cell recruitment compared to $TRAIL^{+/+}$ mice. $TRAIL^{+/+}$ or $TRAIL^{-/-}$ C57BL/6 mice were infected with 1500 EIU of A/PR/8/34. At day 8 post-infection, lungs and spleens were harvested and homogenized, and the isolated cells were stained with anti-CD8α, NP_{366} tetramer, PA_{224} tetramer, and anti-CD3ε. The number of $CD3^{+}CD8^{+}tetramer^{+}$ T cells from the infected $TRAIL^{+/+}$ (●) or $TRAIL^{-/-}$ (▲) mice were enumerated using total pulmonary cell counts and flow cytometry. Symbols represent number in individual mice, bars represent the mean of each group, and data are representative of two experiments.

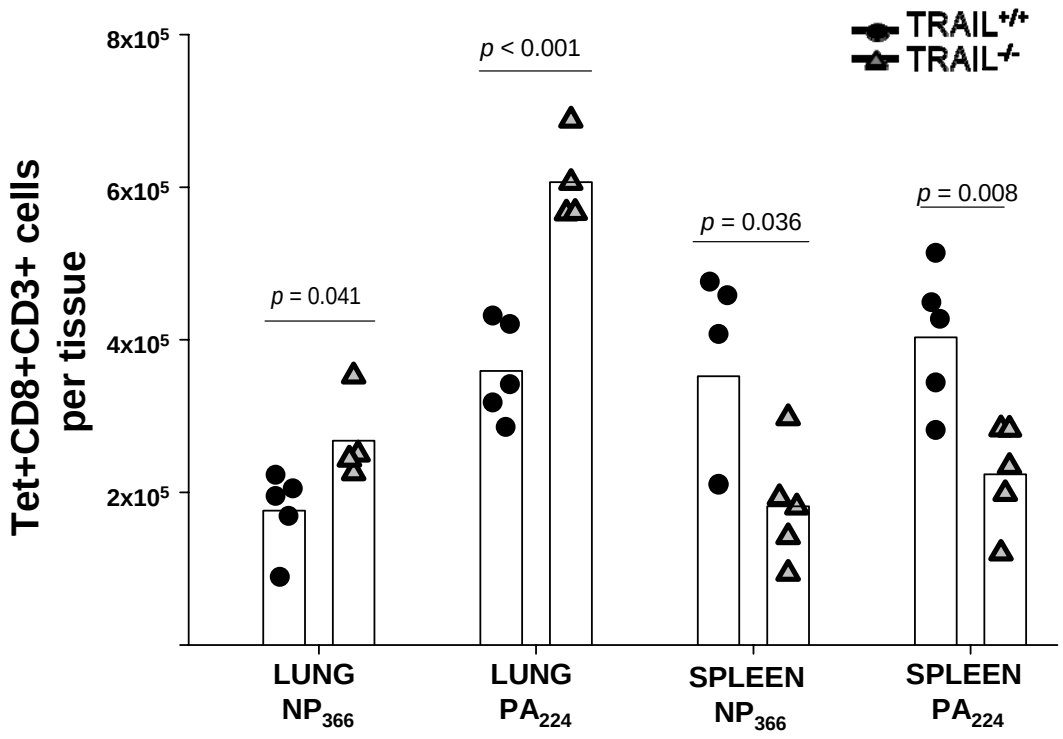
TRAIL+/+
TRAIL-/-
Tet+CD8+CD3+ cells per tissue
8x10^5
6x10^5
4x10^5
2x10^5
p = 0.041
p < 0.001
p = 0.036
p = 0.008
LUNG NP366
LUNG PA224
SPLEEN NP366
SPLEEN PA224

Figure 20. BALB/c TRAIL$^{-/-}$ mice show enhanced pulmonary recruitment of antigen-specific T cells after influenza virus infection. TRAIL$^{+/+}$ or TRAIL$^{-/-}$ BALB/c mice were infected with 1500 EIU of A/PR/8/34. At day 8 post-infection, lungs were harvested and homogenized; isolated cells were stained with anti-CD8α, HA_{533} tetramer, NP_{147} tetramer, and anti-CD3ε. The number of $CD3^+CD8^+$tetramer$^+$ T cells (mean $\pm$ SD) from TRAIL$^{+/+}$ (black bars) or TRAIL$^{-/-}$ (gray bars) were enumerated using total pulmonary cell counts and flow cytometry. Bars represent 4-5 mice per group and data are representative of two independent experiments.

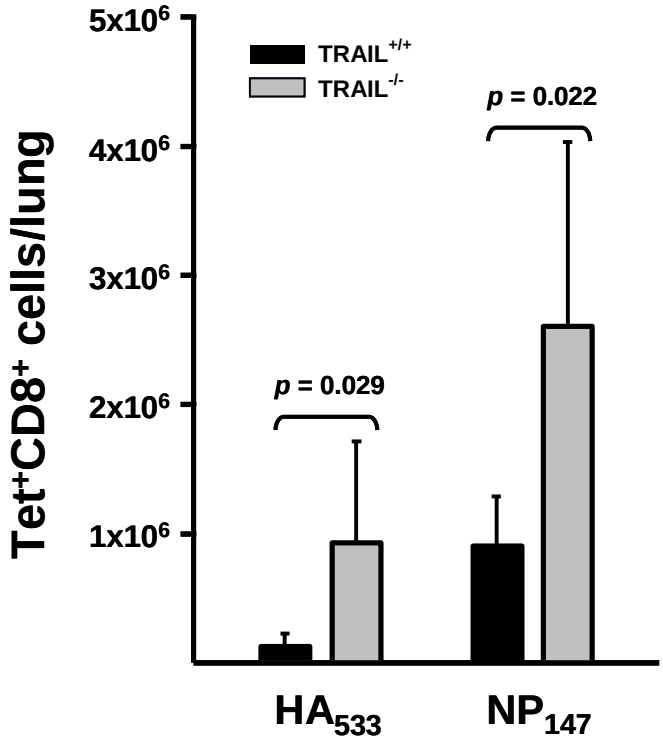
5x10^6
4x10^6
3x10^6
2x10^6
1x10^6
Tet+CD8+ cells/lung
TRAIL+/+
TRAIL-/-
p = 0.029
p = 0.022
HA533
NP147

Figure 21. Given a clinical dose of influenza virus, $TRAIL^{-/-}$ have enhanced *in vivo* cytotoxicity compared with $TRAIL^{+/+}$ mice. The pulmonary influenza-specific $CD8^+$ T cell response in $TRAIL^{+/+}$ (●) or $TRAIL^{-/-}$ (▲) C57BL/6 mice was measured by *in vivo* cytotoxicity assay on day 8 post-infection. Symbols represent killing in individual mice, and bars represent mean killing. Percentage influenza-specific killing was calculated by comparing unpulsed target lysis to influenza peptide-pulsed target lysis. Targets were verified to be $DR5^+$ by flow cytometry (Figure 10C). Target frequencies were normalized to ratios harvested from transfers into naïve mice. Statistical significance was determined using a paired *t* test. Data are representative of three independent experiments.

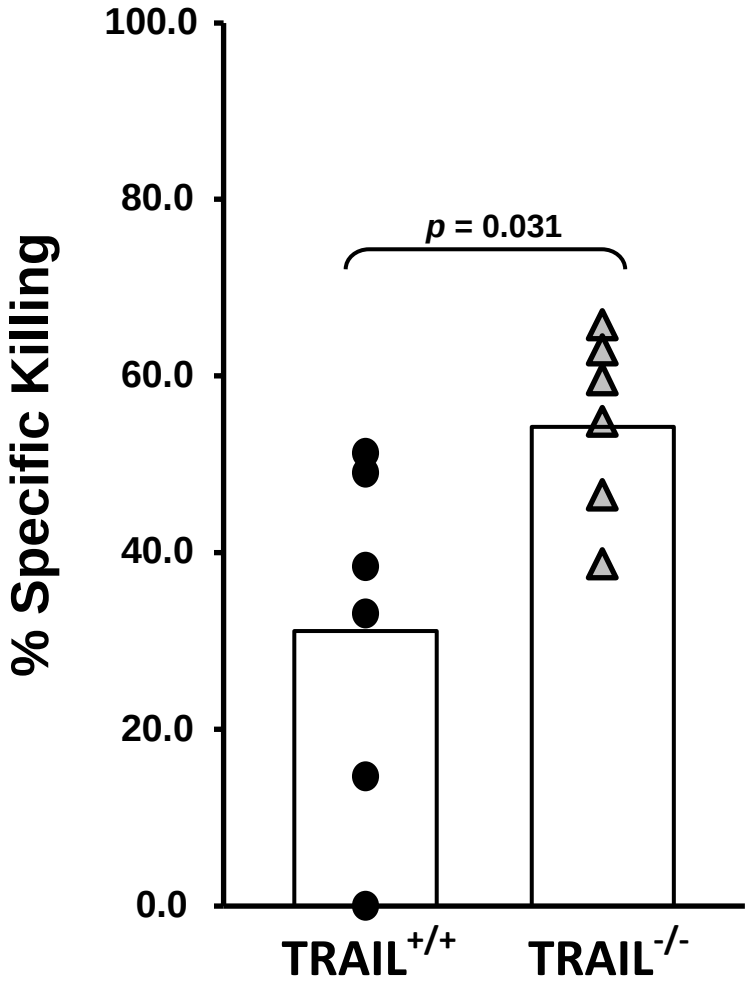
100.0
80.0
60.0
40.0
20.0
0.0
% Specific Killing
p = 0.031
TRAIL+/+
TRAIL-/-

Figure 22. Pulmonary T cells from TRAIL$^{-/-}$ and TRAIL$^{+/+}$ mice have similar *in vitro* killing capacity after clinical-dose influenza virus infection. On day 8 post infection, lungs of infected mice were harvested, and their pulmonary T cells isolated. A portion of the T cells was then stained with anti-CD8a, NP_{366} tetramer, and PA_{224} tetramer. The percentage of tetramer-positive CD8^{+} cells was used to calculate the number of influenza-specific effectors. T cells were cultured for 18 h with ^{51}Cr-labeled target cells (with or without influenza peptides) at a 30:1 ratio (influenza-specific effectors to targets). The killing by the T cells from TRAIL$^{+/+}$ (black bars) or TRAIL$^{-/-}$ (gray bars) C57BL/6 mice was calculated. Bars represent mean killing $\pm$ SD. Percent specific lysis was calculated as: 100 X (experimental c.p.m. - spontaneous c.p.m.)/(total c.p.m. - spontaneous c.p.m.). Spontaneous and total ^{51}Cr release were determined in the presence of either medium alone or 1% NP-40, respectively. Targets were verified to be DR5^{+} by flow cytometry (Figure 10C). Data points represent the mean of triplicate wells. Statistical significance was determined using a paired *t* test.

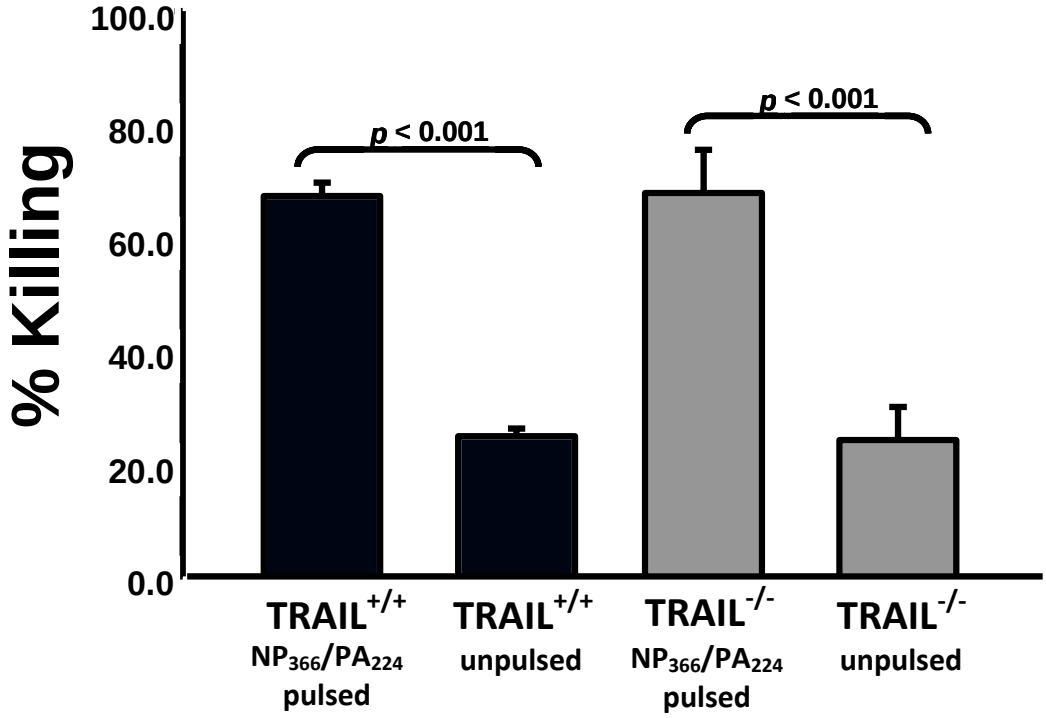
100.0
80.0
60.0
40.0
20.0
0.0
% Killing
p < 0.001
p < 0.001
TRAIL+/+
NP366/PA224
pulsed
TRAIL+/+
unpulsed
TRAIL-/-
NP366/PA224
pulsed
TRAIL-/-
unpulsed

Figure 23. Pulmonary T cells from TRAIL$^{+/+}$ and TRAIL$^{-/-}$ mice have similar expression of effector molecules. TRAIL$^{+/+}$ or TRAIL$^{-/-}$ C57BL/6 mice were infected with 1500 EIU of A/PR/8/34 and then lungs were harvested on day 8 post-infection. For A and B, isolated cells were stained with anti-CD8α, NP_{366} tetramer or PA_{224} tetramer, anti-CD3ε, anti-granzyme B or isotype control antibody, and anti-FasL or isotype control antibody. Histograms represent Granzyme B staining (A) or FasL staining (B) on CD8$^+$tetramer$^+$ cells. Gray histograms represent isotype control staining. Data represent staining on 4-5 mice from 2 independent experiments. For C and D, isolated cells were incubated with NP_{366} or PA_{224} or control media, brefeldin A, and anti CD107a for 5 h. After incubation, the cells were stained with anti-CD8, anti-IFNγ or isotype control antibody, and anti-TNF or isotype control antibody. Histograms represent the TNF expression (C) or CD107a staining (D) of CD8$^+$IFNγ$^+$ cells. Gray histograms represent isotype control staining. Data represent staining on 4 mice from 2 independent experiments.

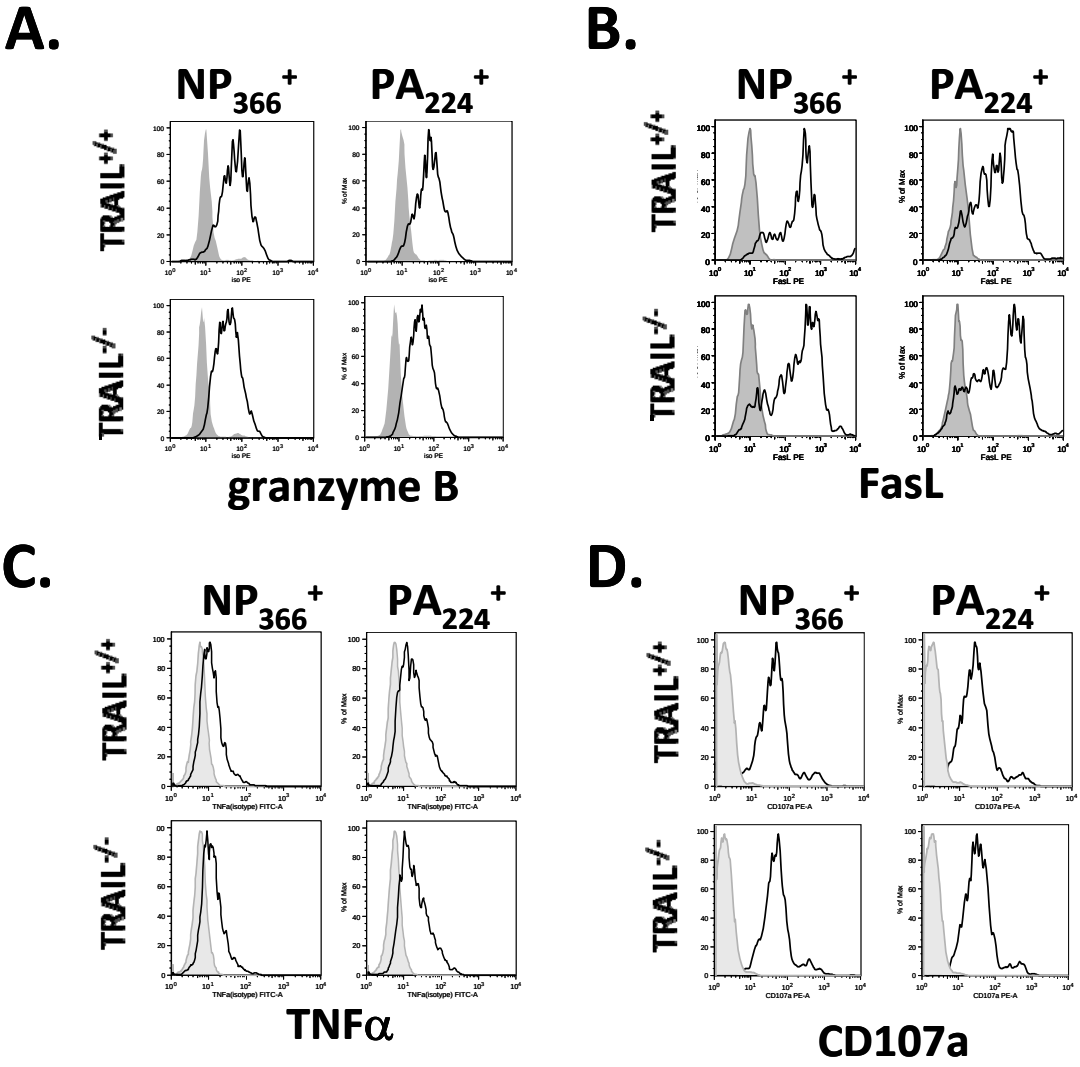
A.
NP366+
PA224+
TRAIL+/+
TRAIL-/-
granzyme B
B.
NP366+
PA224+
TRAIL+/+
TRAIL-/-
FasL
C.
NP366+
PA224+
TRAIL+/+
TRAIL-/-
TNFα
D.
NP366+
PA224+
TRAIL+/+
TRAIL-/-
CD107a

Figure 24. TRAIL$^{-/-}$ mice have increased pulmonary expression of MIG and MIP-1α after clinical dose influenza virus infection compared to TRAIL$^{+/+}$ mice. TRAIL$^{+/+}$ or TRAIL$^{-/-}$ C57BL/6 mice were infected with 1500 EIU of A/PR/8/34. **For A,** the lungs were harvested on day 6 post-infection and homogenized in 3 ml of DMEM. Subsequently, the pulmonary chemokine expression was determined. Data presented are the average chemokine concentration measured from 3-4 TRAIL$^{+/+}$ (black bars) or TRAIL$^{-/-}$ (gray bars) mice, and are representative of two independent experiments. Statistical significance was determined using a paired *t* test. **For B,** lungs were harvested and homogenized on day 8 post-infection, and the isolated cells were stained with anti-CD8α, NP_{366} tetramer, PA_{224} tetramer, and anti-CXCR3, anti-CCR5, or isotype control. Histograms show CXCR3 expression (**on left**) and CCR5 expression (**on right**) on CD8$^+$ tetramer$^+$ T cells from TRAIL$^{+/+}$ (solid line) and TRAIL$^{-/-}$ (dashed line) mice or the isotype control (shaded histogram). Data are representative of 4-5 mice from 2 independent experiments. NS, not significant.

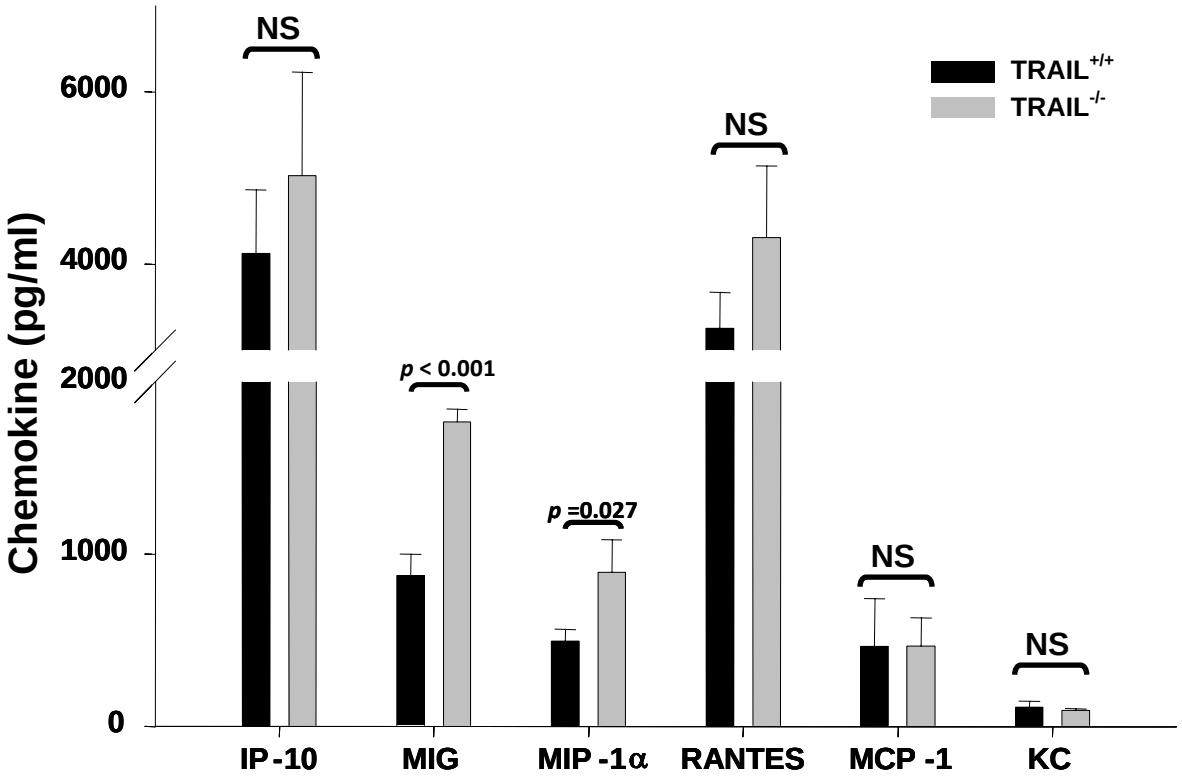
NS
NS
NS
NS
p < 0.001
p =0.027
TRAIL+/+
TRAIL-/-
Chemokine (pg/ml)
6000
4000
2000
1000
0
IP-10
MIG
MIP-1α
RANTES
MCP-1
KC

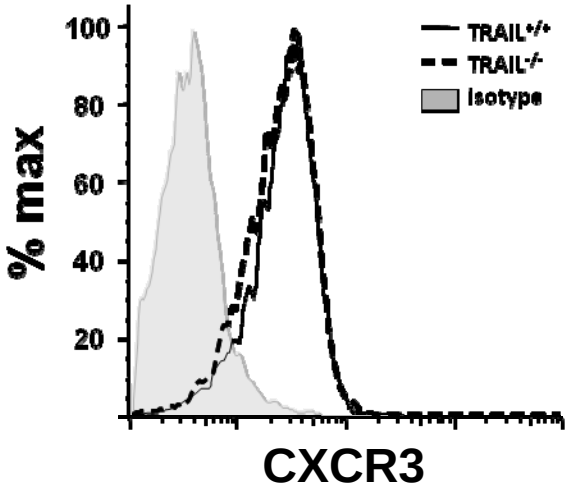
TRAIL+/+
TRAIL-/-
Isotype
% max
100
80
60
40
20
CXCR3

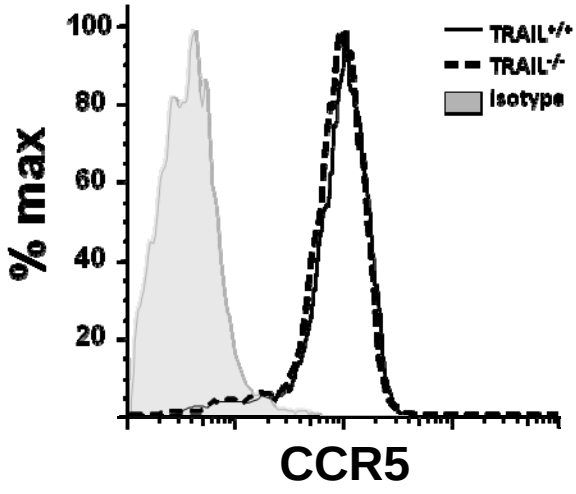
TRAIL+/+
TRAIL-/-
Isotype
% max
100
80
60
40
20
CCR5

Figure 25. Abrogation of chemokine signals to T cells blocks their migration to the lung after influenza virus infection. The experimental design is outlined in A. Briefly, $TRAIL^{-/-}$ recipient mice and WT or $CXCR3^{-/-}$ mice were infected with A/PR/8/34. At day 6 post-infection, dLN were harvested and homogenized. From these cells, $CD8^{+}$ cells were purified. The purified populations were then blocked with anti-CCR5 (or isotype) and stained with PKH-26 or PKH-67, as described in the table insert. The blocked/knockout cells were then mixed with an unblocked, WT reference population and $3.5x10^{5}$ cells were transferred to recipient mice. 20 hours later, the lungs were harvested from the recipient mice, and T cell trafficking was assessed by comparing migration of the blocked/knockout populations to the cotransferred WT population; these values are displayed in B. All values were adjusted to account for variability in input ratios. Bars are normalized to the migration observed in the unblocked/WT population group and the data represent pooled lungs from 3-4 mice/group. Statistical significance was determined using a paired *t* test.

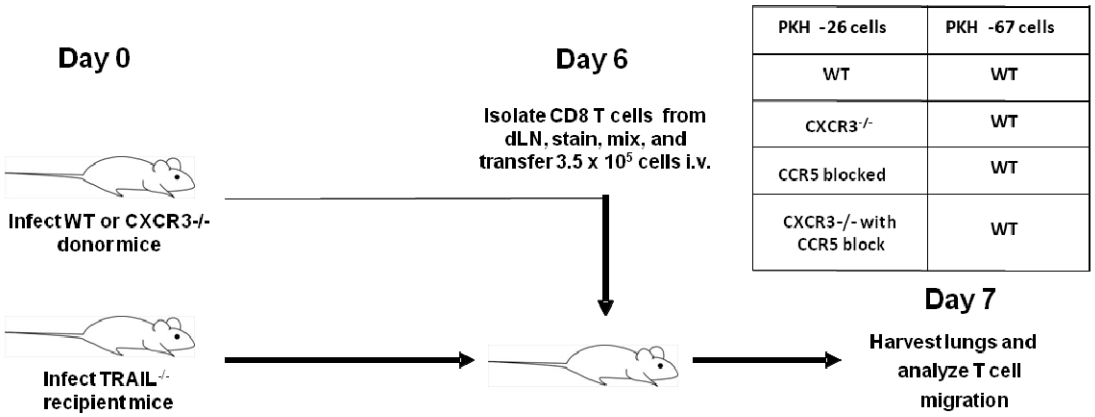
Day 0
Day 6
Day 7
Isolate CD8 T cells from dLN, stain, mix, and transfer 3.5 x 10^5 cells i.v.
Infect WT or CXCR3-/- donor mice
Infect TRAIL-/- recipient mice
Harvest lungs and analyze T cell migration
PKH -26 cells
PKH -67 cells
WT
WT
CXCR3-/-
WT
CCR5 blocked
WT
CXCR3-/- with CCR5 block
WT

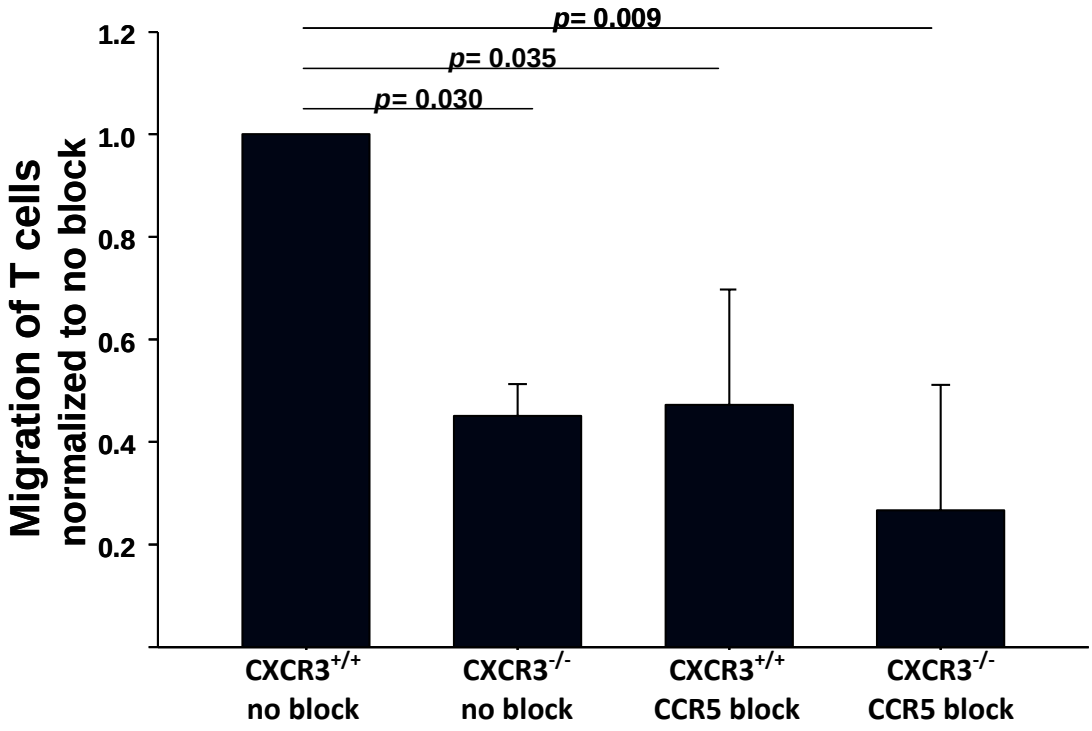
p= 0.009
p= 0.035
p= 0.030
Migration of T cells normalized to no block
1.2
1.0
0.8
0.6
0.4
0.2
CXCR3+/+ no block
CXCR3-/- no block
CXCR3+/+ CCR5 block
CXCR3-/- CCR5 block

CHAPTER IV. INFLUENZA-INDUCED EXPRESSION OF FUNCTIONAL TNF-RELATED APOPTOSIS-INDUCING LIGAND (TRAIL) ON HUMAN PBMC

Abstract

The immunological response to influenza virus infection, like many other viruses, is characterized by robust production of proinflammatory cytokines, including type I and II interferon (IFN), which induce a number of antiviral effects and are essential for priming the innate and adaptive cellular components of the immune response. Here, we demonstrate that influenza virus infection induces the expression of functional TRAIL on human peripheral blood mononuclear cell (PBMC) populations. Consistent with previous studies examining TRAIL upregulation, increased TRAIL expression correlated with increased type I and II IFN levels in PBMC cultures. Interestingly, dilution of these cytokines resulted in decreased expression of TRAIL, TRAIL upregulation was not dependent on active viral infection, and TRAIL was observed on NS-1 negative cells. Furthermore, influenza virus infection of lung adenocarcinoma cells (A549) resulted in increased sensitization to TRAIL-induced apoptosis compared to uninfected A549. Infected PBMC expressing TRAIL preferentially killed infected A549, while not affecting uninfected cells, and the addition of soluble TRAIL-R2:Fc blocked the lysis of infected cells, demonstrating TRAIL-dependent killing of infected cells. Collectively, these data show that TRAIL expression is induced on primary human innate and adaptive immune cells in response to cytokines produced during influenza infection, and that TRAIL-sensitivity is increased in influenza virus-infected cells. These data also suggest that TRAIL is a primary mechanism used by influenza-stimulated human PBMC to kill influenza-infected target cells and reinforce the importance of cytokines produced in response to TLR agonists in enhancing cellular immune effector functions.

Introduction

Influenza virus infection of the respiratory tract induces both innate and adaptive immune responses that are targeted to control and eliminate the viral infection. Studies investigating the protective immunity induced by primary influenza virus infection revealed that the clearance of infected epithelial cells by $CD8^+$ T cells utilizes either Fas or perforin-dependent direct killing mechanisms (65-67). These $CD8^+$ T cells first appear in the lung around day 4-post infection (57, 68, 69), where their continued expansion and accumulation correspond with virus clearance (69). Interestingly, in a subset of animals deficient in both perforin and Fas, decreased influenza virus titers were observed on day 14 relative to day 10 post infection (67), suggesting the existence of an additional mechanism by which $CD8^+$ T cells kill influenza-infected target cells.

In addition to the Fas-FasL and perforin-granzyme B pathways for killing, $CD8^+$ T cells can also utilize a TNF-related apoptosis-inducing ligand (TRAIL)/TRAIL-receptor dependent mechanism to eliminate virally-infected cells (92, 152-156, 197). TRAIL is one of several TNF family members capable of inducing apoptosis (83, 84), and does so in humans through interactions with TRAIL-R1 or -R2 (198). Subsequent to their ligation, both TRAIL-R1 and –R2 stimulate apoptosis through Fas-associated death domains (FADD) recruitment to the trimerized receptor and caspase activation (198). While TRAIL has received great attention in cancer therapy contexts because it selectively induces apoptosis in tumor cells but not normal cells, it is also proving to be a potent inducer of apoptosis in virally-infected cells that are normally TRAIL-resistant when uninfected (92, 152, 197).

More recent reports have implied roles for TRAIL in the immune response to influenza virus infection. A plasmacytoid dendritic cell (pDC) cell line (GEN2.2) showed marked upregulation of TRAIL, as well as increased sensitivity to TRAIL, following influenza virus infection (175). Additionally, primary human macrophages infected with H5N1 or H9N2 influenza virus strains upregulate TRAIL expression and

are able to induce apoptosis in Jurkat T cells using a TRAIL-dependent mechanism (177). The importance of TRAIL in the elimination of influenza virus has been suggested in an animal model where administration of a blocking anti-TRAIL mAb significantly delayed clearance of influenza virus in the lungs (Figure 5) (91). This study also demonstrated that TRAIL expression was increased on a fraction of bulk $CD8^+$ and bulk $CD4^+$ T cells, as well as NK cells, following influenza virus infections. Together, these results suggest a possible role for TRAIL-dependent apoptosis of virus-infected cells following influenza virus infections. However, none of these studies have directly examined TRAIL expression on primary human cells that comprise the innate and adaptive cellular immune response to influenza virus infection.

Based on these previous studies, we hypothesized that human peripheral blood mononuclear cells (PBMC) would respond to influenza *in vitro* by increasing TRAIL expression and show enhanced TRAIL-specific killing. Our data demonstrate that TRAIL expression is upregulated on multiple PBMC populations in response to influenza virus stimulation, and this upregulation is dependent on cytokines produced in response to influenza virus infection or in response to stimulation with the influenza virus genome, but is not dependent on direct infection of the TRAIL-expressing cells. Importantly, our data also show for the first time that TRAIL sensitivity is increased in alveolar epithelial cells infected with influenza virus, as demonstrated with either recombinant TRAIL or TRAIL-expressing, influenza-stimulated PBMC populations. Our findings suggest that TRAIL-induced apoptosis is an additional effector pathway utilized by the cellular immune response to influenza virus infections, and that sensitivity to TRAIL-induced apoptosis is specifically increased in influenza-infected cells compared with uninfected cells.

Materials and Methods

Reagents and mAb

Reagents and sources were as follows: UCHT1, FITC-conjugated IgG1 anti-human CD3; M5E2 (eBioscience, San Diego, CA), FITC-conjugated IgG2a anti-human CD14 (BD Bioscience, San Diego, CA); HIB19, FITC-conjugated IgG1 anti-human CD19 (eBioscience); NCAM16.2, FITC-conjugated IgG2b anti-human CD56; RIK-2, IgG1 anti-human TRAIL (a gift from Dr. H. Yagita, Juntendo University, Tokyo, Japan); IgG1-biotin isotype control (Caltag Laboratories, Inc., Burlingame, CA); 4SB3, PE-conjugated IgG1 anti-human IFN-γ (BD Bioscience, San Diego, CA); IgG1-PE isotype control (Caltag Laboratories, Inc., Burlingame, CA); 1A7, mouse anti-NS1 (a gift from Dr. Jonathan Yewdell, NAIAD); and APC-labeled goat $F(ab')^2$ anti-mouse IgG (Caltag Laboratories, Inc., Burlingame, CA). The soluble fusion proteins TRAIL-R2:Fc and Fas:Fc were purchased from Alexis Biochemicals (San Diego, CA). CpG ODN 2216 (ggGGGACGATCGTCgggggG) was synthesized by Sigma Genosys (The Woodlands, TX), and the sequence is 5′-3′, lower case letters are 5′ of phosphothiorate linkages, and upper case letter are 5′ of phosphodiester linkages. Poly I:C and ssRNA/LyoVec [a single-stranded GU-rich oligonucleotide (5′GCCCGUCUGUUGUGUGACUC-3′ with all phosphothioate linkages) complexed with LyoVec] were purchased from Invivogen (San Diego, CA).

Virus preparation

Influenza A viruses A/PuertoRico/8/34 (PR8; H1N1) was grown in the allantoic fluid of 10 d old embryonated chicken eggs for 2 d at 37°C, as previously described (69). Allantoic fluid was harvested and stored at -80°C. For UV inactivation, virus preparations were dialyzed overnight and subsequently exposed to UV lamp at 15cm for 30 minutes at room temperature.

Tumor cell lines

The human melanoma cell line WM 793 was obtained from Dr. M. Herlyn (Wistar Institute, Philadelphia, PA), and cultured in Dulbecco's modified Eagle's medium (DMEM) supplemented with 10% fetal bovine serum, penicillin, streptomycin, sodium pyruvate, non-essential amino acids, and HEPES (hereafter referred to as complete DMEM). The human lung adenocarcinoma cell line A549 was purchased from ATCC (Manassas, VA) and cultured in RPMI-1640 supplemented as above (complete RPMI).

Isolation of influenza genome

Samples of stock virus were spun twice (3000 rpm for 10 min at 4°C) to remove debris. Supernatants were collected and then spun in an ultracentrifuge to pellet virions (27,000 rpm for 3 h at 4°C in a SW60 rotor). Virions were lysed in detergent (Igepal/Triton X100/PBS) by passing through a syringe and suspended in TRIZOL (Invitrogen, Carlsbad, CA) at a 2:1 TRIZOL:detergent ratio. RNA was then harvested according to manufacturer's protocol.

Preparation of PBMC

PBMC were isolated from normal, healthy donors by standard density gradient centrifugation over Ficoll-Paque Plus (Pharmacia, Uppsala, Sweden). PBMC (5×10^6 cells/2 ml/well in a 6 well plate) were cultured in complete RPMI 1640 alone or in complete RPMI containing CpG ODN (1 μg/ml), poly I:C (1 μg/ml), ssRNA (1 μg/ml) for 24 h. PBMC infection with influenza (1 pfu/cell) was performed by first incubating the cells with virus in PBS on ice for 30 min, then at 37°C for 30 min. Cell were washed twice with PBS, and then cultured for 24 h in complete RPMI. In some experiments, PMBC were infected using the protocol described, then decreasing numbers of infected or uninfected cells were cultured in equivalent volumes of media. In some experiments, plasmacytoid DC (pDC) were depleted from the PBMC using the CD304 (BDCA-

4/Neutropilin-1) microbead kit (Miltenyi Biotec, Auburn CA). pDC depletion was verified by measuring the presence of $CD123^+CD303^+$ (BDCA-2) cells in the PBMC using FITC-conjugated anti-CD123 and PE-conjugated anti-CD303 mAb (Miltenyi Biotec). In every experiment, there were no detectable $CD123^+CD303^+$ cells remaining in the PBMC.

PBMC culture and supernatant transfer

PBMC were depleted of pDC, infected with influenza virus (or not infected), and cultured as described above at a cell density of 10^6 cells/well in 1 ml media. After 24 h, supernatants from infected cultures were collected and transferred to freshly-isolated uninfected PBMC. After another 24 hour culture, the PBMC were harvested and analyzed by flow cytometry as described below. In some cultures, IFN-α and/or IFN-γ were neutralized using 1μg/ml anti-IFN-α (PBL Biomedical, Piscataway, NJ) or 5μg/ml anti-IFN-γ (R&D Systems, Minneapolis, MN) Ab or isotype control Ab for 30 min prior to supernatant transfer. As a positive control for inducing TRAIL expression, uninfected PBMC were treated with 500ng/ml IFN-α (Cell Signaling Technologies, Danvers, MA) for 24 h.

Flow cytometry

Cell analysis was performed on a FACScan (Becton Dickinson, San Jose, CA) with $>10^4$ cells analyzed per sample. For multi-color cell analysis, cells were combined in a 96-well round-bottom plate with 2 μl each of the direct FITC-labeled and biotin-labeled mAb and then incubated at 4°C for 30 min. Following three washes with PBS containing 2 mg/ml BSA and 0.02% NaN_3 (FACS buffer), 40 μl of PE-labeled streptavidin (1:100 dilution; Caltag Laboratories) was added for an additional 30 min. Cells were either analyzed immediately or fixed in 2% paraformaldehyde until analysis. For intracellular stain of NS1 protein, cells were labeled with surface markers as described, fixed in 2% paraformaldehyde, permeabilized in FACS buffer with 0.5% saponin, and incubated with

anti-NS1 or isotype control at 4°C for 30 min. Following three washes with FACS buffer with saponin, 2 μl of APC-labeled anti-mouse IgG was added for an additional 30 min. Cells were either analyzed immediately or fixed in 2% paraformaldehyde until analysis. For intracellular cytokine staining for IFN-γ, brefeldin A was added to the last 5 h of the 24 h cell culture after influenza infection or TLR stimulation; subsequently, cells were labeled with surface markers as described, fixed in 2% paraformaldehyde, permeabilized in FACS buffer with 0.5% saponin, and incubated with anti-IFN-γ or isotype control at 4°C for 30 min. Cells were either analyzed immediately or fixed in 2% paraformaldehyde until analysis.

PBMC-mediated killing

Unstimulated or stimulated PBMC were cultured as described above. WM 793 tumor cells were labeled with 100 μCi of ^{51}Cr for 1 h at 37°C, washed three times, and resuspended in complete medium. To determine TRAIL-induced death, ^{51}Cr-labeled tumor cells (10^4/well) were incubated with varying numbers of effector cells for 14 h. In some cultures, TRAIL-R2:Fc or Fas:Fc (20 μg/ml) were added to the PBMC 15 min prior to adding tumor cell targets. All cytotoxicity assays were performed in 96-well round-bottom plates and the percent specific lysis was calculated as: 100 X (experimental c.p.m. - spontaneous c.p.m.)/(total c.p.m. - spontaneous c.p.m.). Spontaneous and total ^{51}Cr release were determined in the presence of either medium alone or 1% NP-40, respectively. The presence of TRAIL-R2:Fc or Fas:Fc during the assay had no effect on the level of spontaneous release by the targets.

IFN-α and IFN-γ ELISA

Human IFN-α and –γ protein levels produced after influenza virus infection or TLR agonist stimulation were quantified using a sandwich ELISA purchased from R&D Systems (Minneapolis, MN).

Statistics

Statistical analysis was performed using ANOVA to assess differences among the study groups using SigmaStat 3.5 (Systat Software, Richmond, CA), and statistical significance was determined as $p \leq 0.05$.

Results

Influenza virus infection of human PBMC induces the expression of functional TRAIL

Influenza virus infection induces a robust inflammatory reaction, hallmarked by the production of the anti-viral cytokines type I and type II interferon (IFN) (197, 199, 200). The *TRAIL* promoter contains IFN-response elements, resulting in the IFN-driven expression of TRAIL on multiple human PBMC populations (197, 201). Thus, our initial experiments were designed to examine TRAIL expression on human PBMC after influenza virus infection. Peripheral blood T cells ($CD3^+$), Mϕ ($CD14^+$), B cells ($CD19^+$), and NK cells ($CD56^+$) can express functional TRAIL (118, 120, 184); thus, these populations within bulk PBMC were examined by two-color flow cytometry for TRAIL expression 24 h after influenza virus infection. When infected, TRAIL expression was observed on all four major PBMC populations (Figure 26A).

Concurrent experiments were performed to determine whether the TRAIL expressed on the influenza-infected cells was functional. Thus, human PBMC were isolated from normal healthy volunteers and infected with influenza. After culturing for 24 h, the PBMC were then incubated with the TRAIL-sensitive human melanoma tumor cell line WM 793 (123). The uninfected PBMC demonstrated minimal cytotoxic activity toward WM 793, whereas influenza-infected PBMC were efficient killers of these TRAIL-sensitive target cells over a range of effector-target cell ratios (Figure 27A). These data were reproducible using PBMC from multiple donors. To confirm that the observed PBMC cytotoxic activity was indeed TRAIL-dependent, influenza-infected

PBMC were incubated with either TRAIL-R2:Fc (117) or Fas:Fc prior to their incubation with the target cells. Under these conditions, TRAIL-R2:Fc reduced target cell death to control (uninfected PBMC effectors) levels, whereas Fas:Fc did not inhibit the ability of the influenza-infected PBMC to mediate target cell lysis (Figure 27A). Similar results were also observed when infecting the PBMC with UV-inactivated influenza (Figures 26B & 27B), indicating that infection with a replication-competent influenza virus was not required to induce TRAIL expression. Collectively, these results demonstrate that PBMC mediate TRAIL-induced cell lysis following influenza virus infection.

Nucleic acid TLR agonists induce functional TRAIL expression on PBMC

The Toll-like receptors (TLR) serve as first-line receptors for innate immune cell detection of pathogenic infections by recognizing conserved molecular motifs, which are known as pathogen-associated molecular patterns (PAMPs) (2, 202). Ten human TLR have been identified that recognize unique PAMPs from bacteria, viruses, fungi, and protozoa. Viruses that enter endocytic compartments, such as influenza, are recognized by TLR3 (specific for double-stranded RNA (dsRNA)), TLR7 (specific for single-stranded RNA (ssRNA)), and TLR9 (specific for CpG motifs in unmethylated DNA) (2, 202). With this in mind, we next tested the ability of TLR3 (poly I:C), TLR7 (ssRNA), and TLR9 (CpG ODN) agonists to induce TRAIL on PBMC. PBMC stimulation with either the poly I:C or ssRNA led to TRAIL upregulation on multiple PBMC populations, with $CD14^+$ Mϕ showing the highest increase in expression (Figure 26C & D). The broad expression of TRAIL induced by poly I:C and ssRNA also resulted in substantial target cell lysis that was completely inhibited upon inclusion of soluble TRAIL-R2:Fc, but not Fas:Fc (Figure 27C & D). Consistent with previous reports from our laboratory (182, 203), CpG ODN was a potent inducer of TRAIL on all four PBMC populations examined (Figure 26E), resulting in TRAIL-specific cytotoxic activity (Figure 27E).

Stimulation with influenza genome is sufficient to induce TRAIL expression on PBMC

In vitro influenza infection of PBMC could stimulate TRAIL upregulation through a number of different mechanisms. To determine the ability of influenza virus genome to stimulate TRAIL induction, the genetic material from UV-inactivated influenza was isolated and used to stimulate PBMC. The influenza ssRNA genome was a competent TRAIL-inducing agent, as TRAIL was expressed on T cells (Figure 28A), as well as other PBMC populations, following 24 h culture with influenza RNA mixed with DOTAP. In contrast, stimulation of PBMC with influenza proteins was not sufficient to induce TRAIL expression. Interestingly, an examination of TRAIL expression coincidental with influenza virus proteins revealed that TRAIL expression was not dependent on direct infection of the TRAIL-expressing cell, as populations of NS1-negative $CD3^+$, $CD14^+$, and $CD56^+$ cells expressed TRAIL (Figure 28B). Thus, these results demonstrate that upregulation of functional TRAIL on multiple PBMC populations occurs in response to stimulation with the influenza virus genome, but this upregulation is not dependent on direct infection of the TRAIL-expressing cell.

Influenza stimulates IFN-α and -γ production, which induces TRAIL expression on human PBMC

A large proportion of the signaling events in influenza-infected cells, be it epithelial cells or antigen presenting cells, is geared toward the generation of cellular responses designed to limit or prevent the spread of the invading virus in the tissue and the establishment of a persistent infection. A major part of this antiviral response is mediated by the expression and secretion of IFN-α and -γ (199, 200). The recognition of viral components, particularly the viral genetic material, directly triggers signaling pathways that induce IFN-α production (2, 199)**,** as well as production of IFN-γ (200). Thus, we measured the amount of IFN-α and -γ in the supernatants of PBMC stimulated

with influenza or the TLR agonists used in Figures 26 and 27. Our analysis revealed that influenza-infected human PBMC produced ~1500 and 1000 pg/ml IFN-α and IFN-γ, respectively (Figure 29A). As predicted, CpG ODN-stimulated PBMC only produced IFN-α. Stimulation with ssRNA only led to measurable levels of IFN-γ, which is consistent with previous reports (28). This lack of IFN-α production might be explained by the lack of TLR8 on plasmacytoid DC (pDC), which is the human TLR targeted by the ssRNA/LyoVec used. Stimulation of PBMC by poly I:C produced low, but measurable amounts of both IFN-α and –γ. All of these levels of IFN are well within the range of concentrations (100 ng/ml – 10 pg/ml) that induce TRAIL expression on human PBMC (184). Plasmacytoid DC (pDC) are the predominant cell within the peripheral blood to produce type-I IFN (204-208). Depletion of pDC substantially decreased the amount of IFN-α produced by PBMC after influenza virus infection (as well as CpG stimulation), but did not alter IFN-γ production, suggesting that pDC are the sole source of IFN-α after influenza virus stimulation (Figure 29B). Additionally, intracellular cytokine staining revealed that T cells, Mϕ, and NK cells produced IFN-γ after influenza virus stimulation (Figure 29C). Together, these data demonstrate that influenza virus infection of PBMC stimulates multiple cell types to produce type I and II IFN.

Interferon stimulation, not direct infection, causes TRAIL upregulation

While the upregulation of TRAIL in response to stimulation by type I and II IFN has been widely described in tumor models (118, 120, 209) the mechanism of induction in viral systems has not been well-characterized. Examining the coexpression of TRAIL with NS1 demonstrated that a population of PBMC expressed TRAIL that did not have detectable levels of NS1 (Figure 28B), indicating direct infection was not necessary for a cell to express TRAIL. To determine the relative importance of cytokine action on cells versus infection, PBMC were infected as described previously, but the infected cells were

then split into cultures containing decreasing numbers of cells in an equivalent volume. As expected, diluting the number of cells in equivalent volumes of culture media caused a cell number-dependent decrease in IFN-α (Figure 30A) detected in the cultures. Interestingly, the decreased IFN correlated with decreased TRAIL expression on the $CD56^+$ populations (Figure 30B), as well as other PBMC populations. To verify that TRAIL expression was driven by interferon stimulation, supernatants from influenza-infected PBMC cultures were transferred to uninfected cells. As expected, transfer of supernatant from influenza-infected PBMC cultures lead to TRAIL upregulation by uninfected $CD56^+$ cells (Figure 30C) as well as other PBMC populations. When anti-IFN-α and anti-IFN-γ neutralizing antibodies were added to the supernatants prior to transfer, the supernatants failed to induce TRAIL expression on the uninfected PBMCs while supernatants treated with isotype control antibodies stimulated TRAIL upregulation (Figure 30D). Interestingly, neutralization of both IFN-α and IFN-γ was required to ablate TRAIL expression, as only blocking IFN-α or IFN-γ resulted in TRAIL upregulation. Together, these data demonstrate that the upregulation of TRAIL on PBMC is induced by IFN-α and IFN-γ signaling rather than direct infection of the cells.

Influenza-stimulated PBMC utilize TRAIL to kill influenza-infected lung cells, but not uninfected cells

Epithelial cells derived from multiple organs can be sensitized to TRAIL-mediated apoptosis after viral infection. We hypothesized that TRAIL plays an important role in the elimination of influenza-infected lung epithelial cells, and the aforementioned results clearly demonstrate that influenza-stimulated PBMC gain TRAIL-mediated cytotoxic activity. Thus, the following experiments were performed to investigate the other component to our hypothesis—i.e. the sensitization of influenza-infected human lung epithelial cells to TRAIL. We began our analysis by testing the responsiveness of the human lung adenocarcinoma cell line A549 to TRAIL before and after influenza virus

infection. As previously reported, uninfected A549 were not readily killed by recombinant TRAIL (152), but the cells displayed increased sensitivity after influenza virus infection (Figure 31A). Next, we examined the ability of influenza-stimulated PBMC to kill influenza-infected A549. Uninfected target cells were killed at similar levels by both unstimulated and influenza-stimulated PBMC (Figure 31B). However, a significant increase in the lysis of infected target cells by influenza-stimulated PBMC was observed ($p < 0.05$). Further analysis found that the addition of soluble TRAIL-R2:Fc blocked target cell lysis (Figure 31C), whereas the addition of Fas:Fc did not significantly inhibit killing, suggesting that TRAIL is the primary mechanism used by influenza-stimulated PBMC to kill influenza-infected target cells.

Discussion

Each year in the United States, approximately 36,000 people die from influenza virus infection, and more than 200,000 people are hospitalized from influenza complications (210). The World Health Organization estimates that ~5-15% of the entire global population are infected annually, with the elderly and very young most at risk for severe complications (211). Influenza virus infection is immunogenic, stimulating cytotoxic T cells (CTL) to kill infected airway epithelial cells that are primary targets of the influenza virus. Initial recognition of the viral infection by the innate immune system typically triggers an antiviral immune response. In particular, type I and type II IFN are key cytokines produced after influenza virus infection that help to activate the innate and adaptive immune responses (34). Among the multitude of events that occur after IFN stimulation, the acquisition of effector molecules on/in various immune cells is vital for controlling influenza virus infection and eliminating infected cells. To our knowledge, our data show for the first time that human PBMC stimulated with influenza virus upregulate TRAIL, and that these TRAIL-expressing cells have enhanced ability to kill

influenza-infected cells. These observations expand the number of known effector molecules utilized by human immune cells to eliminate influenza virus.

Influenza is a ssRNA virus that infects both the upper and lower respiratory tracts of humans. While various components of the viral coat are strong antigens that can be recognized by the adaptive immune system, the single-stranded RNA (ssRNA) of the influenza genome is immunostimulatory and is initially recognized by the host pattern-recognition receptors that stimulate the production of IFN (212). TLR3 expressed in pulmonary epithelial cells can recognize the dsRNA intermediate produced during viral replication and mRNA synthesis (213-215), resulting in the production of a number of proinflammatory cytokines by bronchial epithelial cells. Additionally, the RNA helicase RIG-I recognition of single-stranded viral genomic RNA bearing a 5'triphosphate end activates type I IFN production (29). This recognition is blocked by the influenza NS1 protein (216, 217), which binds to dsRNA and inhibits various antiviral pathways in infected cells (218). Despite this interference, innate and adaptive immune cells can still respond to influenza by producing IFN-α through TLR7 recognition of ssRNA. Within the blood, pDC express TLR7, and secrete large amounts of IFN-α in response to viral infection (219). The IFN-α produced by pDC upon viral stimulation is critical in the subsequent response of T cells, NK cells, and other DC to the virus.

Our results show that both IFN-α and –γ are produced by human PBMC after influenza virus infection. In our in vitro infection system, the pDC are the primary source of IFN-α, while T cells, monocytes, and NK cells are responsible for IFN-γ production. This observation is consistent with recent report underscoring the role of pDCs as the respiratory DC subset responsible for producing IFN-α and other cytokines in response to influenza virus infection (220). Interestingly, these observations conflict with a recent study of IFN-α production after infection with RNA-viruses, which concluded that alveolar macrophages and conventional DC—but not pDCs—are the primary producers of IFN-α in response to RNA-virus infection (221). While Kumagai

and colleagues convincingly demonstrated that pDCs played a minimal role in IFN-α production to Newcastle disease virus and Sendai virus, their study did not examine the immune response to influenza virus. Taken together, these studies support the notion that immune responses to similar pathogens can be induced by unique mechanisms; further, they reinforce the need to determine the relative contributions of alveolar macrophages and DC subsets during the *in vivo* immune response to influenza virus infection.

Among the multitude of IFN-responsive genes present in human PBMC, the observed induction of TRAIL expression occurs rapidly. The human TRAIL promoter contains multiple transcriptional binding elements, including an IFN sensitive response element (201, 222). Furthermore, human T cells, B cells, NK cells, Mϕ, and DC all can be induced to express TRAIL by IFN (either type I or II IFN) (118, 120, 184, 203, 223). We observed functional TRAIL expressed on multiple PBMC populations after influenza virus infection; further, these cells could kill influenza-infected target cells *in vitro*. This TRAIL expression is dependent on cytokine signaling rather than on direct infection, as cells given equivalent infections showed decreasing levels of TRAIL expression when cell number and cytokine levels were diluted. Furthermore, blocking IFN signals (by pDC depletion and blocking mAb) resulted in lack of TRAIL upregulation in cells stimulated with supernatants from influenza-infected cultures, while transfer of non-blocked supernatants stimulated TRAIL expression. Based on these observations, we can easily speculate that many of the inflammatory cells responding to an influenza virus infection in the lungs will be induced to express TRAIL as they enter the IFN-rich pulmonary microenvironment or the draining lymph nodes where influenza antigens would be presented. Interestingly, animals infected with the influenza A from the 1918 pandemic showed aberrant IFN production and signaling (224) and disrupted expression of TRAIL message (181). These observations, coupled with the dysregulated IFN responses observed in H5N1 infections (178, 199, 225, 226), suggest that altered IFN

signaling and aberrant TRAIL upregulation during the immune response to highly pathogenic influenza strains might contribute to the pathogenicity of these infections.

Many viruses have a substantial impact on host cell metabolism; hence, it might be predicted that cells infected with viruses acquire sensitivity to TRAIL. In addition to the Fas/FasL and perforin:Granzyme B pathways for killing, $CD8^+$ T cells can also utilize a TRAIL/TRAIL receptor-dependent mechanism to induce apoptosis of infected cells during viral infections. TRAIL induces apoptotic cell death (83-85, 227) by recruiting and aggregating caspase 8 upon binding to either TRAIL-R1 or -R2 (85, 86, 89, 228). This aggregation in turn leads to a caspase cascade and eventually to apoptotic death of the TRAIL-R1/-R2-expressing cell (85, 86, 198, 228). Importantly, TRAIL is upregulated on $CD8^+$ T cells, $CD4^+$ T cells, and NK cells following virus infection (91, 92, 197) or during inflammatory responses marked by increases of IFNγ or TNFα (94, 197). In turn, normal cells infected with RSV, human cytomegalovirus, or encephalomyocarditis virus become susceptible to TRAIL-mediated killing (152-154, 197), and IFN-γ and TNF can downregulate TRAIL receptor expression on uninfected cells (197). These previous reports are consistent with our results demonstrating enhanced killing of cells from influenza-infected cultures relative the killing of cells from uninfected cultures. Specifically, we found the TRAIL-resistant human lung adenocarcinoma cell line, A549, could be sensitized to TRAIL following influenza virus infection – much like that seen by Kotelkin et al. who showed that A549 could be rendered TRAIL sensitive after RSV infection (152).

Overall, our results demonstrate that TRAIL-induced apoptosis plays a key role in clearance of virus-infected cells. Understanding of the relative contributions of apoptosis-inducing ligands and other factors that determine the outcome of virus infection *in vitro and in vivo* will help design treatment strategies for highly-pathogenic viruses in which the balance of these contributions is disrupted. Interestingly, aberrant TRAIL signaling might contribute to viral pathology in highly-pathogenic infections

(101). Hence, treatment strategies of highly-pathogenic influenza viruses should seek to optimize TRAIL-induced viral clearance while minimizing the detrimental effects associated with highly-pathogenic infections.

Figure 26. TRAIL expression on human PBMC after influenza virus infection or TLR agonist stimulation. PBMC were infected with **(A)** viable or **(B)** UV-inactivated influenza (as described in the Materials and Methods) or stimulated with the TLR agonists **(C)** poly I:C, **(D)** ssRNA, or **(E)** CpG ODN. Surface TRAIL expression was analyzed 24 h later on $CD3^+$, $CD14^+$, $CD19^+$, and $CD56^+$ cells using two-color flow cytometry. Representative results are shown in histograms based on 10^4 gated cells in all conditions, and cell viability was >95%, as assessed by propidium iodide exclusion. Similar results were observed using at least 4 different PBMC donors.

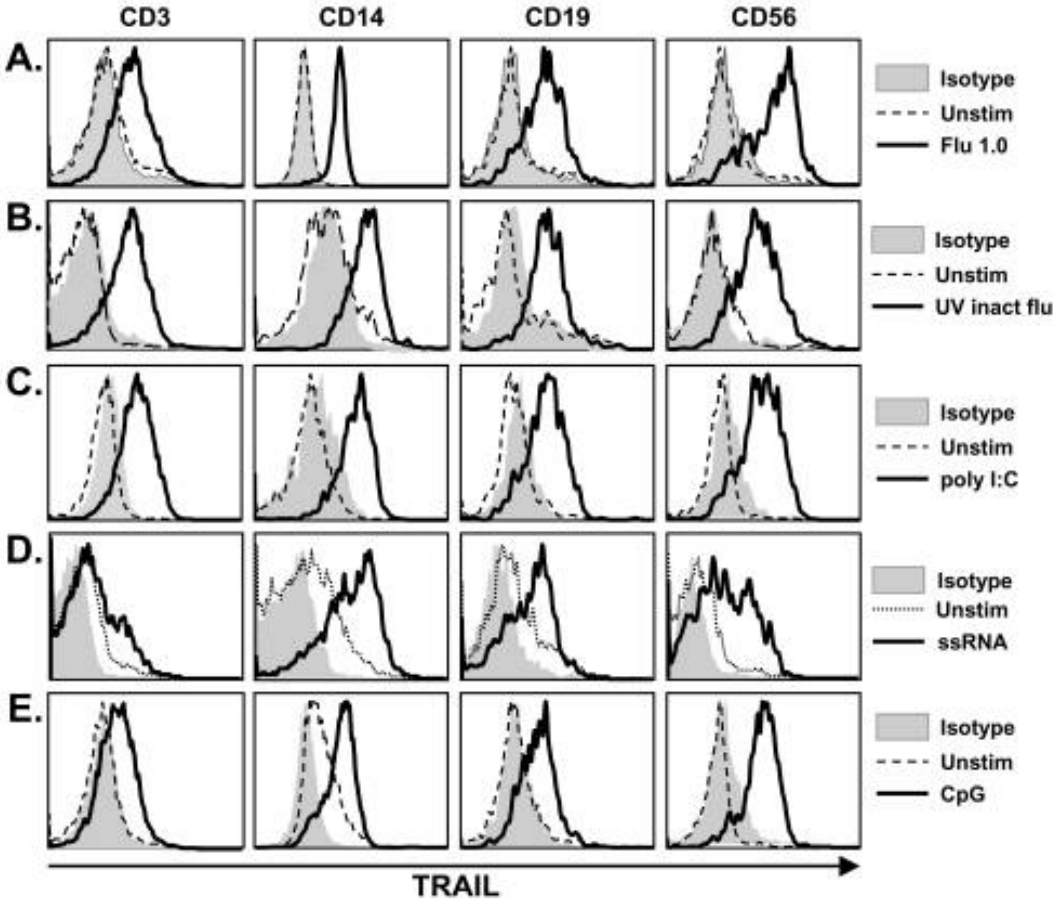
CD3
CD14
CD19
CD56
A.
B.
C.
D.
E.
Isotype
Unstim
Flu 1.0
Isotype
Unstim
UV inact flu
Isotype
Unstim
poly I:C
Isotype
Unstim
ssRNA
Isotype
Unstim
CpG
TRAIL

Figure 27. TRAIL-mediated cytotoxicity by human PBMC occurs after influenza virus infection or stimulation with TLR agonists. PBMC were infected with (A) viable or (B) UV-inactivated influenza (as described in the Materials and Methods) or stimulated with the TLR agonists (C) poly I:C, (D) ssRNA, or (E) CpG ODN. After 24 h, the PBMC were harvested and cultured for 14 h with ^{51}Cr-labeled WM 793 target cells at the indicated effector-target cell ratios. For each condition, TRAIL-R2:Fc (20 μg/ml) inhibited target cell killing, while Fas:Fc (20 μg/ml) did not. Data points represent the mean of triplicate wells, and experiments were repeated at least three times using different donor PBMC with similar results. For clarity, SD bars were omitted from the graphs, but were <10% of the value of all points.

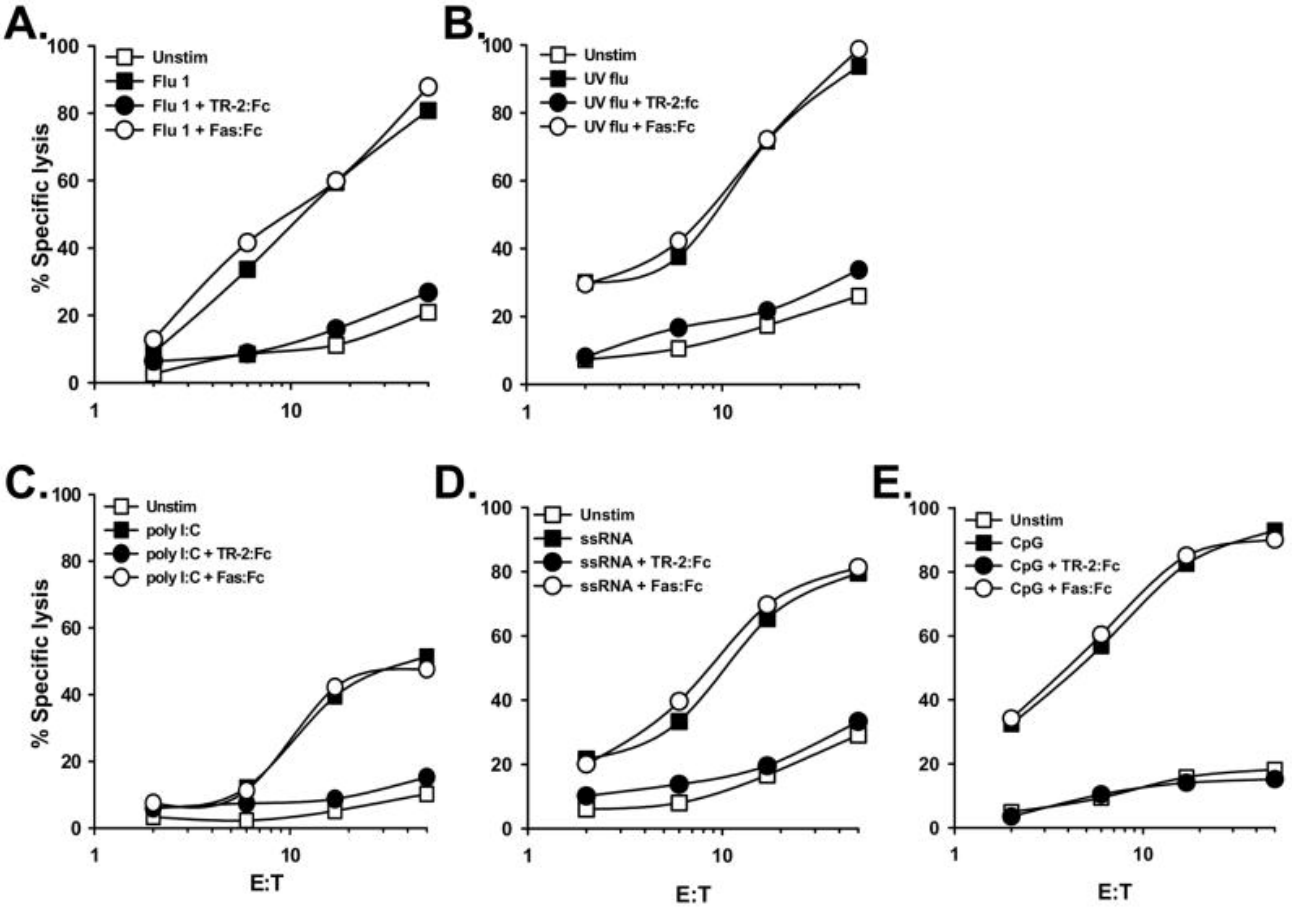
A.
Unstim
Flu 1
Flu 1 + TR-2:Fc
Flu 1 + Fas:Fc
% Specific lysis
B.
Unstim
UV flu
UV flu + TR-2:fc
UV flu + Fas:Fc
C.
Unstim
poly I:C
poly I:C + TR-2:Fc
poly I:C + Fas:Fc
% Specific lysis
E:T
D.
Unstim
ssRNA
ssRNA + TR-2:Fc
ssRNA + Fas:Fc
E:T
E.
Unstim
CpG
CpG + TR-2:Fc
CpG + Fas:Fc
E:T

Figure 28. Influenza RNA stimulates TRAIL expression on human T cells. (A) RNA was isolated from UV-inactivated influenza particles (as described in the Materials and Methods), and used to stimulate PBMC at the indicated concentrations. To facilitate uptake, RNA was mixed with DOTAP. As controls, PBMC were incubated with DOTAP alone or influenza RNA without DOTAP. After 24 h, cells were collected, and processed to examine TRAIL expression on $CD3^+$ T cells. Results are representative of 3 independent experiments using different donor PBMC. (B) PBMC were infected with influenza and cultured for 24 hours. Surface TRAIL expression and intracellular NS1 expression were analyzed on $CD3^+$, $CD14^+$, and $CD56^+$ cells using three-color flow cytometry. Representative results are shown in histograms based on 10^4 gated cells in all conditions, and cell viability was >95%, as assessed by propidium iodide exclusion. Similar results were observed using 2 different PBMC donors.

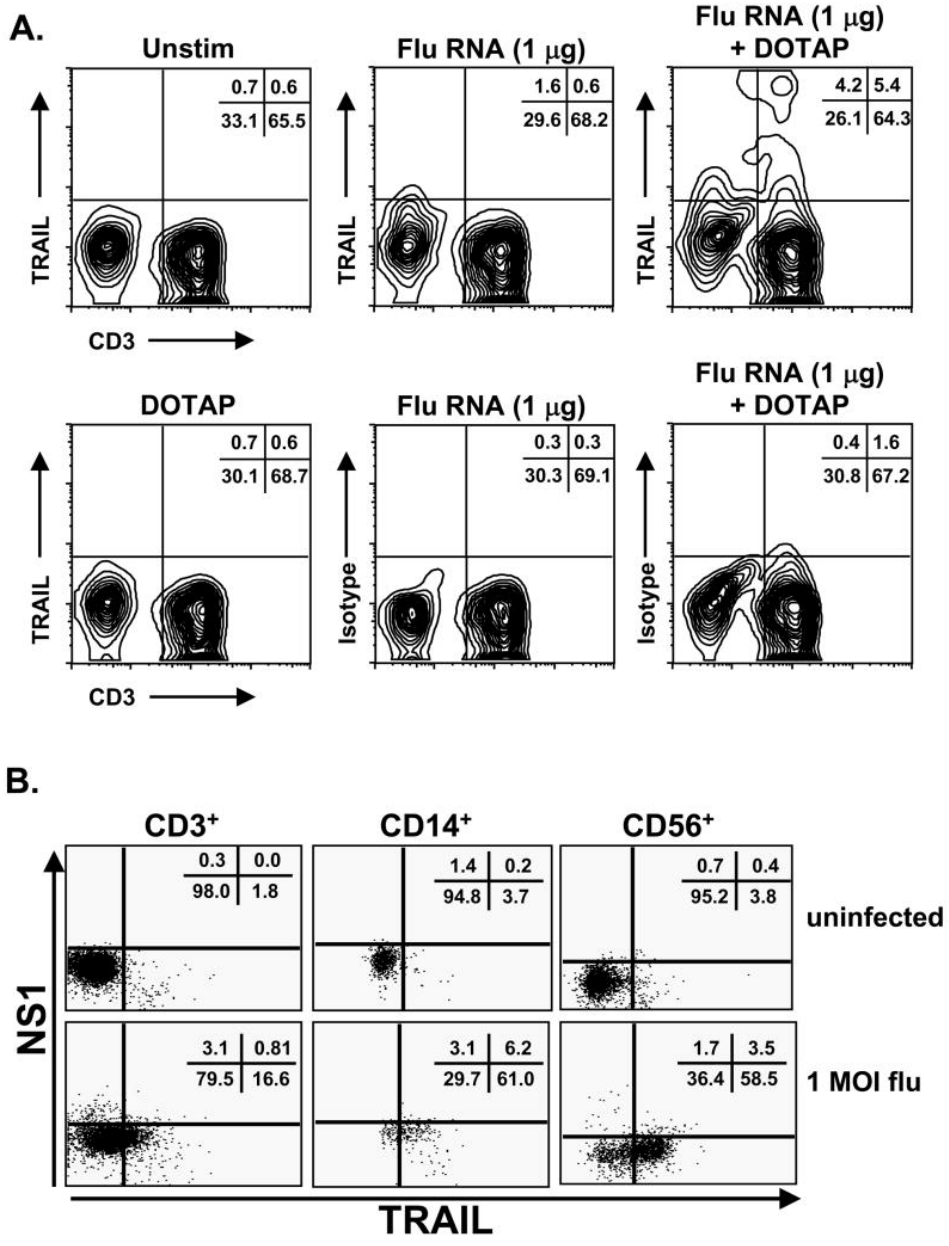
A.
Unstim
Flu RNA (1 μg)
Flu RNA (1 μg) + DOTAP
0.7 0.6
33.1 65.5
1.6 0.6
29.6 68.2
4.2 5.4
26.1 64.3
TRAIL
CD3
DOTAP
Flu RNA (1 μg)
Flu RNA (1 μg) + DOTAP
0.7 0.6
30.1 68.7
0.3 0.3
30.3 69.1
0.4 1.6
30.8 67.2
Isotype
B.
CD3+
CD14+
CD56+
0.3 0.0
98.0 1.8
1.4 0.2
94.8 3.7
0.7 0.4
95.2 3.8
uninfected
3.1 0.81
79.5 16.6
3.1 6.2
29.7 61.0
1.7 3.5
36.4 58.5
1 MOI flu
NS1
TRAIL

Figure 29. Influenza stimulates IFN-α and –γ production from PBMC. (A) PBMC were infected with viable or UV-inactivated influenza (UV-flu) or stimulated with the TLR agonists poly I:C, ssRNA, or CpG ODN. After 24 h, IFN-α and –γ levels were quantified in the culture supernatant by ELISA. Cytokine levels represent the average amount measured from at least four independent experiments using different donors. (B) IFN-α is made by pDC within PBMC after influenza virus infection. PBMC or PBMC depleted of pDC were infected with influenza. After 24 h culture, IFN-α and –γ levels in the culture supernatants were then determined by ELISA. Results represent the average amount measured from 3 independent experiments using different donors. (C) IFN-γ expression by PBMC after influenza virus infection or TLR agonist stimulation. PBMC were infected with viable influenza or stimulated with the TLR agonists poly I:C or ssRNA. Intracellular IFN-γ levels were analyzed 24 h later in $CD3^+$, $CD14^+$, and $CD56^+$ cells using two-color flow cytometry. Representative results are shown based on 10^4 gated cells in all conditions, and cell viability was >95%, as assessed by propidium iodide exclusion. Similar results were observed using at least 3 different PBMC donors.

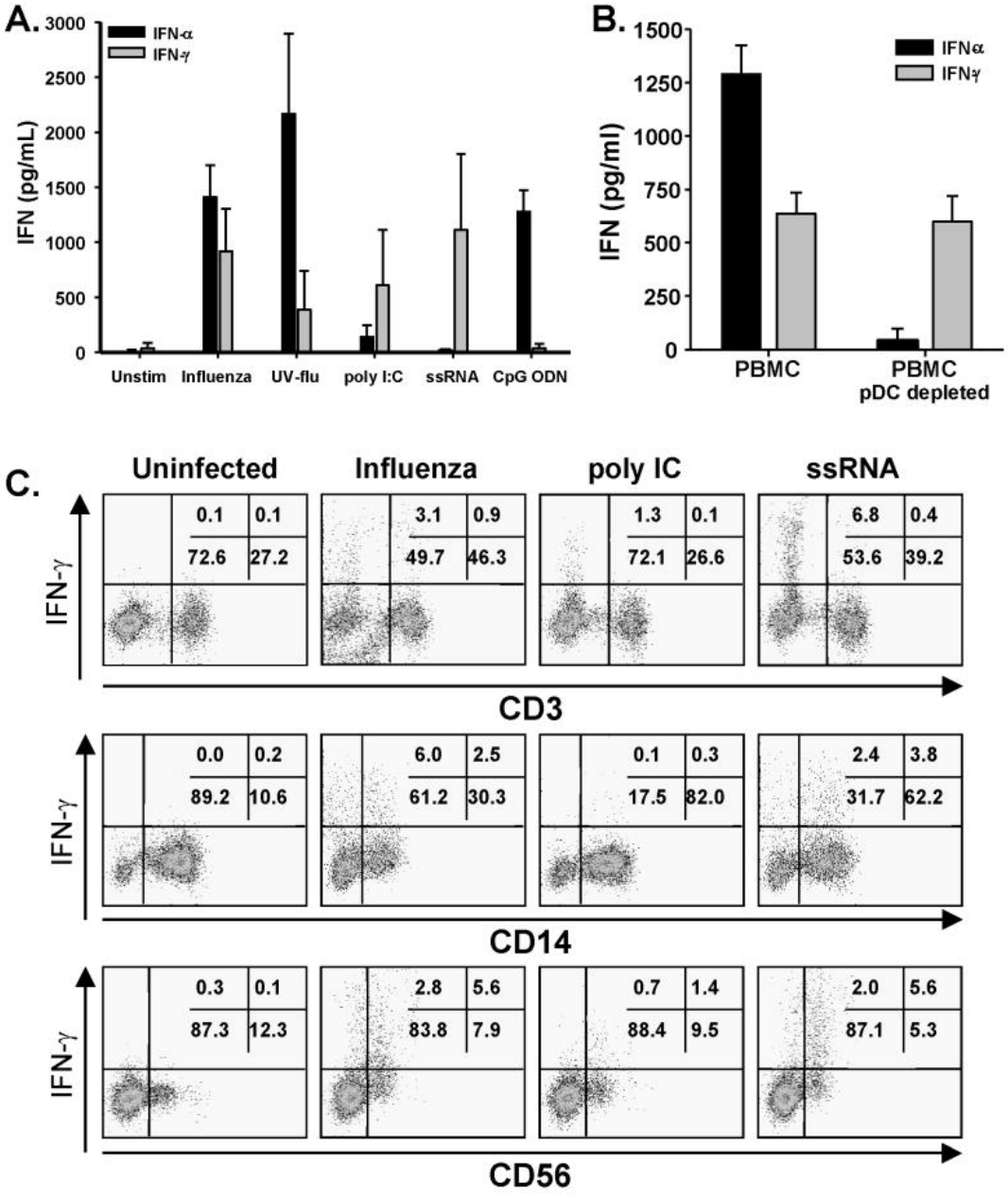
A.
IFN-α
IFN-γ
IFN (pg/mL)
3000
2500
2000
1500
1000
500
0
Unstim
Influenza
UV-flu
poly I:C
ssRNA
CpG ODN
B.
IFNα
IFNγ
IFN (pg/ml)
1500
1250
1000
750
500
250
0
PBMC
PBMC
pDC depleted
C.
Uninfected
Influenza
poly IC
ssRNA
IFN-γ
CD3
0.1 0.1
72.6 27.2
3.1 0.9
49.7 46.3
1.3 0.1
72.1 26.6
6.8 0.4
53.6 39.2
IFN-γ
CD14
0.0 0.2
89.2 10.6
6.0 2.5
61.2 30.3
0.1 0.3
17.5 82.0
2.4 3.8
31.7 62.2
IFN-γ
CD56
0.3 0.1
87.3 12.3
2.8 5.6
83.8 7.9
0.7 1.4
88.4 9.5
2.0 5.6
87.1 5.3

Figure 30. TRAIL induction is driven primarily by cytokines. (A) PBMC were infected with influenza. After infection, decreasing numbers of cells (10^6 – 1.25×10^5 cells) were aliquoted into 2 ml of media. After 24 h culture, IFN-α levels in the culture supernatants were determined by ELISA. Results represent the average amount measured from 2 independent experiments using different donors. * $p < 0.05$ compared to uninfected level. (B) After infection and 24 h culture (as described in 5A), PBMC from cell dilution cultures were analyzed for surface TRAIL expression on $CD3^+$ cells using two-color flow cytometry. Representative results are shown in histograms based on at least 5×10^3 gated cells. Similar results were observed using 2 different PBMC donors. (C) After infection and 24 h culture (as described in 5A), supernatants from 10^6-cell PBMC cultures were transferred to uninfected cells from the same donor. After 24 h incubation, TRAIL expression on uninfected cells (uninfected), uninfected cells with supernatants from influenza-infected cells (Flu sup), or receiving media plus IFN-α (IFN-α) was determined. Representative results for $CD3^+$ cells are shown in histograms based on at least 10^4 gated cells. Similar results were observed using 2 different PBMC donors. (D) PBMC were depleted of pDC, infected with influenza virus, and cultured for 24 h (as described in 5A). Supernatants from 10^6-cell cultures were incubated with an anti-IFN-γ neutralizing mAb, and then transferred to uninfected cells from the same donor. TRAIL expression on uninfected cells cultured with isotype or anti-IFN-γ mAb only, or in supernatants from influenza-infected cells treated with anti-IFN or isotype antibody. Representative results for $CD3^+$ cells are shown in histograms based on at least 10^4 gated cells. Similar results were observed using 2 different PBMC donors.

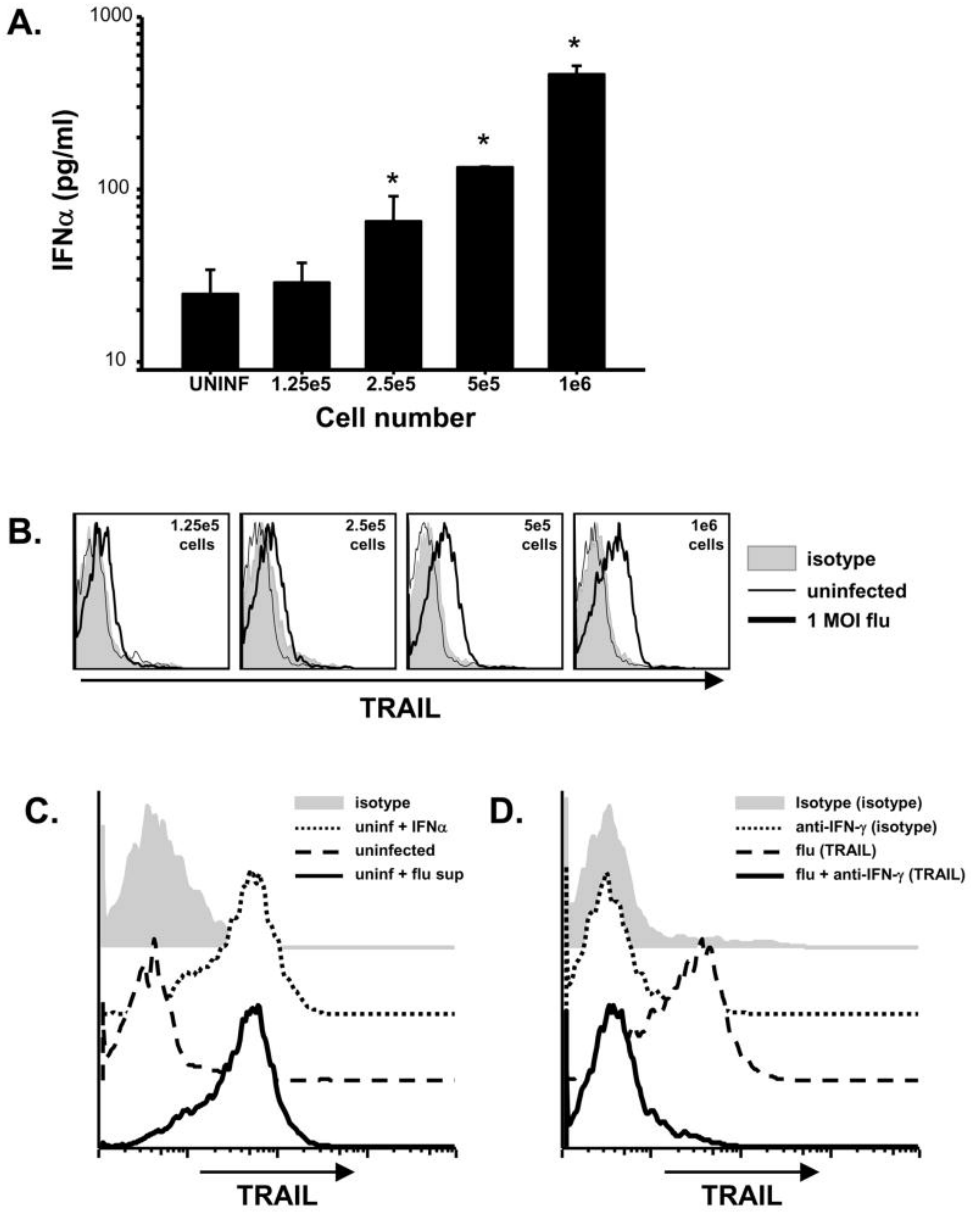
A.
1000
100
10
IFNα (pg/ml)
*
*
*
UNINF
1.25e5
2.5e5
5e5
1e6
Cell number
B.
1.25e5 cells
2.5e5 cells
5e5 cells
1e6 cells
isotype
uninfected
1 MOI flu
TRAIL
C.
isotype
uninf + IFNα
uninfected
uninf + flu sup
TRAIL
D.
Isotype (isotype)
anti-IFN-γ (isotype)
flu (TRAIL)
flu + anti-IFN-γ (TRAIL)
TRAIL

Figure 31. Influenza virus infection alters cell sensitivity to TRAIL. (A) The lung adenocarcinoma cell line, A549, was infected with influenza (1 MOI) for 24 h. The cells were then added to 96-well microtiter plates (4×10^5 cells/well) and cultured with increasing concentrations of recombinant TRAIL (rTRAIL) at the indicated concentrations. Cell death was measured 24 h later. Uninfected A549 cells were tested at the same time. Results are representative of 3 independent experiments, where each data point is the average of 3 wells. (B) Influenza-infected PBMC readily kill influenza-infected A549 cells, but not uninfected A549 cells. PBMC were infected with influenza. After 24 h, the PBMC were harvested and cultured for 14 h with ^{51}Cr-labeled uninfected or influenza-infected (1 MOI for 24 h) A549 target cells at the indicated effector-target cell ratios. (C) Inhibition of influenza-infected PBMC killing of influenza-infected A5499 target cells is blocked by TRAIL-R2:Fc (20 μg/ml), while Fas:Fc (20 μg/ml) did not significantly inhibit killing. The effector:target cells ratio was 50:1. Data points represent the mean of triplicate wells, and experiments were repeated at least three times using different donor PBMC with similar results. * $p < 0.05$.

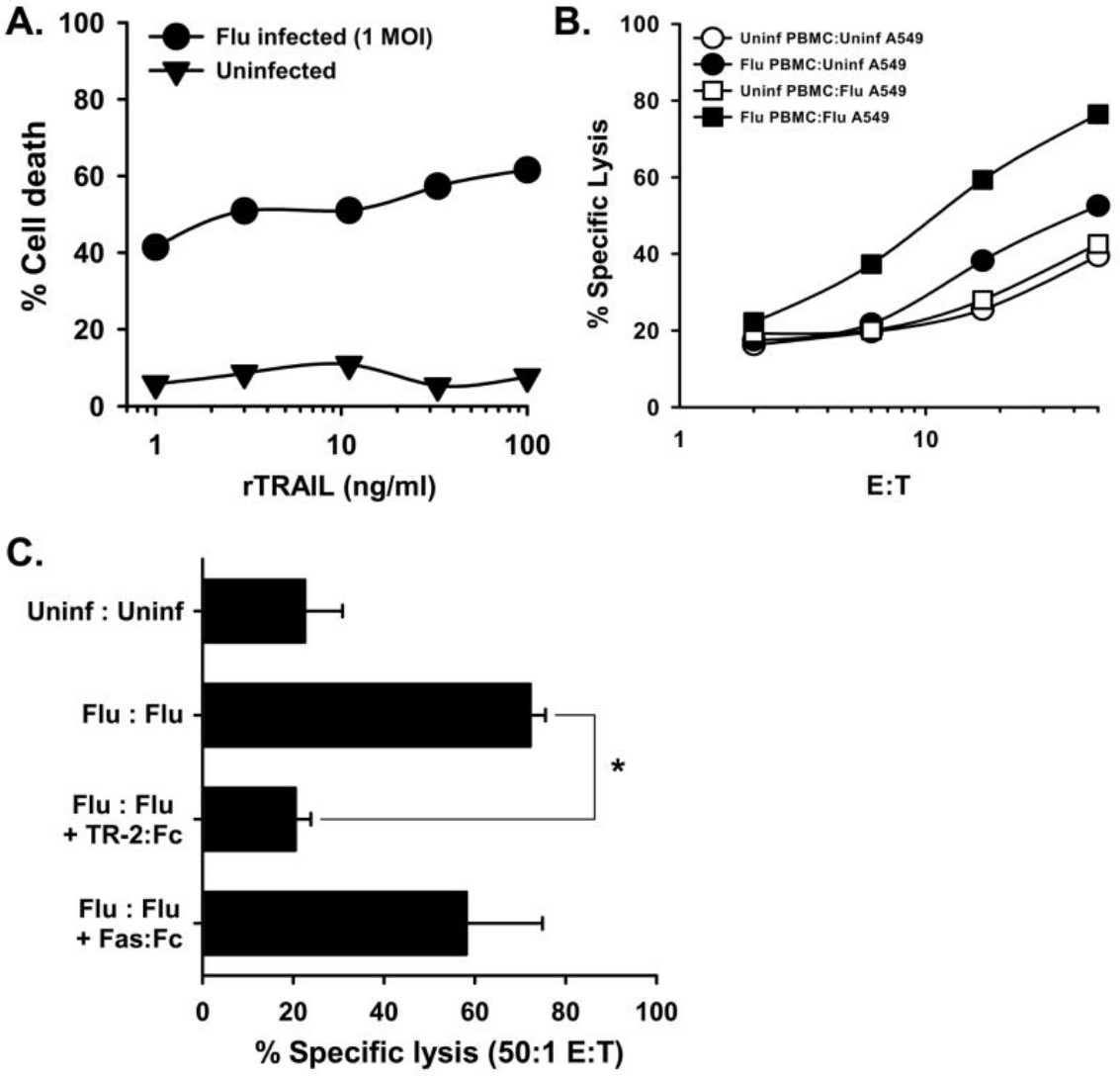
A.
Flu infected (1 MOI)
Uninfected
% Cell death
rTRAIL (ng/ml)
B.
Uninf PBMC:Uninf A549
Flu PBMC:Uninf A549
Uninf PBMC:Flu A549
Flu PBMC:Flu A549
% Specific Lysis
E:T
C.
Uninf : Uninf
Flu : Flu
Flu : Flu
+ TR-2:Fc
Flu : Flu
+ Fas:Fc
*
% Specific lysis (50:1 E:T)

CHAPTER V: DISCUSSION

Regarding Scientific Discoveries

Among the many aims of science is to find models that account for observations, place these observations into a coherent framework, and to use this framework to make predictions of future events. The historian and philosopher Thomas Kuhn examined the history of science in his scholarly essay *The Structure of Scientific Revolutions*, in which he attempted to examine the practice of collecting the body of scientific knowledge, and to fit this practice into a historically coherent framework (229). From this work came the terms *paradigm*, which refers to a dominant model that explains a collection of observations, and *paradigm shift*, which refers to a change from one dominant model to a new explanation of the collection of observations (229).

In subsequent essays, Kuhn went on to expound on the historical structure of scientific discovery—that is the historical pattern that scientific discoveries follow (230). In this explanation, he advised that discoveries go through three stages: 1) discovery of an anomaly (when an observation does not fit into the current paradigm; this marks the opening of a period of discovery), 2) normal science/discovery (development of an anomaly—when the observations are made to fill in the gaps surrounding the anomaly), and 3) assimilation of the discovery (after the process of normal science has sufficiently filled in the gaps around a discovery, and the discovery is the foundation of a new paradigm as well as the framework for new technologies) (229, 230).

Relating these stages of discovery to the concept of paradigms, the discovery of an anomaly would be an observation inconsistent with or not supporting a current paradigm. During the maturation of a discovery, the discord between the previously-established paradigm and a new paradigm can result in the formation of a new paradigm—i.e. necessitate a paradigm shift (229, 230). Historically, paradigm shifts abound in science. Repeated observations and adaptations of models for planetary

motion stimulated a shift from a geo-centric, Ptolemaic model to a helio-centric, Copernican model. Albert Einstein's conceptual prediction and subsequent testing shifted the Newtonian idea of "conservation of mass" to a relativistic "conservation of mass/energy". Charles Darwin's theory of evolution by natural selection supplanted Lemarckian theories of evolution by inheritance of acquired characteristics.

While these examples are of obvious historical significance, the relatively short history of immunology has its share of paradigm shifts. The discovery by Zinkernagel and Doherty revealed that recognition of virally-infected cells needed recognition of both MHC and antigen (231); this discovery altered perceptions of how T cells were activated, lead to the discovery of the TCR, generated insights to central and peripheral tolerance, and has advanced to a stage where we can utilize TCR-transgenic T cells as a resource for the study other immunological problems. A 1982 study of autoimmune oophoritis demonstrated that $CD4^+CD8^-$ thymocytes were able to inhibit autoimmune disease (232, 233); this discovery lead to the discovery that $CD4^+CD25^+$ cells represent a regulatory phenotype and established a new paradigm for the regulation of immune responses.

In another area of study, a 1991 study revealed that Toll, a protein important in the embryonic development of *Drosophila melanogaster*, was highly homologous to the IL-1 receptor (234). When subsequent studies revealed that Toll was involved in the immune responses of *Drosophila (235, 236)*, the door was opened for the establishment of a new paradigm for Toll-like receptors and other pattern recognition receptors activating immune responses through recognition of pathogen-associated molecular patterns commonly expressed by infectious pathogens. The "normal science" discoveries related to the original Toll/IL-1R anomaly have revolutionized our understanding of immune activation by pathogens—explaining 30-year-old puzzles (i.e. the lack of response in C3H/Hej mice stimulated with LPS) (237), improving our understanding of human susceptibility to infectious diseases (238-242), and even enhancing our vaccination strategies (243-245) and tumor immunotherapy strategies (203, 246-249).

Regarding additional observations

Part of the investigation to determine the mechanism behind the enhanced T cell response targeted the phenotype and function of DC. Since $CD8^+$ T cells are activated and proliferate in the lung-draining LN prior to their migration into the lungs, it was reasoned that LN-derived factors/interactions were likely responsible for the increased $CD8^+$ T cell response in clinical dose-infected $TRAIL^{-/-}$ mice. Programming of the T cell response in the lung-draining LN is mediated by DC through both direct cell-to-cell contact and cytokine-dependent mechanisms. Interestingly, no distinct differences were observed in the costimulatory molecule expression; however, a significant increase in the number of $CD8^+$ dendritic cells in the lung-draining LN at day 6p.i. was noted (Figure 32A; $p < 0.001$). The increased number of DC in the dLN of $TRAIL^{-/-}$ mice correlated with a decrease in the apoptosis of DC populations in the dLN (Figure 32B). Consistent with these data, an increase in DR5 expression was observed on lung-draining LN-resident DC after influenza infection (Figure 32C), as well as TRAIL upregulation on NK cells, $CD4^+$ T cells, and $CD8^+$ T cells from $TRAIL^{+/+}$ mice (Figure 32D).

DC:T cell interactions are common during T cell priming in the dLN, and an emerging body of evidence supports DC:NK cell interactions during the initiation of immune responses. TRAIL and DR5 on these potentially interacting populations suggests the potential for differential induction of apoptosis of DC in $TRAIL^{+/+}$ and $TRAIL^{-/-}$ mice. Further, the Diehl study demonstrated increased inflammatory cytokine production after TLR stimulation of DR5-deficient cells. Considering these results together, it is intriguing to speculate that TRAIL:DR5 interactions might be responsible for shaping immune responses by inducing DC apoptosis or by influencing the production of cytokines that augment DC survival.

Immunopathology in influenza infection system has been attributed in part to $CD8^+$ T cells, which produce TNF that activates epithelial chemokine expression. These chemokines, in turn, recruit macrophages that contribute to an inflammatory response

resulting in tissue damage not related to viral clearance (108). We speculated that the increased T cell response might be associated with increases in pulmonary TNF expression and associated lung damage. While increases in TNF in the TRAIL-/- mice were observed, subsequent experiments to neutralize TNF during infection resulted in exacerbated disease in the $TRAIL^{-/-}$ mice. Determining the possible relationship between TNF expression and TRAIL expression could reveal if TRAIL has a direct effect on TNF expression (by blocking of transcription after a cell receives a signal from TRAIL) or an indirect effect (by blocking chemokine/cytokine expression that influence TNF production). Alternatively, the expression of these cytokines could be unrelated to one another, and only appear in response to an out-of-control influenza infection. Further, it would help us to better understand the role of TNF expression in immune responses to influenza, which is especially interesting given the fact that it does not help clear the virus, yet is consistently expressed in response to influenza virus infections.

In efforts to determine the cause of the death of the mice during the clinical dose infections, the death of pulmonary cells after infection in relation to their infection status was examined. As predicted, at day 4 post-infection there was an increased incidence of apoptosis in influenza infected cells compared with uninfected cells, as measured by the presence or absence of influenza HA on the cell surface; this observation was similar in $TRAIL^{+/+}$ and $TRAIL^{-/-}$ mice (Top panel, Figure 33). However, when the apoptosis in the lungs of $TRAIL^{-/-}$ mice at day 6 post-infection was examined, substantially increased apoptosis was observed in the uninfected cell population (Bottom panel, Figure 33). Understanding the mechanism that is causing this increased death would be another interesting line of investigation. Given the increased chemokine/cytokine expression in the lungs of $TRAIL^{-/-}$ mice, this increased death could be indicative of increased inflammation leading to uncontrolled tissue damage—similar to that observed with TNF induction in the Enelow influenza immunopathology study. Alternatively, the timing of

Figure 32. Decreased CD8+DC apoptosis in the draining LN correlates with increased CD8+DC numbers in TRAIL-/- mice compared to WT mice. $TRAIL^{+/+}$ or $TRAIL^{-/-}$ C57BL/6 mice were infected with 1500 E.I.U. of A/PR/8/34. At various days post infection, lung-draining lymph nodes were harvested, homogenized, and stained with anti-ClassII, anti-CD11c, DX5 (anti-NK cell), anti-CD3, anti-CD4, anti-CD8, anti-DR5 or isotype control antibody, and anti-TRAIL or isotype control antibody. For A, the number of $CD8^+CD11c^+ClassII^+$ cells (mean $\pm$ SD) from $TRAIL^{+/+}$ (black bars) or $TRAIL^{-/-}$ (gray bars) were enumerated using total LN cell counts and flow cytometry. DC numbers were normalized to the number of lymph nodes harvested from each mouse. Bars represent 3-4 mice per group and data are representative of three experiments. For B, the single-cell suspensions from A were also stained with Annexin V. The data represent the percentage of Annexin V^+ of $CD8^+CD11c^+ClassII^+$ cells from individual $TRAIL^{+/+}$ (●) or $TRAIL^{-/-}$ (▲) mice; bars represent the mean for each group. The data for C represent the DR5 expression on bulk DC (i.e. $CD11c^+ClassII^+$ cells) or $CD8^+$ DC (i.e. $CD8^+CD11c^+ClassII^+$ cells). Solid lines represent expression on DC from influenza-infected mice; dashed lines represent expression on DC from uninfected mice; shaded histograms represent isotype control. The data for D represent the TRAIL expression on NK cells (i.e. $DX5^+CD3^{NEG}$ cells), $CD4^+CD3^+$ T cells or $CD8^+CD3^+$ T cells. Solid lines represent expression on cells from influenza-infected mice (*bottom row; "flu"*) or from uninfected mice (*top row; "uninf"*); shaded histograms represent isotype control staining. Data are representative of 4-5 mice from 2 independent experiments. *p*-values determined using a paired *t* test.

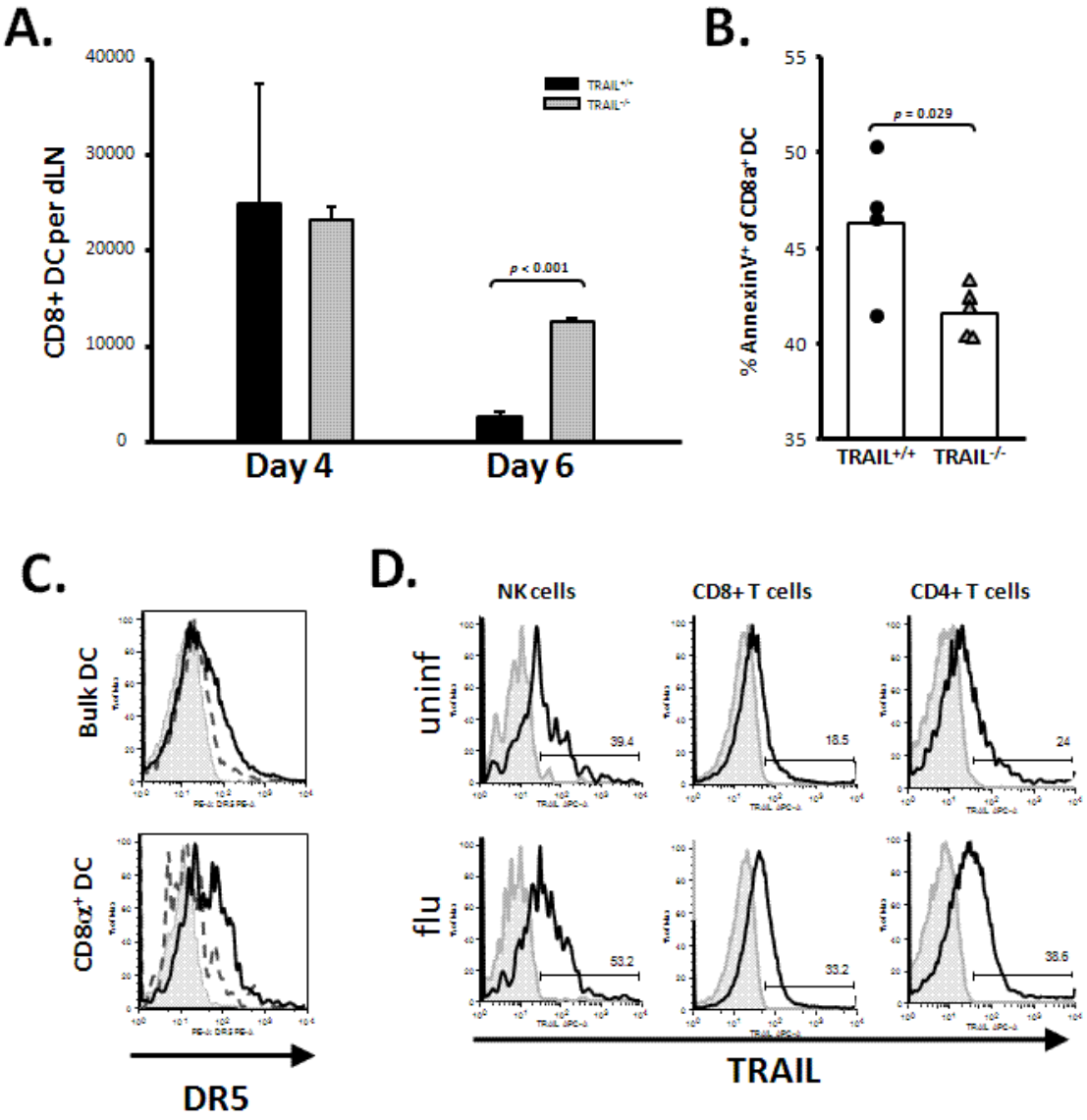
A.
CD8+ DC per dLN
40000
30000
20000
10000
0
TRAIL+/+
TRAIL-/-
p < 0.001
Day 4
Day 6
B.
% AnnexinV+ of CD8a+ DC
55
50
45
40
35
p = 0.029
TRAIL+/+
TRAIL-/-
C.
Bulk DC
CD8α+ DC
DR5
D.
NK cells
CD8+ T cells
CD4+ T cells
uninf
flu
39.4
18.5
24
53.2
33.2
38.6
TRAIL

Figure 33. TRAIL-/- mice have increased pulmonary Annexin V staining of influenza-negative cells, but similar staining of influenza-infected cells. C57Bl/6 or TRAIL-/- mice were infected i.n. with A/PR/8. At various days post infection, lungs were harvested, stained with anti-HA antibody and AnnexinV/7AAD and analyzed by flow cytometry. The top panel shows apoptosis of influenza-positive and influenza-negative populations on day 4, while the bottom panel shows similar results from day 6. Data are representative of 2 independent experiments.

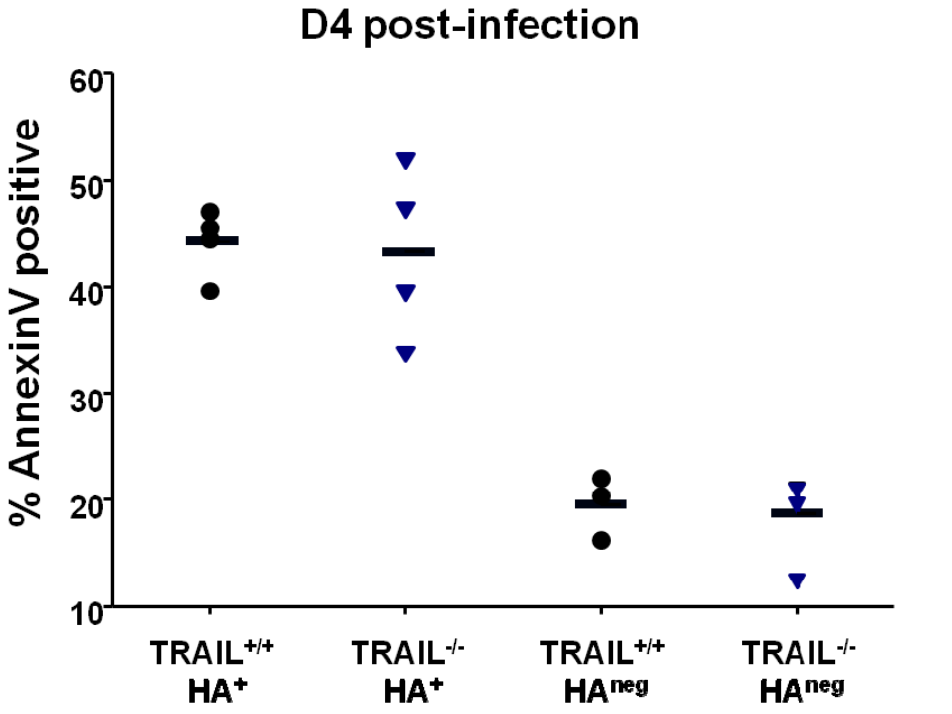
D4 post-infection
% AnnexinV positive
60
50
40
30
20
10
TRAIL+/+ HA+
TRAIL-/- HA+
TRAIL+/+ HAneg
TRAIL-/- HAneg

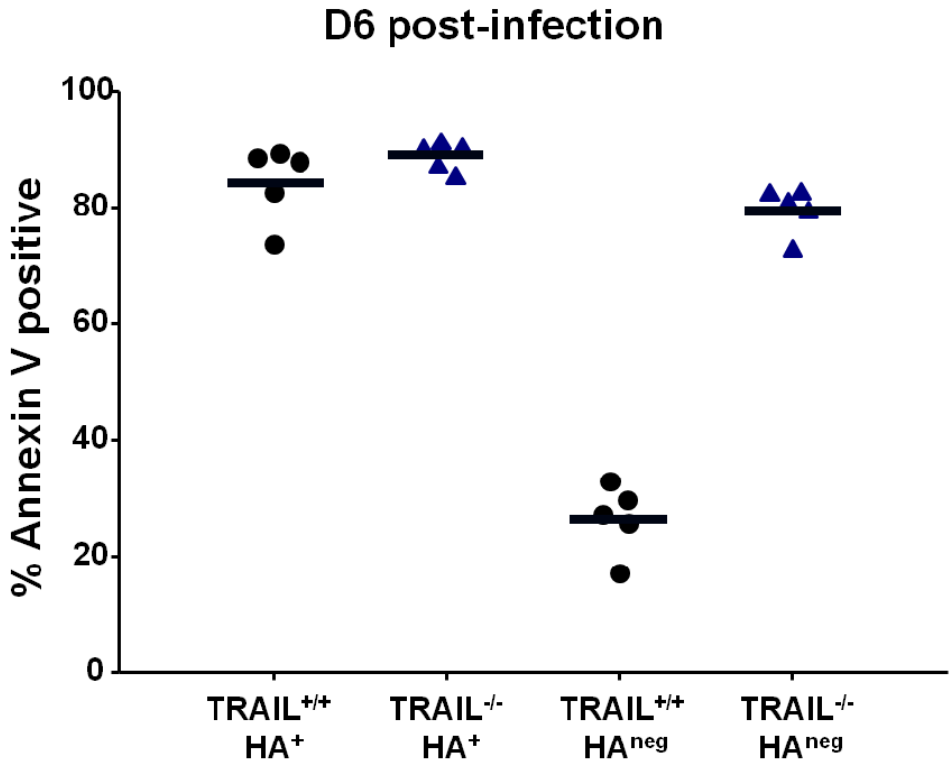
D6 post-infection
% Annexin V positive
100
80
60
40
20
0
TRAIL+/+ HA+
TRAIL-/- HA+
TRAIL+/+ HAneg
TRAIL-/- HAneg

the increased uninfected cell death is consistent with the recruitment of T cells to the lungs; hence, the observed increases in death of uninfected cells could be a result of bystander killing by T cells. Understanding the mechanism of this bystander killing would offer insight to the stimulus that drives bystander killing by T cells; and given that the bystander killing was only observed in the $TRAIL^{-/-}$ environment, such studies would also expand the understanding of how TRAIL controls immune responses.

Regarding the Data

Prior to the work presented herein, the literature describing roles for TRAIL emphasized its involvement in tumor therapies—in which cells of the immune system can utilize TRAIL to specifically induce the apoptosis of transformed cells, while leaving normal cells unaffected. Other studies had demonstrated roles for TRAIL in the elimination of helpless CD8+ T cells upon secondary challenge (250), in regulating autoimmune inflammation (143), and in controlling eosinophil survival in a model of allergic asthma (251). Additionally, studies of TRAIL/TRAIL-receptor involvement in the immune response to viruses supported their involvement in the immune response to measles (154), HIV-1 (252, 253), RSV (152), and hepatitis (219, 254). However, the clearance of virus after primary infection of a naïve host stated that clearance was mediated by $CD8^{+}$ T cells that clear virus through perforin- and Fas-dependent mechanisms (74). While expression of TRAIL had been observed during the immune response to influenza virus infection (91), no definitive evidence existed proving a role for TRAIL in clearing influenza.

The data from Chapter 2 examine the potential role for TRAIL in clearing primary influenza virus infections. These data demonstrate that TRAIL deficiency results in increased morbidity and higher viral titers than in $TRAIL^{+/+}$ hosts. Recognizing the aforementioned evidence that $CD8^{+}$ T cells are responsible for clearing virus, TRAIL expression was examined on these cells and determined that TRAIL was expressed

primarily on antigen-specific $CD8^+$ T cells. Examination of killing by these antigen specific T cells revealed that pulmonary $CD8^+$ T cells with TRAIL could kill influenza-specific target cells more effectively than $CD8^+$ T cells deficient in TRAIL. Consistent with this decreased killing capacity by $CD8^+$ T cells in $TRAIL^{-/-}$ mice, clearance of virus was delayed in the $TRAIL^{-/-}$ mice relative the $TRAIL^{+/+}$ mice. Further, the TRAIL-sufficient $CD8^+$ T cells could protect lethally infected mice from death, while those receiving TRAIL-deficient $CD8^+$ T cells were not protected from lethal challenge. Together, these data support a role for $CD8^+$ T cell-expressed TRAIL in clearing primary influenza virus infections. In the broader context of immunity to influenza virus infections, they suggest the inclusion of TRAIL as an additional effector pathway that $CD8^+$ T cells can use to kill influenza-infected cells.

While the data from Chapter 2 support a role for TRAIL in the clearing of influenza-infected cells by $CD8^+$ T cells, this study—like most quality studies—leads to more questions than it answers. The inclusion of TRAIL:DR5 interactions, along with Fas:FasL and Granzyme B/perforin, as an effector pathway provides evidence of three pathways by which infected cells can be killed during influenza infections. A single deficiency in TRAIL resulted in a delay of viral clearance, while a single deficiency of Fas (on target cells) or perforin (on effectors) resulted in no significant change in viral clearance in the previous studies (74). Given these data, one might speculate that TRAIL is the dominant pathway by which $CD8^+$ T cells clear influenza virus infections. This claim is likely overstating or overinterpreting the completed results, as the studies were completed with different initial doses of virus and utilized different strains of influenza. Hence, to make comparisons of the relative importance of FasL, granzyme B, and TRAIL in the clearance of influenza virus infections would require a side-by-side comparison of singly- and doubly-deficient T cells in animals given equivalent infections with the same influenza virus strain. Such comparisons would help determine the extent to which the granzyme B-induced, FasL-induced, and TRAIL-induced cytotoxicity of CD8 T cells is

dependent on the other pathways as well as the ability of these pathways to induce apoptosis independently from the other effector pathways.

Adoptive transfers of single-deficient and double-deficient T cells into OT-I TCR transgenic mice followed by influenza virus infection of these mice would allow the effects of specific effector molecule deficiency on T cells to be determined. In this adoptive transfer system, only the transferred T cells would be able to respond to influenza virus infections, as the OVA-specific OT-I transgenic T cells would not be responsive to influenza-virus-associated epitopes. By examining the killing capacity of singly-deficient T cells in these mice, the viral clearance from these mice, and the outcome of viral infections of these mice, one could determine the necessity of the singly-knocked out pathways to the cytotoxic function of the intact pathways (e.g. transfer of $TRAIL^{-/-}$ T cells would determine the necessity of TRAIL signals to the apoptosis induced by granzyme B and FasL as well as the necessity of TRAIL for viral clearance and host survival). By examining the killing capacity of doubly-deficient T cells in these mice, the viral clearance from these mice, and the outcome of viral infections of these mice, one could determine if singly-intact pathways were sufficient to induce apoptosis of infected cells and to protect mice from influenza virus infections (e.g. transfer of $FasL^{-/-}perforin^{-/-}$ T cells would eliminate the effects of FasL and granzyme killing by T cells, and help determine if TRAIL was sufficient to kill virally-infected cells, as well as if TRAIL was sufficient for viral clearance and host survival).

These experiments with single-knockout and double-knockout T cells would help determine if the apoptosis-inducing pathways are working in tandem or independently. Given the overlap in the signaling induced by TRAIL and FasL (both recruit FADD and activate the caspase cascade upon ligation of their respective receptors), these two ligands working together to more effectively induce apoptosis would not be surprising. Alternatively, both TRAIL:DR5 interactions (138, 255) and FasL:Fas interactions (255-257) can induce non-apoptotic signaling in their target cells. It is interesting to speculate

that signaling through both receptors might be necessary to induce apoptosis of the cell, while signaling through only one or the other would induce the nonapoptotic effects—such as the activation of NF-κB signaling (130-132) or the upregulation of anti-apoptotic molecules (133, 134, 137). If studies of the single- vs. double-deficient T cells implied that one receptor was necessary for the induction of apoptosis by the other, subsequent experiments could examine the differences in signaling that lead to the induction of apoptosis vs. alternative signals. These comparisons of the single-deficient T cells versus double-deficient T cells could examine the molecules in the apoptotic pathway that are more proximal to the receptor (i.e. the recruitment of FADD and the activation of Caspases 8 and 10), the mitochondria-associated events (i.e. the activation/recruitment of Bid/Bax/Bak, release of cytochrome C, the activation of Caspase 9), or the terminal events of apoptosis (i.e. Caspase 3 activation, DNA fragmentation). Such studies would improve the understanding of the requirements for the induction of apoptosis in influenza infected cells. Extended further, such studies would have potential implications for improving vaccine design—to optimize the T cell expression/utilization of both TRAIL and FasL; as well, these studies could offer additional insight regarding the sensitivity or resistance of tumors to TRAIL-induced apoptosis.

Determining the relative contributions of these pathways to influenza-induced immunopathology (or controlling that immunopathology) is another area that would be explored with the adoptive transfer system. Specifically, a transfer system that utilized $TRAIL^{+/+}$ or $TRAIL^{-/-}$ T cells transferred into $TRAIL^{+/+}$ or $TRAIL^{-/-}$ hosts would determine how TRAIL on T cells contributes to immunopathology or helps to control immunopathology. Further, the adoptive transfers into $TRAIL^{-/-}$ mice would determine the extent to which TRAIL expression on other cells (i.e. non-CD8 T cells) contributes to immunopathology or to the control of immunopathology. Antigen-specific expression of TNF can mediate pulmonary immunopathology by $CD8^{+}$ T cells after influenza virus infection (108), but the induction of immunopathology is not limited to T cells during

influenza virus infections. Indeed, in a study of H5N1 influenza infection, macrophages were found to upregulate TRAIL; this TRAIL expression lead to the death of T cells that were responding to the infection (101). TRAIL can be expressed by a considerable portion of immune cells in response to interferon signals (119, 153, 156, 201, 222), and influenza virus infection results in interferon production despite the presence/action of NS1 (29, 196, 215, 217). Hence, determining the contributions of TRAIL on CD8 T cells and non-CD8 T cells to immunopathology would help broaden the understanding of how TRAIL contributes to influenza-induced immunopathology (as well as how TRAIL on these cells might help control immunopathology).

A cell-specific knockout of TRAIL would be an important tool in helping determine the importance of TRAIL expression in specific cell types. While the effect of TRAIL deficiency in specific cells can be accomplished for some cell types through adoptive transfer studies (e.g. the CD8 T cell transfers described above), developing a transgenic mouse with a floxxed TRAIL gene would be useful. Once developed, the TRAIL-flox mice could be crossed to the appropriate cre-expressing strains (e.g. CD4-cre to knock out TRAIL in T cells or CD11c-cre to knock out TRAIL in DC) to allow for cell-type specific knockouts. These new strains with more specific deletions of TRAIL would help to reveal potential roles TRAIL on individual cell types, allowing investigations to determine the contributions to immunopathology as well as the contributions to controlling virus load and clearance.

A complicating factor in understanding the immune response to influenza virus infections is the highly-variable nature of the virus itself. Even among the commonly used laboratory influenza strains, immune responses vary; this challenge is broadened when one further considers highly pathogenic strains like the 1918 strain or recently-emerged H5N1 avian influenza strains. In an effort to broaden the studies from Chapter 2 to a more clinically relevant model of influenza infection, the dose of influenza virus used for infection in the studies in Chapter 3 was increased. The prediction was that the

increase in infectious dose would increase the morbidity/mortality that was observed, which it did in both the TRAIL$^{+/+}$ and TRAIL$^{-/-}$ mice. Surprisingly, the increased dose reversed the *in vivo* cytotoxicity as compared to the results in Chapter 2; that is, clinical-dose infection resulted in better pulmonary CD8^{+} T cell killing in the TRAIL$^{-/-}$ than in the TRAIL$^{+/+}$ mice. This killing was not because of a difference in effector function by the T cells, as expression of FasL, granzyme B, TNF, and CD107a were all similar in/on the T cells from TRAIL$^{-/-}$ and TRAIL$^{+/+}$ mice. Further, the *in vitro* assessment of T cell killing revealed that the T cells from TRAIL$^{+/+}$ mice and TRAIL$^{-/-}$ mice could kill targets similarly on a per cell basis. Therefore, the difference in *in vivo* killing seen in the TRAIL$^{-/-}$ and TRAIL$^{+/+}$ mice seems to be due to enhanced recruitment of T cells to the lungs of TRAIL$^{-/-}$ mice. This enhanced recruitment correlated with increased expression of MIG and MIP-1α, two chemokines associated with pulmonary T cell recruitment. Inhibiting the ability of T cells to respond to these chemokines (by either blocking or though use of receptor knockout animals) resulted in decreased migration of the transferred T cells to the lungs of infected mice.

To definitively verify that the observed difference in killing was due solely to the enhanced recruitment of T cells, however, additional experiments to confirm the *in vitro* per-cell killing by the T cells in TRAIL$^{-/-}$ should be completed. Exploring a wider range of E:T ratios would help confirm the results from figure 22. If the killing by TRAIL$^{-/-}$ and TRAIL$^{+/+}$ T cells is similar on a per cell basis, then the killing difference is likely due to differences in T cell number. Alternatively, if the killing difference between TRAIL$^{-/-}$ T cells and TRAIL$^{+/+}$ T cells persists in *in vitro* killing experiments, some other mechanism would be responsible for the difference in killing. Given that similar expression of FasL, granzyme B, TNF, and CD107a was observed, the differential killing could involve differences in the expression of other cytolytic molecules (e.g. granzyme A, granzyme K) that are also upregulated in T cells after influenza infection (258, 259). Alternatively, differences in T cell expression of LFA-1 could influence lytic synapse

formation and associated killing ability (260). Hence, if differences in T cell cytotoxicity on a per cell basis were observed, subsequent studies would examine differential expression of other cytolytic molecules as well as differential expression of adhesion molecules. Further, the function of T cells from TRAIL$^{-/-}$ and TRAIL$^{+/+}$ mice would be determined by microscopy studies to examine the frequency of T-cell:infected-cell interactions, T-cell:infected-cell contact/interaction times, and the per cell killing capacity of individual T cells.

Beyond confirming the results included herein, further *in vitro* analysis of killing by CD8^{+} T cells from the TRAIL$^{-/-}$ could help to determine the effector functions utilized by the TRAIL$^{-/-}$ T cells. Interestingly, infection with a sub-clinical dose resulted in the priming TRAIL$^{-/-}$ T cells that had diminished cytotoxicity compared to those from TRAIL$^{+/+}$ mice. Conversely, infection with a clinical dose resulted TRAIL$^{-/-}$ T cells with cytotoxic function similar to their TRAIL$^{+/+}$ counterparts. Side-by-side comparison of the TRAIL$^{-/-}$ T cells from sub-clinical dose infection and from clinical dose infections would help to determine the difference in the T cells in the two infection settings. Such comparisons would include comparisons of surface phenotypes (e.g. expression of CD69, CD62L, CD25, PD-1, KLRG1), comparisons of the expression of effector molecules (e.g. expression of granzyme B, FasL, IFNγ, TNFα) and side-by-side comparisons of *in vitro* cytotoxicity. The effector molecule analysis would likely reveal differential expression of a known effector pathway (e.g. FasL or Granzyme B), and would lead to additional *in vitro* cytotoxicity experiments to block/inhibit the altered pathway and confirm its role in the differential killing. If differential effector molecule expression was not observed/confirmed on T cells from sub-clinical versus clinical doses of infection, subsequent experiments would examine inhibitory molecule expression (e.g. PD-1 or CTLA-4, both of which are associated with T cell exhaustion (261)) or the production of inhibitory cytokines (e.g. IL-10, which can be produced by CD8+ T cells after influenza virus infection (262, 263). Observing differences in inhibitory molecule expression or in

inhibitory cytokines would lead to neutralization studies to verify their role in the differential function of the T cells from sub-clinical versus clinical dose infections.

Other studies of the differential T cell response from the sub-clinical dose infections compared to clinical dose infections could examine the cause of the differential response; that is, determine if the differential T cell responses are due to differences in the priming of the T cells. The DC populations in the lung-draining LN play a key role in initiating T cell responses to influenza virus infection (53, 57, 58). Comparing the phenotype of DC (e.g. upregulation of costimulatory molecules and secretion of cytokines) and the function of DC (e.g. migration from lung to the lung-draining LN and ability to activate naïve T cells) after sub-clinical and clinical dose infections would help determine if differences in DC are the cause of the differential T cell response. Alternatively, the differential T cell responses could result from differences in the pulmonary environment induced by a sub-clinical dose infection versus a clinical dose infection. Clearly, signals received in the LN are not the only determining factor for T cell responses—as after T cell migration from the lung-draining LN to the lung, DC:T cell interactions in the lung environment are important to T cell survival and accumulation in the airways (59, 60). Differential survival/activation signals from pulmonary DC populations could influence the T cell function in a sub-clinical dose versus a clinical dose. Determining the influence of these DC populations (and their cytokine expression, costimulatory molecule expression, MHC expression) in a sub-clinical dose versus a clinical dose would reveal the potential roles for the pulmonary environment in influencing T cell function. Further, these studies of DC function in the draining LN and in the lung environment would expand understanding of how the influenza dose alters DC function to influence T cell responses.

Considering the differences in sub-clinical dose infection and clinical dose infection from a different perspective, determining how the initial inoculum of virus differentially stimulates/activates the viral sensing pathways (e.g. TLR and NLR) would

be of interest. Initial experiments would be completed to determine the involvement of specific TLR/NLR by blocking these pathways in TRAIL$^{-/-}$ mice receiving sub-clinical and clinical doses of infection or by crossing the TRAIL$^{-/-}$ mice to TLR/NLR knockouts (e.g. Nalp3$^{-/-}$, TLR3$^{-/-}$, TLR7$^{-/-}$). Involvement of the pathways would be determined by comparing the pulmonary chemokine production (e.g. MIG, IP-10, MIP-1α, MIP-1β), pulmonary cytokine production (IFNα, IFNγ, IL-6, IL-12, IL-10), and the antigen-specific CD8^{+} T cell responses induced by a sub-clinical dose versus a clinical dose. If/when the involvement of these pathways was confirmed, the results would be applied to determining how the TLR/NLR activation alters DC function and T cell priming. Future experiments would determine the extent to which TLR/NLR activation altered DC migration from the lung to the dLN was altered, altered DC activation (e.g. expression of costimulatory molecules or production of cytokines), altered T cell activation (e.g. stimulation of T cell proliferation and upregulation of T cell activation markers), and influenced T cells inhibition (e.g. by signals through PD-1 or from IL-10).

While the previous paragraphs have emphasized comparisons between the sub-clinical infectious dose and the clinical infectious dose, similar studies would be completed to determine the differential T cell responses in TRAIL$^{+/+}$ and TRAIL$^{-/-}$ mice given clinical dose infections. Of specific interest might be a comparison of killing mechanisms used by the TRAIL$^{+/+}$ and TRAIL$^{-/-}$ T cells at the clinical dose infection. Considering the lack of difference in *in vitro* killing by CD8 T cells after a clinical dose infection, comparing the relative importance of FasL, TRAIL, and granzyme B to the cytotoxic function of CD8^{+} T cells would be of interest. Utilizing the adoptive transfer system of single-deficient and double-deficient T cells outlined above, the effectiveness of the individual pathways in killing infected cells, in clearing virus, and in protecting from infection would be determined. If comparisons of sub-clinical responses to clinical dose responses revealed differential expression and utilization of FasL, subsequent studies would determine how TRAIL regulates FasL expression. Additionally,

comparing T cell activation (e.g. ability to proliferate and expression of CD69/CD25) as well as T cell inhibition/exhaustion marker expression (e.g. PD-1, KLRG1) on the $TRAIL^{+/+}$ and $TRAIL^{-/-}$ T cells would help verify the similarities between the T cells in the respective immune responses to clinical-dose influenza virus infection. Should differences in T cell activation and/or inhibition in the $TRAIL^{+/+}$ and $TRAIL^{-/-}$ mice be revealed, subsequent studies would seek to determine the extent to which TRAIL regulates T cell activation and proliferation, T cell expression of inhibition/exhaustion markers, and the interactions of T cells with infected target cells after clinical dose infections of $TRAIL^{+/+}$ and $TRAIL^{-/-}$ mice.

Differences in DC function could also contribute to the differential T cell responses observed in the $TRAIL^{+/+}$ and $TRAIL^{-/-}$ mice. As mentioned in the discussion of sub-clinical versus clinical dose infections in the $TRAIL^{-/-}$ mice above, altered DC function could exist in the lung-draining LN as well as in the lung environment itself. To address these possibilities, experiments would be conducted to examine DC function in the lung-draining LN including DC costimulatory molecule expression (e.g. CD80, CD86), DC chemokine production (e.g. IL-12), and DC ability to prime naïve T cells (e.g. stimulate T cell proliferation and upregulation of activation markers). Additional experiments would evaluate DC functions in the lung environment, including chemokine/cytokine production (e.g. IL-12, IL-15), MHC expression, and ability to stimulate T cell survival in the lung environment. Subsequently, followup experiments would be aimed at determining how TRAIL expression alter the DC function. These experiments would determine how TRAIL expression influences DC apoptosis in the LN and lung environment (including determining how TRAIL induced apoptosis influences DC numbers, determining the cells responsible for stimulating the apoptosis of DC, and determining the specific DC subsets undergoing apoptosis). Additionally, these experiments would determine the extent to which TRAIL expression stimulates non-apoptotic effects on DC in the LN and lung environments (including determining how

TRAIL expression influences DC chemokine/cytokine production and determining how TRAIL expression influences the DC expression of costimulatory and inhibitory molecules on the surface of DC).

The data from Chapter 3 support a role for TRAIL:DR5 interactions as a mechanism of regulating immune responses, which reinforces the discovery by Diehl, et.al. that established a role for TRAIL as a regulator of immune responses. While the data from Chapter 3 clearly demonstrated increased chemokine expression in the absence of TRAIL, the mechanism of this regulation was not determined. Given the strong evidence for TRAIL as an inducer of apoptosis and the emerging evidence for non-apoptotic TRAIL signaling, either of these is a possible means for controlling pulmonary chemokine expression. TRAIL expression could result in killing the chemokine expressing cells; alternatively, TRAIL expression could induce signaling pathways that shut down the chemokine production. Considering the recent report suggesting that cIAP is required for activation of the inflammasome (264), that TRAIL signaling can downregulate cIAP (265), and the reports that influenza activates the inflammasome through NLRP3 (32, 33), the intersection of TRAIL signals with inflammasome signaling provides an intriguing possibility for how TRAIL might modulate cytokine and chemokine expression. This possible regulation is further supported by a study connecting IL-1β (a major product of inflammasome activation) to the induction of CXC chemokines (266). Future studies to examine the possible connections between cIAP modulation by TRAIL, as well as the effects of this modulation on chemokine/cytokine production, would expand the understanding of non-apoptotic TRAIL signaling as well as provide a mechanism by which TRAIL regulates chemokine/cytokine production during immune responses.

During primary influenza infection, CCR5-deficiency results in enhanced disease correlated to increased immunopathology. In subsequent studies, it was determined that loss of both CXCR3 and CCR5 pathways resulted in amelioration of the

immunopathology observed in the CCR5-deficient hosts (267). These data suggest the existence of multiple T cells subsets responding to the infection, which are differentially recruited by CXCR3- and CCR5-associated chemokines. Interestingly, $CXCR3^{-/-}$ resulted in decreased leukocyte infiltration to the airway, but had no effect on viral clearance (61). Given the increase in pulmonary CXCR3-associated chemokines and the increased immunopathology that is observed in the $TRAIL^{-/-}$ mice after clinical-dose influenza virus infection, exploring the link between CXCR3-chemokine expression and immunopathology would be an interesting followup study. Breeding $TRAIL^{-/-}CXCR3^{-/-}$ mice would allow the importance of the CXCR3-associated chemokines in the induction of immunopathology in the $TRAIL^{-/-}$ system. Additionally, such experiments would allow further assessment of the overall importance of CXCR3-associated chemokines in driving immunopathology during influenza virus infections. These experiments might reveal the existence of a specific subset of T cells (presumably CXCR3-expressing) that induce immunopathology after influenza virus infections; or conversely, examination of the CCR5-deficient system might reveal a specific subset of T cells (presumably CCR5-expressing) that help to control immunopathology after influenza virus infection. Observing either of these outcomes would reveal an additional role for TRAIL in controlling immunopathology after influenza virus infection. Subsequent studies would seek to determine the mechanism by which TRAIL controls chemokine expression (e.g. by the direct apoptosis of chemokine-producing cells or by non-apoptotic signals to the chemokine-producing cells that results in stopping their chemokine production).

In related, complementary studies it would be of interest to determine the specific cell types producing the cytokines/chemokines in the $TRAIL^{+/+}$ and $TRAIL^{-/-}$ airways, as both epithelial cells and leukocytes are capable of producing these products. While similar levels of infection in the lung were observed in $TRAIL^{-/-}$ and $TRAIL^{+/+}$ mice (figures 14 & 16), determining how infection relates to chemokine expression could reveal additional means of regulation. Primary future explorations should examine the

production of MIG and MIP-1a (as well as other chemokines) in the airway—specifically, determining the cell population(s) responsible for production. Once this determination has been made, subsequent experiments could explore the importance of the chemokines as well as the chemokine source in determining the outcome of infection. Further, determining the chemokine source(s) would allow better-defined experiments to be conducted regarding how TRAIL:DR5 interactions are controlling chemokine expression.

For example, consider a case in which both epithelial cells and macrophages are infected and producing cytokine. In a $TRAIL^{+/+}$ environment, TRAIL signals would presumably kill the infected cells, thus eliminating the chemokine production by these cells; however, in a $TRAIL^{-/-}$ environment, no death of these cells would occur and the chemokine production would persist. Further, the potential non-apoptotic signals mentioned above could also act differentially on the various populations that are infected, as the distribution of inflammasome components varies from cell type to cell type (268). TRAIL-receptor expression might relate to a cell's susceptibility to TRAIL-induced regulation/apoptosis. Examining the relative effect of TRAIL signaling on infected ($NP^{+}DR5^{HIGH}$) cells in comparison to uninfected ($NP^{NEG}DR5^{LOW}$) could offer insight to the control of chemokine production. Such experiments would help determine if apoptotic versus nonapoptotic signaling relates to the intensity of TRAIL receptor expression on the cells as well as the chemokine/cytokine production by these cells.

Among the many influences chemokines and cytokines have on the immune response is the formation and maturation of nasopharyns-associated lymphoid tissue (NALT) and bronchus-associated lymphoid tissue (BALT) (269-271). While the chemokines associated with establishing BALT and NALT (SLC, MIP-3β, CXCL13, and CCL19) were not specifically examined in the investigations, the aberrant expression of chemokines in the lung after influenza virus infection could extend to the chemokines related to NALT/BALT cell recruitment. Determining the mechanisms controlling

chemokine expression will offer potential insight about the control of chemokines in the NALT/BALT, but the effects of TRAIL:DR5 interactions on BALT/NALT-associated chemokines has not been examined. Further, considering the specific upregulation of MIG and MIP-1α, but not other chemokines, the potential role that TRAIL:DR5 interactions have in the control of NALT/BALT-associated chemokines is difficult to predict. Determining the effects on the expression of these chemokines would not only reveal the roles for TRAIL in BALT/NALT function, but would also reveal mechanisms of regulation for specific chemokines by TRAIL:DR5 interactions.

While most effects of TRAIL are associated with signaling induced when its receptor is ligated on a target cell, reports also indicate that some cell-intrinsic "reverse signaling" can occur. Cross-linking TRAIL with plate-bound TRAIL-receptor Fc resulted in enhanced $CD4^+$ proliferation and IFNγ production (272, 273). Further, this reverse signaling isn't just an *in vitro* artifact, as this TRAIL signaling was shown to have a potential role in the development of autoimmune disease (273). Alveolar macrophages and influenza-specific T cells—both of which have been associated with inducing immunopathology—express TRAIL after influenza virus infection. Determining the effects of reverse signaling through TRAIL in these cell types would initially require moving from *in vivo* infection models into the more controlled system of T cell and macrophage cell lines. Examining the effects of DR5 engagement on cytokine production and proliferation as well as determining the signaling pathways activated by ligand engagement. Of particular interest in this regard would be the studies examining the potential for differential signals by the various TRAIL receptors, particularly in the human system. If the different receptors were discovered to differentially "back signal" through TRAIL, it would add another intriguing level of complexity of immune regulation via TRAIL. In such a case, immune regulation (including the regulation T cell activation and proliferation, regulation of cytokine and chemokine production, and regulation DC activation and function) could result from modulation of either TRAIL

expression or from modulation of the TRAIL-receptor expression. Future studies would aim to determine how the modulation of specific TRAIL-receptor expression correlates with disease outcome after influenza virus infection.

Prior to the investigations of the role for TRAIL in the human immune response to influenza virus, TRAIL was thought to be involved primarily in the response to tumors. Multiple lines of research focused on how TRAIL fights tumors and how TRAIL can be upregulated/exploited to help fight tumors. Investigations of TRAIL expression in human influenza infections have revealed potentially harmful roles for TRAIL—based largely on *in vitro* studies of TRAIL expression on various cell types after influenza stimulation. TLR stimuli and direct infection of PBMC resulted in TRAIL upregulation. Given that both influenza infection and the TLR stimuli used caused the production of type I and type II interferons, the expression of TRAIL on these cells is not surprising. Considering that all of the TRAIL-expressing cell types that were examined have been shown to kill TRAIL-sensitive targets in vitro, these TRAIL expression data did not shift any long-established thoughts in the field; however, they did serve to reinforce a positive role for TRAIL in the immune response to influenza virus infection that had been implied by the mouse studies. Future examination of TRAIL in the human immune response to influenza virus infection should target the *in vivo* response to influenza infections. Such studies would help establish a "normal" baseline response that could be used as a context in which to interpret data from *in vitro* studies. Without an *in vivo* baseline to serve as a reference point, the data from *in vitro* studies are difficult to interpret without bias influencing the explanation of outcomes.

Perhaps the most interesting finding from the human studies was the discovery that infection of epithelial cells sensitizes them to TRAIL-induced apoptosis, but not FasL. This rapid sensitization to killing by TRAIL raises many questions for future study. Consistent with previous reports, the sensitization to TRAIL was not due to modulation of TRAIL-receptor expression. However, the infection did cause a change in

the balance of pro-and anti-apoptotic message in these epithelial cells. Subsequent studies to determine if these changes are interferon-driven or infection-driven would offer better understanding of the role of TRAIL/TRAIL-receptor in the response to influenza virus, but could potentially help explain the TRAIL-associated immunopathology that was observed in the recent study by Herold, et.al. that showed TRAIL as an inducer of immunopathology (101). Determining the mechanism of TRAIL sensitization could offer treatment strategies that would prevent potential immunopathology after infection.

Subsequent studies into TRAIL's role in the human response to influenza virus infections should also seek to correlate the mouse studies with human responses. First, it would be interesting to determine if the $CD8^+$ T cells responding to infection express TRAIL in an influenza-specific fashion, and if these influenza-specific cells use the TRAIL expressed on their surface to kill infected cells. An upregulation of TRAIL in the *in vitro* cultures was observed, but examining TRAIL expression during a "normal" priming response *in vivo* would reinforce the data obtained in the mouse studies. Further, determining the importance of TRAIL:TRAIL-receptor interactions in healthy patient responses could improve the understanding of the TRAIL system and how it contributes to immune responses to influenza virus infection. Further, determining how the various receptors in the human system contribute to apoptotic versus nonapoptotic signals during influenza infections could improve the understanding of the TRAIL:TRAIL-receptor system in humans and could help elucidate roles for TRAIL in the regulation of human immune responses and the mechanisms by which TRAIL regulates these responses. And as mentioned previously in the discussion, examining how the various TRAIL receptors might cause differential "reverse signaling" to TRAIL-expression cells would be of interest. Additionally, analysis of human cancer patients has revealed polymorphisms of TRAIL-R1 that have been correlated with increased susceptibility to disease. Examining how these polymorphisms might influence the other roles for TRAIL could offer additional insight for how TRAIL functions in the immune response.

Regarding Scientific Discoveries and Paradigm Shifts

Considering the data presented herein, I believe that the discoveries described in this dissertation make considerable contributions toward further developing, if not shifting, established paradigms in immunology. Chapter two outlines an additional pathway by which $CD8^+$ T cells can kill infected cells after influenza virus infection. This finding not only shifts the paradigm of how the T cells kill, but also supports the paradigm that TRAIL has roles outside the realm of tumor immunology. The discoveries described in Chapter three reinforce a relatively new paradigm—one in which TRAIL acts as a regulator of immune responses. Though the mechanistic details of this regulation are still to be determined, future studies to examine how TRAIL acts to regulate immune responses will push forward the fields of immune regulation and TRAIL signaling. Chapter four complements the data from chapter two, reinforcing a role for TRAIL in the immune response to influenza virus infections; but perhaps most substantially, these data demonstrate that infected epithelial cells are sensitized to TRAIL-induced apoptosis—implying that the control of influenza infection by TRAIL need not be antigen-specific killing by CD8 T cells. Together, the discoveries made during the investigations that contributed to this dissertation have filled in some of the knowledge gaps of existing paradigms while forcing subtle shifts in other paradigms.

All that said, Max Plank is credited with the adage that "Old paradigms don't die because the practitioners agree with the superior reasoning of the new paradigm. The old ideas die when the practitioners die." So while the data in this thesis show new mechanisms of killing infected cells as well as new roles for TRAIL in regulating immune responses, it will likely take some time before TRAIL is regularly included as a major mechanism by which $CD8^+$ T cells clear influenza virus infections. Further, next week a new set of data could emerge that adds to or even refutes the findings made herein—inducing additional shifts the current paradigms. Such shifts are neither grounds for despair nor grounds for elation—they are just the nature of the science.

REFERENCES

1. LaForce, F. M., K. L. Nichol, and N. J. Cox. 1994. Influenza: virology, epidemiology, disease, and prevention. *Am J Prev Med* 10 Suppl:31-44.

2. Thompson, W. W., D. K. Shay, E. Weintraub, L. Brammer, N. Cox, L. J. Anderson, and K. Fukuda. 2003. Mortality associated with influenza and respiratory syncytial virus in the United States. *Jama* 289:179-186.

3. CDC, C. f. D. C. i. e. 2008. Influenza Fact Sheet.

4. Barker, W. H., and J. P. Mullooly. 1982. Pneumonia and influenza deaths during epidemics: implications for prevention. *Arch Intern Med* 142:85-89.

5. Zimmerman, R. K., D. B. Middleton, and N. J. Smith. 2003. Vaccines for persons at high risk due to medical conditions, occupation, environment, or lifestyle, 2003. *J Fam Pract* 52:S22-35.

6. Heikkinen, T., H. Silvennoinen, V. Peltola, T. Ziegler, R. Vainionpaa, T. Vuorinen, L. Kainulainen, T. Puhakka, T. Jartti, P. Toikka, P. Lehtinen, T. Routi, and T. Juven. 2004. Burden of influenza in children in the community. *J Infect Dis* 190:1369-1373.

7. Subbarao, K., B. R. Murphy, and A. S. Fauci. 2006. Development of effective vaccines against pandemic influenza. *Immunity* 24:5-9.

8. Horimoto, T., and Y. Kawaoka. 2005. Influenza: lessons from past pandemics, warnings from current incidents. *Nat Rev Microbiol* 3:591-600.

9. Palese, P. 2004. Influenza: old and new threats. *Nat Med* 10:S82-87.

10. Fauci, A. S. 2005. Race against time. *Nature* 435:423-424.

11. CDC. 2009. Flu View: A Weekly Influenza Surveillance Report Prepared by the Influenza Division. 2009-2010 Influenza Season Week 43 ending October 31, 2009 ed. I. D. o. t. CDC, ed. Centers for Disease Control and Prevention, Atlanta, GA.

12. 2009. Will swine flu push the world into deflation? In *Economic Outlook*. Oxford Economics, Ltd.

13. Lamb, R. A., and P. W. Choppin. 1983. The gene structure and replication of influenza virus. *Annu Rev Biochem* 52:467-506.

14. Morgan, C., K. C. Hsu, R. A. Rifkind, A. W. Knox, and H. M. Rose. 1961. The Application of Ferritin-Conjugated Antibody to Electron Microscopic Studies of Influenza Virus in Infected Cells : Ii. the Interior of the Cell. *J Exp Med* 114:833-836.

15. Murphy, J. S., and F. B. Bang. 1952. Observations with the electron microscope on cells of the chick chorio-allantoic membrane infected with influenza virus. *J Exp Med* 95:259-268.

16. Laver, W. G., and R. C. Valentine. 1969. Morphology of the isolated hemagglutinin and neuraminidase subunits of influenza virus. *Virology* 38:105-119.

17. Schnell, J. R., and J. J. Chou. 2008. Structure and mechanism of the M2 proton channel of influenza A virus. *Nature* 451:591-595.

18. Hale, B. G., R. E. Randall, J. Ortin, and D. Jackson. 2008. The multifunctional NS1 protein of influenza A viruses. *J Gen Virol* 89:2359-2376.

19. Neumann, G., M. T. Hughes, and Y. Kawaoka. 2000. Influenza A virus NS2 protein mediates vRNP nuclear export through NES-independent interaction with hCRM1. *Embo J* 19:6751-6758.

20. Robb, N. C., M. Smith, F. T. Vreede, and E. Fodor. 2009. NS2/NEP protein regulates transcription and replication of the influenza virus RNA genome. *J Gen Virol* 90:1398-1407.

21. Chen, W., P. A. Calvo, D. Malide, J. Gibbs, U. Schubert, I. Bacik, S. Basta, R. O'Neill, J. Schickli, P. Palese, P. Henklein, J. R. Bennink, and J. W. Yewdell. 2001. A novel influenza A virus mitochondrial protein that induces cell death. *Nat Med* 7:1306-1312.

22. Isin, B., P. Doruker, and I. Bahar. 2002. Functional motions of influenza virus hemagglutinin: a structure-based analytical approach. *Biophys J* 82:569-581.

23. Shapiro, G. I., and R. M. Krug. 1988. Influenza virus RNA replication in vitro: synthesis of viral template RNAs and virion RNAs in the absence of an added primer. *J Virol* 62:2285-2290.

24. Dias, A., D. Bouvier, T. Crepin, A. A. McCarthy, D. J. Hart, F. Baudin, S. Cusack, and R. W. Ruigrok. 2009. The cap-snatching endonuclease of influenza virus polymerase resides in the PA subunit. *Nature* 458:914-918.

25. Leser, G. P., and R. A. Lamb. 2005. Influenza virus assembly and budding in raft-derived microdomains: a quantitative analysis of the surface distribution of HA, NA and M2 proteins. *Virology* 342:215-227.

26. Air, G. M., and W. G. Laver. 1989. The neuraminidase of influenza virus. *Proteins* 6:341-356.

27. Meurs, E., K. Chong, J. Galabru, N. S. Thomas, I. M. Kerr, B. R. Williams, and A. G. Hovanessian. 1990. Molecular cloning and characterization of the human double-stranded RNA-activated protein kinase induced by interferon. *Cell* 62:379-390.

28. Barchet, W., A. Krug, M. Cella, C. Newby, J. A. Fischer, A. Dzionek, A. Pekosz, and M. Colonna. 2005. Dendritic cells respond to influenza virus through TLR7- and PKR-independent pathways. *Eur J Immunol* 35:236-242.

29. Le Goffic, R., J. Pothlichet, D. Vitour, T. Fujita, E. Meurs, M. Chignard, and M. Si-Tahar. 2007. Cutting Edge: Influenza A virus activates TLR3-dependent inflammatory and RIG-I-dependent antiviral responses in human lung epithelial cells. *J Immunol* 178:3368-3372.

30. Hornung, V., J. Ellegast, S. Kim, K. Brzozka, A. Jung, H. Kato, H. Poeck, S. Akira, K. K. Conzelmann, M. Schlee, S. Endres, and G. Hartmann. 2006. 5'-Triphosphate RNA is the ligand for RIG-I. *Science* 314:994-997.

31. Pichlmair, A., O. Schulz, C. P. Tan, T. I. Naslund, P. Liljestrom, F. Weber, and C. Reis e Sousa. 2006. RIG-I-mediated antiviral responses to single-stranded RNA bearing 5'-phosphates. *Science* 314:997-1001.

32. Thomas, P. G., P. Dash, J. R. Aldridge, Jr., A. H. Ellebedy, C. Reynolds, A. J. Funk, W. J. Martin, M. Lamkanfi, R. J. Webby, K. L. Boyd, P. C. Doherty, and T. D. Kanneganti. 2009. The intracellular sensor NLRP3 mediates key innate and healing responses to influenza A virus via the regulation of caspase-1. *Immunity* 30:566-575.

33. Allen, I. C., M. A. Scull, C. B. Moore, E. K. Holl, E. McElvania-TeKippe, D. J. Taxman, E. H. Guthrie, R. J. Pickles, and J. P. Ting. 2009. The NLRP3 inflammasome mediates in vivo innate immunity to influenza A virus through recognition of viral RNA. *Immunity* 30:556-565.

34. Katze, M. G., Y. He, and M. Gale, Jr. 2002. Viruses and interferon: a fight for supremacy. *Nat Rev Immunol* 2:675-687.

35. Ghosh, S. K., J. Kusari, S. K. Bandyopadhyay, H. Samanta, R. Kumar, and G. C. Sen. 1991. Cloning, sequencing, and expression of two murine 2'-5'-oligoadenylate synthetases. Structure-function relationships. *J Biol Chem* 266:15293-15299.

36. Zhou, A., B. A. Hassel, and R. H. Silverman. 1993. Expression cloning of 2-5A-dependent RNAase: a uniquely regulated mediator of interferon action. *Cell* 72:753-765.

37. Pavlovic, J., O. Haller, and P. Staeheli. 1992. Human and mouse Mx proteins inhibit different steps of the influenza virus multiplication cycle. *J Virol* 66:2564-2569.

38. Turan, K., M. Mibayashi, K. Sugiyama, S. Saito, A. Numajiri, and K. Nagata. 2004. Nuclear MxA proteins form a complex with influenza virus NP and inhibit the transcription of the engineered influenza virus genome. *Nucleic Acids Res* 32:643-652.

39. Talon, J., C. M. Horvath, R. Polley, C. F. Basler, T. Muster, P. Palese, and A. Garcia-Sastre. 2000. Activation of interferon regulatory factor 3 is inhibited by the influenza A virus NS1 protein. *J Virol* 74:7989-7996.

40. Servant, M. J., N. Grandvaux, and J. Hiscott. 2002. Multiple signaling pathways leading to the activation of interferon regulatory factor 3. *Biochem Pharmacol* 64:985-992.

41. Servant, M. J., B. Tenoever, and R. Lin. 2002. Overlapping and distinct mechanisms regulating IRF-3 and IRF-7 function. *J Interferon Cytokine Res* 22:49-58.

42. Kumar, K. P., K. M. McBride, B. K. Weaver, C. Dingwall, and N. C. Reich. 2000. Regulated nuclear-cytoplasmic localization of interferon regulatory factor 3, a subunit of double-stranded RNA-activated factor 1. *Mol Cell Biol* 20:4159-4168.

43. Bilyk, N., and P. G. Holt. 1995. Cytokine modulation of the immunosuppressive phenotype of pulmonary alveolar macrophage populations. *Immunology* 86:231-237.

44. Holt, P. G. 1978. Inhibitory activity of unstimulated alveolar macrophages on T-lymphocyte blastogenic response. *Am Rev Respir Dis* 118:791-793.

45. Becker, S., J. Quay, and J. Soukup. 1991. Cytokine (tumor necrosis factor, IL-6, and IL-8) production by respiratory syncytial virus-infected human alveolar macrophages. *J Immunol* 147:4307-4312.

46. Dawson, T. C., M. A. Beck, W. A. Kuziel, F. Henderson, and N. Maeda. 2000. Contrasting effects of CCR5 and CCR2 deficiency in the pulmonary inflammatory response to influenza A virus. *Am J Pathol* 156:1951-1959.

47. Lin, K. L., Y. Suzuki, H. Nakano, E. Ramsburg, and M. D. Gunn. 2008. CCR2+ monocyte-derived dendritic cells and exudate macrophages produce influenza-induced pulmonary immune pathology and mortality. *J Immunol* 180:2562-2572.

48. Perrone, L. A., J. K. Plowden, A. Garcia-Sastre, J. M. Katz, and T. M. Tumpey. 2008. H5N1 and 1918 pandemic influenza virus infection results in early and excessive infiltration of macrophages and neutrophils in the lungs of mice. *PLoS Pathog* 4:e1000115.

49. Tumpey, T. M., A. Garcia-Sastre, J. K. Taubenberger, P. Palese, D. E. Swayne, M. J. Pantin-Jackwood, S. Schultz-Cherry, A. Solorzano, N. Van Rooijen, J. M. Katz, and C. F. Basler. 2005. Pathogenicity of influenza viruses with genes from the 1918 pandemic virus: functional roles of alveolar macrophages and neutrophils in limiting virus replication and mortality in mice. *J Virol* 79:14933-14944.

50. Kim, H. M., Y. W. Lee, K. J. Lee, H. S. Kim, S. W. Cho, N. van Rooijen, Y. Guan, and S. H. Seo. 2008. Alveolar macrophages are indispensable for controlling influenza viruses in lungs of pigs. *J Virol* 82:4265-4274.

51. Albert, M. L., B. Sauter, and N. Bhardwaj. 1998. Dendritic cells acquire antigen from apoptotic cells and induce class I-restricted CTLs. *Nature* 392:86-89.

52. Brydon, E. W., H. Smith, and C. Sweet. 2003. Influenza A virus-induced apoptosis in bronchiolar epithelial (NCI-H292) cells limits pro-inflammatory cytokine release. *J Gen Virol* 84:2389-2400.

53. Bhardwaj, N., A. Bender, N. Gonzalez, L. K. Bui, M. C. Garrett, and R. M. Steinman. 1994. Influenza virus-infected dendritic cells stimulate strong proliferative and cytolytic responses from human CD8+ T cells. *J Clin Invest* 94:797-807.

54. Banchereau, J., and R. M. Steinman. 1998. Dendritic cells and the control of immunity. *Nature* 392:245-252.

55. Legge, K. L., and T. J. Braciale. 2003. Accelerated migration of respiratory dendritic cells to the regional lymph nodes is limited to the early phase of pulmonary infection. *Immunity* 18:265-277.

56. Belz, G. T., C. M. Smith, L. Kleinert, P. Reading, A. Brooks, K. Shortman, F. R. Carbone, and W. R. Heath. 2004. Distinct migrating and nonmigrating dendritic cell populations are involved in MHC class I-restricted antigen presentation after lung infection with virus. *Proc Natl Acad Sci U S A* 101:8670-8675.

57. Lawrence, C. W., and T. J. Braciale. 2004. Activation, differentiation, and migration of naive virus-specific CD8+ T cells during pulmonary influenza virus infection. *J Immunol* 173:1209-1218.

58. Macatonia, S. E., P. M. Taylor, S. C. Knight, and B. A. Askonas. 1989. Primary stimulation by dendritic cells induces antiviral proliferative and cytotoxic T cell responses in vitro. *J Exp Med* 169:1255-1264.

59. McGill, J., N. Van Rooijen, and K. L. Legge. 2008. Protective influenza-specific CD8 T cell responses require interactions with dendritic cells in the lungs. *J Exp Med* 205:1635-1646.

60. McGill, J., J. W. Heusel, and K. L. Legge. 2009. Innate immune control and regulation of influenza virus infections. *J Leukoc Biol* 86:803-812.

61. Wareing, M. D., A. B. Lyon, B. Lu, C. Gerard, and S. R. Sarawar. 2004. Chemokine expression during the development and resolution of a pulmonary leukocyte response to influenza A virus infection in mice. *J Leukoc Biol* 76:886-895.

62. Wareing, M. D., A. Lyon, C. Inglis, F. Giannoni, I. Charo, and S. R. Sarawar. 2007. Chemokine regulation of the inflammatory response to a low-dose influenza infection in CCR2-/- mice. *J Leukoc Biol* 81:793-801.

63. Wareing, M. D., A. L. Shea, C. A. Inglis, P. B. Dias, and S. R. Sarawar. 2007. CXCR2 is required for neutrophil recruitment to the lung during influenza virus infection, but is not essential for viral clearance. *Viral Immunol* 20:369-378.

64. Proudfoot, A. E. 2002. Chemokine receptors: multifaceted therapeutic targets. *Nat Rev Immunol* 2:106-115.

65. Doherty, P. C. 1996. Cytotoxic T cell effector and memory function in viral immunity. *Curr Top Microbiol Immunol* 206:1-14.

66. Lukacher, A. E., V. L. Braciale, and T. J. Braciale. 1984. In vivo effector function of influenza virus-specific cytotoxic T lymphocyte clones is highly specific. *J Exp Med* 160:814-826.

67. Topham, D. J., R. A. Tripp, and P. C. Doherty. 1997. CD8+ T cells clear influenza virus by perforin or Fas-dependent processes. *J Immunol* 159:5197-5200.

68. Lawrence, C. W., R. M. Ream, and T. J. Braciale. 2005. Frequency, specificity, and sites of expansion of CD8+ T cells during primary pulmonary influenza virus infection. *J Immunol* 174:5332-5340.

69. Legge, K. L., and T. J. Braciale. 2005. Lymph node dendritic cells control CD8+ T cell responses through regulated FasL expression. *Immunity* 23:649-659.

70. Epstein, S. L., C. Y. Lo, J. A. Misplon, and J. R. Bennink. 1998. Mechanism of protective immunity against influenza virus infection in mice without antibodies. *J Immunol* 160:322-327.

71. Graham, M. B., and T. J. Braciale. 1997. Resistance to and recovery from lethal influenza virus infection in B lymphocyte-deficient mice. *J Exp Med* 186:2063-2068.

72. Tripp, R. A., S. R. Sarawar, and P. C. Doherty. 1995. Characteristics of the influenza virus-specific CD8+ T cell response in mice homozygous for disruption of the H-2lAb gene. *J Immunol* 155:2955-2959.

73. Mozdzanowska, K., M. Furchner, K. Maiese, and W. Gerhard. 1997. CD4+ T cells are ineffective in clearing a pulmonary infection with influenza type A virus in the absence of B cells. *Virology* 239:217-225.

74. Topham, D. J., and P. C. Doherty. 1998. Clearance of an influenza A virus by CD4+ T cells is inefficient in the absence of B cells. *J Virol* 72:882-885.

75. Banchereau, J., F. Bazan, D. Blanchard, F. Briere, J. P. Galizzi, C. van Kooten, Y. J. Liu, F. Rousset, and S. Saeland. 1994. The CD40 antigen and its ligand. *Annu Rev Immunol* 12:881-922.

76. Gray, D., K. Siepmann, and G. Wohlleben. 1994. CD40 ligation in B cell activation, isotype switching and memory development. *Semin Immunol* 6:303-310.

77. Tanchot, C., and B. Rocha. 2003. CD8 and B cell memory: same strategy, same signals. *Nat Immunol* 4:431-432.

78. Kaech, S. M., and R. Ahmed. 2003. Immunology. CD8 T cells remember with a little help. *Science* 300:263-265.

79. Brown, D. M., E. Roman, and S. L. Swain. 2004. CD4 T cell responses to influenza infection. *Semin Immunol* 16:171-177.

80. Suarez, D. L., and S. Schultz-Cherry. 2000. Immunology of avian influenza virus: a review. *Dev Comp Immunol* 24:269-283.

81. Gerhard, W., K. Mozdzanowska, M. Furchner, G. Washko, and K. Maiese. 1997. Role of the B-cell response in recovery of mice from primary influenza virus infection. *Immunol Rev* 159:95-103.

82. Gerhard, W., K. Mozdzanowska, and D. Zharikova. 2006. Prospects for universal influenza virus vaccine. *Emerg Infect Dis* 12:569-574.

83. Pitti, R. M., S. A. Marsters, S. Ruppert, C. J. Donahue, A. Moore, and A. Ashkenazi. 1996. Induction of apoptosis by Apo-2 ligand, a new member of the tumor necrosis factor cytokine family. *J Biol Chem* 271:12687-12690.

84. Wiley, S. R., K. Schooley, P. J. Smolak, W. S. Din, C. P. Huang, J. K. Nicholl, G. R. Sutherland, T. D. Smith, C. Rauch, C. A. Smith, and et al. 1995. Identification and characterization of a new member of the TNF family that induces apoptosis. *Immunity* 3:673-682.

85. Ashkenazi, A., and V. M. Dixit. 1998. Death receptors: signaling and modulation. *Science* 281:1305-1308.

86. Sheridan, J. P., S. A. Marsters, R. M. Pitti, A. Gurney, M. Skubatch, D. Baldwin, L. Ramakrishnan, C. L. Gray, K. Baker, W. I. Wood, A. D. Goddard, P. Godowski, and A. Ashkenazi. 1997. Control of TRAIL-induced apoptosis by a family of signaling and decoy receptors. *Science* 277:818-821.

87. Pan, G., J. Ni, Y. F. Wei, G. Yu, R. Gentz, and V. M. Dixit. 1997. An antagonist decoy receptor and a death domain-containing receptor for TRAIL. *Science* 277:815-818.

88. Pan, G., K. O'Rourke, A. M. Chinnaiyan, R. Gentz, R. Ebner, J. Ni, and V. M. Dixit. 1997. The receptor for the cytotoxic ligand TRAIL. *Science* 276:111-113.

89. Wu, G. S., T. F. Burns, Y. Zhan, E. S. Alnemri, and W. S. El-Deiry. 1999. Molecular cloning and functional analysis of the mouse homologue of the KILLER/DR5 tumor necrosis factor-related apoptosis-inducing ligand (TRAIL) death receptor. *Cancer Res* 59:2770-2775.

90. Griffith, T. S., and D. H. Lynch. 1998. TRAIL: a molecule with multiple receptors and control mechanisms. *Curr Opin Immunol* 10:559-563.

91. Ishikawa, E., M. Nakazawa, M. Yoshinari, and M. Minami. 2005. Role of tumor necrosis factor-related apoptosis-inducing ligand in immune response to influenza virus infection in mice. *J Virol* 79:7658-7663.

92. Clarke, P., S. M. Meintzer, S. Gibson, C. Widmann, T. P. Garrington, G. L. Johnson, and K. L. Tyler. 2000. Reovirus-induced apoptosis is mediated by TRAIL. *J Virol* 74:8135-8139.

93. Sedger, L. M., D. M. Shows, R. A. Blanton, J. J. Peschon, R. G. Goodwin, D. Cosman, and S. R. Wiley. 1999. IFN-gamma mediates a novel antiviral activity through dynamic modulation of TRAIL and TRAIL receptor expression. *J Immunol* 163:920-926.

94. Takeda, K., M. J. Smyth, E. Cretney, Y. Hayakawa, N. Yamaguchi, H. Yagita, and K. Okumura. 2001. Involvement of tumor necrosis factor-related apoptosis-inducing ligand in NK cell-mediated and IFN-gamma-dependent suppression of subcutaneous tumor growth. *Cell Immunol* 214:194-200.

95. Cheung, C. Y., L. L. Poon, A. S. Lau, W. Luk, Y. L. Lau, K. F. Shortridge, S. Gordon, Y. Guan, and J. S. Peiris. 2002. Induction of proinflammatory cytokines in human macrophages by influenza A (H5N1) viruses: a mechanism for the unusual severity of human disease? *Lancet* 360:1831-1837.

96. Hussell, T., A. Pennycook, and P. J. Openshaw. 2001. Inhibition of tumor necrosis factor reduces the severity of virus-specific lung immunopathology. *Eur J Immunol* 31:2566-2573.

97. Jayasekera, J. P., C. G. Vinuesa, G. Karupiah, and N. J. King. 2006. Enhanced antiviral antibody secretion and attenuated immunopathology during influenza virus infection in nitric oxide synthase-2-deficient mice. *J Gen Virol* 87:3361-3371.

98. Peper, R. L., and H. Van Campen. 1995. Tumor necrosis factor as a mediator of inflammation in influenza A viral pneumonia. *Microb Pathog* 19:175-183.

99. Snelgrove, R. J., L. Edwards, A. J. Rae, and T. Hussell. 2006. An absence of reactive oxygen species improves the resolution of lung influenza infection. *Eur J Immunol* 36:1364-1373.

100. Akaike, T., and H. Maeda. 2000. Nitric oxide and virus infection. *Immunology* 101:300-308.

101. Herold, S., M. Steinmueller, W. von Wulffen, L. Cakarova, R. Pinto, S. Pleschka, M. Mack, W. A. Kuziel, N. Corazza, T. Brunner, W. Seeger, and J. Lohmeyer. 2008. Lung epithelial apoptosis in influenza virus pneumonia: the role of macrophage-expressed TNF-related apoptosis-inducing ligand. *J Exp Med* 205:3065-3077.

102. Fesq, H., M. Bacher, M. Nain, and D. Gemsa. 1994. Programmed cell death (apoptosis) in human monocytes infected by influenza A virus. *Immunobiology* 190:175-182.

103. La Gruta, N. L., K. Kedzierska, K. Pang, R. Webby, M. Davenport, W. Chen, S. J. Turner, and P. C. Doherty. 2006. A virus-specific CD8+ T cell immunodominance hierarchy determined by antigen dose and precursor frequencies. *Proc Natl Acad Sci U S A* 103:994-999.

104. Bruder, D., A. Srikiatkhachorn, and R. I. Enelow. 2006. Cellular immunity and lung injury in respiratory virus infection. *Viral Immunol* 19:147-155.

105. Bekker, L. G., A. L. Moreira, A. Bergtold, S. Freeman, B. Ryffel, and G. Kaplan. 2000. Immunopathologic effects of tumor necrosis factor alpha in murine mycobacterial infection are dose dependent. *Infect Immun* 68:6954-6961.

106. Liu, J., M. Q. Zhao, L. Xu, C. V. Ramana, W. Declercq, P. Vandenabeele, and R. I. Enelow. 2005. Requirement for tumor necrosis factor-receptor 2 in alveolar chemokine expression depends upon the form of the ligand. *Am J Respir Cell Mol Biol* 33:463-469.

107. Rutigliano, J. A., and B. S. Graham. 2004. Prolonged production of TNF-alpha exacerbates illness during respiratory syncytial virus infection. *J Immunol* 173:3408-3417.

108. Xu, L., H. Yoon, M. Q. Zhao, J. Liu, C. V. Ramana, and R. I. Enelow. 2004. Cutting edge: pulmonary immunopathology mediated by antigen-specific expression of TNF-alpha by antiviral CD8+ T cells. *J Immunol* 173:721-725.

109. Zhou, J., M. Matsuoka, H. Cantor, R. Homer, and R. I. Enelow. 2008. Cutting edge: engagement of NKG2A on CD8+ effector T cells limits immunopathology in influenza pneumonia. *J Immunol* 180:25-29.

110. Ostler, T., W. Davidson, and S. Ehl. 2002. Virus clearance and immunopathology by CD8(+) T cells during infection with respiratory syncytial virus are mediated by IFN-gamma. *Eur J Immunol* 32:2117-2123.

111. Wiley, J. A., A. Cerwenka, J. R. Harkema, R. W. Dutton, and A. G. Harmsen. 2001. Production of interferon-gamma by influenza hemagglutinin-specific CD8 effector T cells influences the development of pulmonary immunopathology. *Am J Pathol* 158:119-130.

112. Chen, X., H. Thakkar, F. Tyan, S. Gim, H. Robinson, C. Lee, S. K. Pandey, C. Nwokorie, N. Onwudiwe, and R. K. Srivastava. 2001. Constitutively active Akt is an important regulator of TRAIL sensitivity in prostate cancer. *Oncogene* 20:6073-6083.

113. Dunn, C., M. Brunetto, G. Reynolds, T. Christophides, P. T. Kennedy, P. Lampertico, A. Das, A. R. Lopes, P. Borrow, K. Williams, E. Humphreys, S. Afford, D. H. Adams, A. Bertoletti, and M. K. Maini. 2007. Cytokines induced during chronic hepatitis B virus infection promote a pathway for NK cell-mediated liver damage. *J Exp Med* 204:667-680.

114. Barbey, C., P. Baumgaertner, E. Devevre, V. Rubio-Godoy, L. Derre, G. Bricard, P. Guillaume, I. F. Luescher, D. Lienard, J. C. Cerottini, P. Romero, N. Rufer, and D. E. Speiser. 2007. IL-12 controls cytotoxicity of a novel subset of self-antigen-specific human CD28+ cytolytic T cells. *J Immunol* 178:3566-3574.

115. Cha, S. S., M. S. Kim, Y. H. Choi, B. J. Sung, N. K. Shin, H. C. Shin, Y. C. Sung, and B. H. Oh. 1999. 2.8 A resolution crystal structure of human TRAIL, a cytokine with selective antitumor activity. *Immunity* 11:253-261.

116. Ludwig, A. T., J. M. Moore, Y. Luo, X. Chen, N. A. Saltsgaver, M. A. O'Donnell, and T. S. Griffith. 2004. Tumor necrosis factor-related apoptosis-inducing ligand: a novel mechanism for Bacillus Calmette-Guerin-induced antitumor activity. *Cancer Res* 64:3386-3390.

117. Degli-Esposti, M. A., P. J. Smolak, H. Walczak, J. Waugh, C. P. Huang, R. F. DuBose, R. G. Goodwin, and C. A. Smith. 1997. Cloning and characterization of TRAIL-R3, a novel member of the emerging TRAIL receptor family. *J Exp Med* 186:1165-1170.

118. Kayagaki, N., N. Yamaguchi, M. Nakayama, H. Eto, K. Okumura, and H. Yagita. 1999. Type I interferons (IFNs) regulate tumor necrosis factor-related apoptosis-inducing ligand (TRAIL) expression on human T cells: A novel mechanism for the antitumor effects of type I IFNs. *J Exp Med* 189:1451-1460.

119. Fanger, N. A., C. R. Maliszewski, K. Schooley, and T. S. Griffith. 1999. Human dendritic cells mediate cellular apoptosis via tumor necrosis factor-related apoptosis-inducing ligand (TRAIL). *J Exp Med* 190:1155-1164.

120. Zamai, L., M. Ahmad, I. M. Bennett, L. Azzoni, E. S. Alnemri, and B. Perussia. 1998. Natural killer (NK) cell-mediated cytotoxicity: differential use of TRAIL and Fas ligand by immature and mature primary human NK cells. *J Exp Med* 188:2375-2380.

121. Griffith, T. S., C. T. Rauch, P. J. Smolak, J. Y. Waugh, N. Boiani, D. H. Lynch, C. A. Smith, R. G. Goodwin, and M. Z. Kubin. 1999. Functional analysis of TRAIL receptors using monoclonal antibodies. *J. Immunol.* 162:2597-2605.

122. Emery, J. G., P. McDonnell, M. B. Burke, K. C. Deen, S. Lyn, C. Silverman, E. Dul, E. R. Appelbaum, C. Eichman, R. DiPrinzio, R. A. Dodds, I. E. James, M. Rosenberg, J. C. Lee, and P. R. Young. 1998. Osteoprotegerin is a receptor for the cytotoxic ligand TRAIL. *J Biol Chem* 273:14363-14367.

123. Griffith, T. S., W. A. Chin, G. C. Jackson, D. H. Lynch, and M. Z. Kubin. 1998. Intracellular regulation of TRAIL-induced apoptosis in human melanoma cells. *J. Immunol.* 161:2833-2840.

124. Cretney, E., K. Takeda, and M. J. Smyth. 2007. Cancer: novel therapeutic strategies that exploit the TNF-related apoptosis-inducing ligand (TRAIL)/TRAIL receptor pathway. *Int J Biochem Cell Biol* 39:280-286.

125. Cretney, E., A. Shanker, H. Yagita, M. J. Smyth, and T. J. Sayers. 2006. TNF-related apoptosis-inducing ligand as a therapeutic agent in autoimmunity and cancer. *Immunol Cell Biol* 84:87-98.

126. Griffith, T. S., W. A. Chin, G. C. Jackson, D. H. Lynch, and M. Z. Kubin. 1998. Intracellular regulation of TRAIL-induced apoptosis in human melanoma cells. *J Immunol* 161:2833-2840.

127. Ozoren, N., and W. S. El-Deiry. 2003. Cell surface Death Receptor signaling in normal and cancer cells. *Semin Cancer Biol* 13:135-147.

128. Zhang, X. D., X. Y. Zhang, C. P. Gray, T. Nguyen, and P. Hersey. 2001. Tumor necrosis factor-related apoptosis-inducing ligand-induced apoptosis of human melanoma is regulated by smac/DIABLO release from mitochondria. *Cancer Res* 61:7339-7348.

129. Di Pietro, R., and G. Zauli. 2004. Emerging non-apoptotic functions of tumor necrosis factor-related apoptosis-inducing ligand (TRAIL)/Apo2L. *J Cell Physiol* 201:331-340.

130. Chaudhary, P. M., M. Eby, A. Jasmin, A. Bookwalter, J. Murray, and L. Hood. 1997. Death receptor 5, a new member of the TNFR family, and DR4 induce FADD-dependent apoptosis and activate the NF-kappaB pathway. *Immunity* 7:821-830.

131. Degli-Esposti, M. A., W. C. Dougall, P. J. Smolak, J. Y. Waugh, C. A. Smith, and R. G. Goodwin. 1997. The novel receptor TRAIL-R4 induces NF-kappaB and protects against TRAIL-mediated apoptosis, yet retains an incomplete death domain. *Immunity* 7:813-820.

132. Schneider, P., M. Thome, K. Burns, J. L. Bodmer, K. Hofmann, T. Kataoka, N. Holler, and J. Tschopp. 1997. TRAIL receptors 1 (DR4) and 2 (DR5) signal FADD-dependent apoptosis and activate NF-kappaB. *Immunity* 7:831-836.

133. Beg, A. A., and D. Baltimore. 1996. An essential role for NF-kappaB in preventing TNF-alpha-induced cell death. *Science* 274:782-784.

134. Liu, Z. G., H. Hsu, D. V. Goeddel, and M. Karin. 1996. Dissection of TNF receptor 1 effector functions: JNK activation is not linked to apoptosis while NF-kappaB activation prevents cell death. *Cell* 87:565-576.

135. Van Antwerp, D. J., S. J. Martin, T. Kafri, D. R. Green, and I. M. Verma. 1996. Suppression of TNF-alpha-induced apoptosis by NF-kappaB. *Science* 274:787-789.

136. Wang, C. Y., M. W. Mayo, and A. S. Baldwin, Jr. 1996. TNF- and cancer therapy-induced apoptosis: potentiation by inhibition of NF-kappaB. *Science* 274:784-787.

137. Wang, C. Y., M. W. Mayo, R. G. Korneluk, D. V. Goeddel, and A. S. Baldwin, Jr. 1998. NF-kappaB antiapoptosis: induction of TRAF1 and TRAF2 and c-IAP1 and c-IAP2 to suppress caspase-8 activation. *Science* 281:1680-1683.

138. Diehl, G. E., H. H. Yue, K. Hsieh, A. A. Kuang, M. Ho, L. A. Morici, L. L. Lenz, D. Cado, L. W. Riley, and A. Winoto. 2004. TRAIL-R as a negative regulator of innate immune cell responses. *Immunity* 21:877-889.

139. Sedger, L. M., M. B. Glaccum, J. C. Schuh, S. T. Kanaly, E. Williamson, N. Kayagaki, T. Yun, P. Smolak, T. Le, R. Goodwin, and B. Gliniak. 2002. Characterization of the in vivo function of TNF-alpha-related apoptosis-inducing ligand, TRAIL/Apo2L, using TRAIL/Apo2L gene-deficient mice. *Eur J Immunol* 32:2246-2254.

140. Prescott, S., K. James, T. B. Hargreave, G. D. Chisholm, and J. F. Smyth. 1992. Intravesical Evans strain BCG therapy: quantitative immunohistochemical analysis of the immune response within the bladder wall. *J. Urol.* 147:1636-1642.

141. Takeda, K., M. J. Smyth, E. Cretney, Y. Hayakawa, N. Kayagaki, H. Yagita, and K. Okumura. 2002. Critical role for tumor necrosis factor-related apoptosis-inducing ligand in immune surveillance against tumor development. *J. Exp. Med.* 195:161-169.

142. Seki, N., Y. Hayakawa, A. D. Brooks, J. Wine, R. H. Wiltrout, H. Yagita, J. E. Tanner, M. J. Smyth, and T. J. Sayers. 2003. Tumor necrosis factor-related apoptosis-inducing ligand-mediated apoptosis is an important endogenous mechanism for resistance to liver metastases in murine renal cancer. *Cancer Res.* 63:207-213.

143. Song, K., Y. Chen, R. Goke, A. Wilmen, C. Seidel, A. Goke, B. Hilliard, and Y. Chen. 2000. Tumor necrosis factor-related apoptosis-inducing ligand (TRAIL) is an inhibitor of autoimmune inflammation and cell cycle progression. *J Exp Med* 191:1095-1104.

144. Lamhamedi-Cherradi, S. E., S. J. Zheng, K. A. Maguschak, J. Peschon, and Y. H. Chen. 2003. Defective thymocyte apoptosis and accelerated autoimmune diseases in TRAIL-/- mice. *Nat Immunol* 4:255-260.

145. Mi, Q. S., D. Ly, S. E. Lamhamedi-Cherradi, K. V. Salojin, L. Zhou, M. Grattan, C. Meagher, P. Zucker, Y. H. Chen, J. Nagle, D. Taub, and T. L. Delovitch. 2003. Blockade of tumor necrosis factor-related apoptosis-inducing ligand exacerbates type 1 diabetes in NOD mice. *Diabetes* 52:1967-1975.

146. Lamhamedi-Cherradi, S. E., S. Zheng, R. M. Tisch, and Y. H. Chen. 2003. Critical roles of tumor necrosis factor-related apoptosis-inducing ligand in type 1 diabetes. *Diabetes* 52:2274-2278.

147. Barry, M., and G. McFadden. 1998. Apoptosis regulators from DNA viruses. *Curr Opin Immunol* 10:422-430.

148. Meinl, E., H. Fickenscher, M. Thome, J. Tschopp, and B. Fleckenstein. 1998. Anti-apoptotic strategies of lymphotropic viruses. *Immunol Today* 19:474-479.

149. Heinkelein, M., S. Pilz, and C. Jassoy. 1996. Inhibition of CD95 (Fas/Apo1)-mediated apoptosis by vaccinia virus WR. *Clin Exp Immunol* 103:8-14.

150. Macen, J. L., K. A. Graham, S. F. Lee, M. Schreiber, L. K. Boshkov, and G. McFadden. 1996. Expression of the myxoma virus tumor necrosis factor receptor homologue and M11L genes is required to prevent virus-induced apoptosis in infected rabbit T lymphocytes. *Virology* 218:232-237.

151. Upton, C., J. L. Macen, M. Schreiber, and G. McFadden. 1991. Myxoma virus expresses a secreted protein with homology to the tumor necrosis factor receptor gene family that contributes to viral virulence. *Virology* 184:370-382.

152. Kotelkin, A., E. A. Prikhod'ko, J. I. Cohen, P. L. Collins, and A. Bukreyev. 2003. Respiratory syncytial virus infection sensitizes cells to apoptosis mediated by tumor necrosis factor-related apoptosis-inducing ligand. *J Virol* 77:9156-9172.

153. Sato, K., S. Hida, H. Takayanagi, T. Yokochi, N. Kayagaki, K. Takeda, H. Yagita, K. Okumura, N. Tanaka, T. Taniguchi, and K. Ogasawara. 2001. Antiviral response by natural killer cells through TRAIL gene induction by IFN-alpha/beta. *Eur J Immunol* 31:3138-3146.

154. Vidalain, P. O., O. Azocar, B. Lamouille, A. Astier, C. Rabourdin-Combe, and C. Servet-Delprat. 2000. Measles virus induces functional TRAIL production by human dendritic cells. *J Virol* 74:556-559.

155. Washburn, B., M. A. Weigand, A. Grosse-Wilde, M. Janke, H. Stahl, E. Rieser, M. R. Sprick, V. Schirrmacher, and H. Walczak. 2003. TNF-related apoptosis-inducing ligand mediates tumoricidal activity of human monocytes stimulated by Newcastle disease virus. *J Immunol* 170:1814-1821.

156. Zeng, J., P. Fournier, and V. Schirrmacher. 2002. Induction of interferon-alpha and tumor necrosis factor-related apoptosis-inducing ligand in human blood mononuclear cells by hemagglutinin-neuraminidase but not F protein of Newcastle disease virus. *Virology* 297:19-30.

157. Swain, S. L., R. W. Dutton, and D. L. Woodland. 2004. T cell responses to influenza virus infection: effector and memory cells. *Viral Immunol* 17:197-209.

158. Jenkins, M. R., K. Kedzierska, P. C. Doherty, and S. J. Turner. 2007. Heterogeneity of effector phenotype for acute phase and memory influenza A virus-specific CTL. *J Immunol* 179:64-70.

159. Mirandola, P., C. Ponti, G. Gobbi, I. Sponzilli, M. Vaccarezza, L. Cocco, G. Zauli, P. Secchiero, F. A. Manzoli, and M. Vitale. 2004. Activated human NK and CD8+ T cells express both TNF-related apoptosis-inducing ligand (TRAIL) and TRAIL receptors but are resistant to TRAIL-mediated cytotoxicity. *Blood* 104:2418-2424.

160. Lum, J. J., A. A. Pilon, J. Sanchez-Dardon, B. N. Phenix, J. E. Kim, J. Mihowich, K. Jamison, N. Hawley-Foss, D. H. Lynch, and A. D. Badley. 2001. Induction of cell death in human immunodeficiency virus-infected macrophages and resting memory CD4 T cells by TRAIL/Apo2l. *J Virol* 75:11128-11136.

161. Yoneyama, H., K. Matsuno, E. Toda, T. Nishiwaki, N. Matsuo, A. Nakano, S. Narumi, B. Lu, C. Gerard, S. Ishikawa, and K. Matsushima. 2005. Plasmacytoid DCs help lymph node DCs to induce anti-HSV CTLs. *J Exp Med* 202:425-435.

162. Finnberg, N., J. J. Gruber, P. Fei, D. Rudolph, A. Bric, S. H. Kim, T. F. Burns, H. Ajuha, R. Page, G. S. Wu, Y. Chen, W. G. McKenna, E. Bernhard, S. Lowe, T. Mak, and W. S. El-Deiry. 2005. DR5 knockout mice are compromised in radiation-induced apoptosis. *Mol Cell Biol* 25:2000-2013.

163. Hanson, H. L., D. L. Donermeyer, H. Ikeda, J. M. White, V. Shankaran, L. J. Old, H. Shiku, R. D. Schreiber, and P. M. Allen. 2000. Eradication of established tumors by CD8+ T cell adoptive immunotherapy. *Immunity* 13:265-276.

164. Lo, D., J. Freedman, S. Hesse, R. D. Palmiter, R. L. Brinster, and L. A. Sherman. 1992. Peripheral tolerance to an islet cell-specific hemagglutinin transgene affects both CD4+ and CD8+ T cells. *Eur J Immunol* 22:1013-1022.

165. Belz, G. T., W. Xie, J. D. Altman, and P. C. Doherty. 2000. A previously unrecognized H-2D(b)-restricted peptide prominent in the primary influenza A virus-specific CD8(+) T-cell response is much less apparent following secondary challenge. *J Virol* 74:3486-3493.

166. Crowe, S. R., S. C. Miller, R. M. Shenyo, and D. L. Woodland. 2005. Vaccination with an acidic polymerase epitope of influenza virus elicits a potent antiviral T cell response but delayed clearance of an influenza virus challenge. *J Immunol* 174:696-701.

167. VanOosten, R. L., J. M. Moore, B. Karacay, and T. S. Griffith. 2005. Histone deacetylase inhibitors modulate renal cell carcinoma sensitivity to TRAIL/Apo-2L-induced apoptosis by enhancing TRAIL-R2 expression. *Cancer Biol Ther* 4:1104-1112.

168. Ruitenberg, J., S. Ghanekar, D. Brockstedt, and H. Maecker. 2007. Simultaneous detection of murine antigen-specific intracellular cytokines and CD107a/CD107b by flow cytometry. In *Nature Protocols*.

169. Shirasawa, M., N. Fujiwara, S. Hirabayashi, H. Ohno, J. Iida, K. Makita, and Y. Hata. 2004. Receptor for advanced glycation end-products is a marker of type I lung alveolar cells. *Genes Cells* 9:165-174.

170. Vitiello, A., L. Yuan, R. W. Chesnut, J. Sidney, S. Southwood, P. Farness, M. R. Jackson, P. A. Peterson, and A. Sette. 1996. Immunodominance analysis of CTL responses to influenza PR8 virus reveals two new dominant and subdominant Kb-restricted epitopes. *J Immunol* 157:5555-5562.

171. Mariani, S. M., and P. H. Krammer. 1998. Surface expression of TRAIL/Apo-2 ligand in activated mouse T and B cells. *Eur J Immunol* 28:1492-1498.

172. van Stipdonk, M. J., G. Hardenberg, M. S. Bijker, E. E. Lemmens, N. M. Droin, D. R. Green, and S. P. Schoenberger. 2003. Dynamic programming of CD8+ T lymphocyte responses. *Nat Immunol* 4:361-365.

173. Mercado, R., S. Vijh, S. E. Allen, K. Kerksiek, I. M. Pilip, and E. G. Pamer. 2000. Early programming of T cell populations responding to bacterial infection. *J Immunol* 165:6833-6839.

174. Bevan, M. J., and P. J. Fink. 2001. The CD8 response on autopilot. *Nat Immunol* 2:381-382.

175. Chaperot, L., A. Blum, O. Manches, G. Lui, J. Angel, J. P. Molens, and J. Plumas. 2006. Virus or TLR agonists induce TRAIL-mediated cytotoxic activity of plasmacytoid dendritic cells. *J Immunol* 176:248-255.

176. Strater, J., H. Walczak, T. Pukrop, L. Von Muller, C. Hasel, M. Kornmann, T. Mertens, and P. Moller. 2002. TRAIL and its receptors in the colonic epithelium: a putative role in the defense of viral infections. *Gastroenterology* 122:659-666.

177. Li, W. M., W. Liu, C. Gao, B. G. Zhou, S. S. Yang, Z. Wang, R. H. Zhang, R. T. Gan, Y. H. Kong, and Y. Li. 2006. Antigen-specific tolerance induced by IL-10 gene modified immature dendritic cells in experimental autoimmune myocarditis in rats. *Chin Med J (Engl)* 119:1646-1652.

178. Tumpey, T. M., X. Lu, T. Morken, S. R. Zaki, and J. M. Katz. 2000. Depletion of lymphocytes and diminished cytokine production in mice infected with a highly virulent influenza A (H5N1) virus isolated from humans. *J Virol* 74:6105-6116.

179. Horisberger, M. A. 1995. Interferons, Mx genes, and resistance to influenza virus. *Am J Respir Crit Care Med* 152:S67-71.

180. Jewell, N. A., N. Vaghefi, S. E. Mertz, P. Akter, R. S. Peebles, Jr., L. O. Bakaletz, R. K. Durbin, E. Flano, and J. E. Durbin. 2007. Differential type I interferon induction by respiratory syncytial virus and influenza a virus in vivo. *J Virol* 81:9790-9800.

181. Kash, J. C., T. M. Tumpey, S. C. Proll, V. Carter, O. Perwitasari, M. J. Thomas, C. F. Basler, P. Palese, J. K. Taubenberger, A. Garcia-Sastre, D. E. Swayne, and M. G. Katze. 2006. Genomic analysis of increased host immune and cell death responses induced by 1918 influenza virus. *Nature* 443:578-581.

182. Kemp, T. J., B. D. Elzey, and T. S. Griffith. 2003. Plasmacytoid dendritic cell-derived IFN-alpha induces TNF-related apoptosis-inducing ligand/Apo-2L-mediated antitumor activity by human monocytes following CpG oligodeoxynucleotide stimulation. *J Immunol* 171:212-218.

183. Miura, Y., T. Tsujioka, Y. Nishimura, H. Sakaguchi, M. Maeda, H. Hayashi, M. Dong, F. Hyodoh, K. Yata, H. Wada, T. Sugihara, and T. Otsuki. 2006. TRAIL expression up-regulated by interferon-gamma via phosphorylation of STAT1 induces myeloma cell death. *Anticancer Res* 26:4115-4124.

184. Griffith, T. S., S. R. Wiley, M. Z. Kubin, L. M. Sedger, C. R. Maliszewski, and N. A. Fanger. 1999. Monocyte-mediated tumoricidal activity via the tumor necrosis factor-related cytokine, TRAIL. *J. Exp. Med.* 189:1343-1354.

185. Brando, C., S. Mukhopadhyay, E. Kovacs, R. Medina, P. Patel, T. L. Catina, K. S. Campbell, and D. Santoli. 2005. Receptors and lytic mediators regulating anti-tumor activity by the leukemic killer T cell line TALL-104. *J Leukoc Biol* 78:359-371.

186. Brincks, E. L., A. Katewa, T. A. Kucaba, T. S. Griffith, and K. L. Legge. 2008. CD8 T cells utilize TRAIL to control influenza virus infection. *J Immunol* 181:4918-4925.

187. Brincks, E. L., T. A. Kucaba, K. L. Legge, and T. S. Griffith. 2008. Influenza-induced expression of functional tumor necrosis factor-related apoptosis-inducing ligand on human peripheral blood mononuclear cells. *Hum Immunol* 69:634-646.

188. Lund, J. M., L. Alexopoulou, A. Sato, M. Karow, N. C. Adams, N. W. Gale, A. Iwasaki, and R. A. Flavell. 2004. Recognition of single-stranded RNA viruses by Toll-like receptor 7. *Proc Natl Acad Sci U S A* 101:5598-5603.

189. Zhou, J., H. K. Law, C. Y. Cheung, I. H. Ng, J. S. Peiris, and Y. L. Lau. 2006. Functional tumor necrosis factor-related apoptosis-inducing ligand production by avian influenza virus-infected macrophages. *J Infect Dis* 193:945-953.

190. Ichinohe, T., H. K. Lee, Y. Ogura, R. Flavell, and A. Iwasaki. 2009. Inflammasome recognition of influenza virus is essential for adaptive immune responses. *J Exp Med* 206:79-87.

191. Owen, D. M., and M. Gale, Jr. 2009. Fighting the flu with inflammasome signaling. *Immunity* 30:476-478.

192. Szretter, K. J., S. Gangappa, X. Lu, C. Smith, W. J. Shieh, S. R. Zaki, S. Sambhara, T. M. Tumpey, and J. M. Katz. 2007. Role of host cytokine responses in the pathogenesis of avian H5N1 influenza viruses in mice. *J Virol* 81:2736-2744.

193. Itoh, Y., K. Shinya, M. Kiso, T. Watanabe, Y. Sakoda, M. Hatta, Y. Muramoto, D. Tamura, Y. Sakai-Tagawa, T. Noda, S. Sakabe, M. Imai, Y. Hatta, S. Watanabe, C. Li, S. Yamada, K. Fujii, S. Murakami, H. Imai, S. Kakugawa, M. Ito, R. Takano, K. Iwatsuki-Horimoto, M. Shimojima, T. Horimoto, H. Goto, K. Takahashi, A. Makino, H. Ishigaki, M. Nakayama, M. Okamatsu, K. Takahashi, D. Warshauer, P. A. Shult, R. Saito, H. Suzuki, Y. Furuta, M. Yamashita, K. Mitamura, K. Nakano, M. Nakamura, R. Brockman-Schneider, H. Mitamura, M. Yamazaki, N. Sugaya, M. Suresh, M. Ozawa, G. Neumann, J. Gern, H. Kida, K. Ogasawara, and Y. Kawaoka. 2009. In vitro and in vivo characterization of new swine-origin H1N1 influenza viruses. *Nature* 460:1021-1025.

194. Maines, T. R., A. Jayaraman, J. A. Belser, D. A. Wadford, C. Pappas, H. Zeng, K. M. Gustin, M. B. Pearce, K. Viswanathan, Z. H. Shriver, R. Raman, N. J. Cox, R. Sasisekharan, J. M. Katz, and T. M. Tumpey. 2009. Transmission and pathogenesis of swine-origin 2009 A(H1N1) influenza viruses in ferrets and mice. *Science* 325:484-487.

195. Zeng, H., C. Goldsmith, P. Thawatsupha, M. Chittaganpitch, S. Waicharoen, S. Zaki, T. M. Tumpey, and J. M. Katz. 2007. Highly pathogenic avian influenza H5N1 viruses elicit an attenuated type i interferon response in polarized human bronchial epithelial cells. *J Virol* 81:12439-12449.

196. Szretter, K. J., S. Gangappa, J. A. Belser, H. Zeng, H. Chen, Y. Matsuoka, S. Sambhara, D. E. Swayne, T. M. Tumpey, and J. M. Katz. 2009. Early control of H5N1 influenza virus replication by the type I interferon response in mice. *J Virol* 83:5825-5834.

197. Sedger, L. M., D. M. Shows, R. A. Blanton, J. J. Peschon, R. G. Goodwin, D. Cosman, and S. R. Wiley. 1999. IFN-gamma mediates a novel antiviral activity through dynamic modulation of TRAIL and TRAIL receptor expression. *J. Immunol.* 163:920-926.

198. Griffith, T. S., and D. H. Lynch. 1998. TRAIL: a molecule with multiple receptors and control mechanisms. *Curr. Opin. Immunol.* 10:559-563.

199. Chan, M. C., C. Y. Cheung, W. H. Chui, S. W. Tsao, J. M. Nicholls, Y. O. Chan, R. W. Chan, H. T. Long, L. L. Poon, Y. Guan, and J. S. Peiris. 2005. Proinflammatory cytokine responses induced by influenza A (H5N1) viruses in primary human alveolar and bronchial epithelial cells. *Respir Res* 6:135.

200. Graham, M. B., D. K. Dalton, D. Giltinan, V. L. Braciale, T. A. Stewart, and T. J. Braciale. 1993. Response to influenza infection in mice with a targeted disruption in the interferon gamma gene. *J Exp Med* 178:1725-1732.

201. Wang, Q., Y. Ji, X. Wang, and B. M. Evers. 2000. Isolation and molecular characterization of the 5'-upstream region of the human TRAIL gene. *Biochem Biophys Res Commun* 276:466-471.

202. Noppert, S. J., K. A. Fitzgerald, and P. J. Hertzog. 2007. The role of type I interferons in TLR responses. *Immunol Cell Biol* 85:446-457.

203. Kemp, T. J., J. M. Moore, and T. S. Griffith. 2004. Human B cells express functional TRAIL/Apo-2 ligand after CpG-containing oligodeoxynucleotide stimulation. *J Immunol* 173:892-899.

204. Jarrossay, D., G. Napolitani, M. Colonna, F. Sallusto, and A. Lanzavecchia. 2001. Specialization and complementarity in microbial molecule recognition by human myeloid and plasmacytoid dendritic cells. *Eur J Immunol* 31:3388-3393.

205. Hornung, V., S. Rothenfusser, S. Britsch, A. Krug, B. Jahrsdorfer, T. Giese, S. Endres, and G. Hartmann. 2002. Quantitative expression of toll-like receptor 1-10 mRNA in cellular subsets of human peripheral blood mononuclear cells and sensitivity to CpG oligodeoxynucleotides. *J Immunol* 168:4531-4537.

206. Krug, A., S. Rothenfusser, V. Hornung, B. Jahrsdorfer, S. Blackwell, Z. K. Ballas, S. Endres, A. M. Krieg, and G. Hartmann. 2001. Identification of CpG oligonucleotide sequences with high induction of IFN-alpha/beta in plasmacytoid dendritic cells. *Eur. J. Immunol.* 31:2154-2163.

207. Bauer, M., V. Redecke, J. W. Ellwart, B. Scherer, J. P. Kremer, H. Wagner, and G. B. Lipford. 2001. Bacterial CpG-DNA triggers activation and maturation of human CD11c-, CD123+ dendritic cells. *J Immunol* 166:5000-5007.

208. Krug, A., A. Towarowski, S. Britsch, S. Rothenfusser, V. Hornung, R. Bals, T. Giese, H. Engelmann, S. Endres, A. M. Krieg, and G. Hartmann. 2001. Toll-like receptor expression reveals CpG DNA as a unique microbial stimulus for plasmacytoid dendritic cells which synergizes with CD40 ligand to induce high amounts of IL-12. *Eur. J. Immunol.* 31:3026-3037.

209. Griffith, T. S., S. R. Wiley, M. Z. Kubin, L. M. Sedger, C. R. Maliszewski, and N. A. Fanger. 1999. Monocyte-mediated tumoricidal activity via the tumor necrosis factor-related cytokine, TRAIL. *J Exp Med* 189:1343-1354.

210. CDC. 2005. Fact Sheet: Key Facts about Influenza and Influenza Vaccine. Department of Health and Human Services.

211. WHO, W. H. O. i. e. 2008. WHO Influenza web page.

212. Kato, H., O. Takeuchi, S. Sato, M. Yoneyama, M. Yamamoto, K. Matsui, S. Uematsu, A. Jung, T. Kawai, K. J. Ishii, O. Yamaguchi, K. Otsu, T. Tsujimura, C. S. Koh, C. Reis e Sousa, Y. Matsuura, T. Fujita, and S. Akira. 2006. Differential roles of MDA5 and RIG-I helicases in the recognition of RNA viruses. *Nature* 441:101-105.

213. Guillot, L., R. Le Goffic, S. Bloch, N. Escriou, S. Akira, M. Chignard, and M. Si-Tahar. 2005. Involvement of toll-like receptor 3 in the immune response of lung epithelial cells to double-stranded RNA and influenza A virus. *J Biol Chem* 280:5571-5580.

214. Li, S., J. Y. Min, R. M. Krug, and G. C. Sen. 2006. Binding of the influenza A virus NS1 protein to PKR mediates the inhibition of its activation by either PACT or double-stranded RNA. *Virology* 349:13-21.

215. Min, J. Y., and R. M. Krug. 2006. The primary function of RNA binding by the influenza A virus NS1 protein in infected cells: Inhibiting the 2'-5' oligo (A) synthetase/RNase L pathway. *Proc Natl Acad Sci U S A* 103:7100-7105.

216. Mibayashi, M., L. Martinez-Sobrido, Y. M. Loo, W. B. Cardenas, M. Gale, Jr., and A. Garcia-Sastre. 2007. Inhibition of retinoic acid-inducible gene I-mediated induction of beta interferon by the NS1 protein of influenza A virus. *J Virol* 81:514-524.

217. Opitz, B., A. Rejaibi, B. Dauber, J. Eckhard, M. Vinzing, B. Schmeck, S. Hippenstiel, N. Suttorp, and T. Wolff. 2007. IFNbeta induction by influenza A virus is mediated by RIG-I which is regulated by the viral NS1 protein. *Cell Microbiol* 9:930-938.

218. Cella, M., F. Facchetti, A. Lanzavecchia, and M. Colonna. 2000. Plasmacytoid dendritic cells activated by influenza virus and CD40L drive a potent TH1 polarization. *Nat Immunol* 1:305-310.

219. Saitou, Y., K. Shiraki, H. Fuke, T. Inoue, K. Miyashita, Y. Yamanaka, Y. Yamaguchi, N. Yamamoto, K. Ito, K. Sugimoto, and T. Nakano. 2005. Involvement of tumor necrosis factor-related apoptosis-inducing ligand and tumor necrosis factor-related apoptosis-inducing ligand receptors in viral hepatic diseases. *Hum Pathol* 36:1066-1073.

220. Hao, X., T. S. Kim, and T. J. Braciale. 2008. Differential response of respiratory dendritic cell subsets to influenza virus infection. *J Virol* 82:4908-4919.

221. Kumagai, Y., O. Takeuchi, H. Kato, H. Kumar, K. Matsui, E. Morii, K. Aozasa, T. Kawai, and S. Akira. 2007. Alveolar macrophages are the primary interferon-alpha producer in pulmonary infection with RNA viruses. *Immunity* 27:240-252.

222. Gong, B., and A. Almasan. 2000. Genomic organization and transcriptional regulation of human Apo2/TRAIL gene. *Biochem Biophys Res Commun* 278:747-752.

223. Fanger, N. A., C. R. Maliszewski, K. Schooley, and T. S. Griffith. 1999. Human dendritic cells mediate cellular apoptosis via tumor necrosis factor-related apoptosis-inducing ligand (TRAIL). *J. Exp. Med.* 190:1155-1164.

224. Kobasa, D., S. M. Jones, K. Shinya, J. C. Kash, J. Copps, H. Ebihara, Y. Hatta, J. H. Kim, P. Halfmann, M. Hatta, F. Feldmann, J. B. Alimonti, L. Fernando, Y. Li, M. G. Katze, H. Feldmann, and Y. Kawaoka. 2007. Aberrant innate immune response in lethal infection of macaques with the 1918 influenza virus. *Nature* 445:319-323.

225. Hsieh, S. M., and S. C. Chang. 2006. Insufficient perforin expression in CD8+ T cells in response to hemagglutinin from avian influenza (H5N1) virus. *J Immunol* 176:4530-4533.

226. Seo, S. H., E. Hoffmann, and R. G. Webster. 2002. Lethal H5N1 influenza viruses escape host anti-viral cytokine responses. *Nat Med* 8:950-954.

227. Nagata, S. 1997. Apoptosis by death factor. *Cell* 88:355-365.

228. Baize, S., J. Kaplon, C. Faure, D. Pannetier, M. C. Georges-Courbot, and V. Deubel. 2004. Lassa virus infection of human dendritic cells and macrophages is productive but fails to activate cells. *J Immunol* 172:2861-2869.

229. Pajares, F. 2009. The Structure of Scientific Revolutions. http://www.philosophersnet.com/. A Synopsis from the original by Professor Frank Pajares.

230. Kuhn, T. S. 1962. Historical structure of scientific discovery. *Science* 136:760-764.

231. Zinkernagel, R. M., and P. C. Doherty. 1974. Restriction of in vitro T cell-mediated cytotoxicity in lymphocytic choriomeningitis within a syngeneic or semiallogeneic system. *Nature* 248:701-702.

232. Sakaguchi, S., T. Takahashi, and Y. Nishizuka. 1982. Study on cellular events in postthymectomy autoimmune oophoritis in mice. I. Requirement of Lyt-1 effector cells for oocytes damage after adoptive transfer. *J Exp Med* 156:1565-1576.

233. Sakaguchi, S., T. Takahashi, and Y. Nishizuka. 1982. Study on cellular events in post-thymectomy autoimmune oophoritis in mice. II. Requirement of Lyt-1 cells in normal female mice for the prevention of oophoritis. *J Exp Med* 156:1577-1586.

234. Gay, N. J., and F. J. Keith. 1991. Drosophila Toll and IL-1 receptor. *Nature* 351:355-356.

235. Ip, Y. T., M. Reach, Y. Engstrom, L. Kadalayil, H. Cai, S. Gonzalez-Crespo, K. Tatei, and M. Levine. 1993. Dif, a dorsal-related gene that mediates an immune response in Drosophila. *Cell* 75:753-763.

236. Lemaitre, B., E. Nicolas, L. Michaut, J. M. Reichhart, and J. A. Hoffmann. 1996. The dorsoventral regulatory gene cassette spatzle/Toll/cactus controls the potent antifungal response in Drosophila adults. *Cell* 86:973-983.

237. Poltorak, A., X. He, I. Smirnova, M. Y. Liu, C. Van Huffel, X. Du, D. Birdwell, E. Alejos, M. Silva, C. Galanos, M. Freudenberg, P. Ricciardi-Castagnoli, B. Layton, and B. Beutler. 1998. Defective LPS signaling in C3H/HeJ and C57BL/10ScCr mice: mutations in Tlr4 gene. *Science* 282:2085-2088.

238. Cook, D. N., D. S. Pisetsky, and D. A. Schwartz. 2004. Toll-like receptors in the pathogenesis of human disease. *Nat Immunol* 5:975-979.

239. Schroder, N. W., I. Diterich, A. Zinke, J. Eckert, C. Draing, V. von Baehr, D. Hassler, S. Priem, K. Hahn, K. S. Michelsen, T. Hartung, G. R. Burmester, U. B. Gobel, C. Hermann, and R. R. Schumann. 2005. Heterozygous Arg753Gln polymorphism of human TLR-2 impairs immune activation by Borrelia burgdorferi and protects from late stage Lyme disease. *J Immunol* 175:2534-2540.

240. Mockenhaupt, F. P., L. Hamann, C. von Gaertner, G. Bedu-Addo, C. von Kleinsorgen, R. R. Schumann, and U. Bienzle. 2006. Common polymorphisms of toll-like receptors 4 and 9 are associated with the clinical manifestation of malaria during pregnancy. *J Infect Dis* 194:184-188.

241. Misch, E. A., and T. R. Hawn. 2008. Toll-like receptor polymorphisms and susceptibility to human disease. *Clin Sci (Lond)* 114:347-360.

242. Misch, E. A., M. Macdonald, C. Ranjit, B. R. Sapkota, R. D. Wells, M. R. Siddiqui, G. Kaplan, and T. R. Hawn. 2008. Human TLR1 Deficiency Is Associated with Impaired Mycobacterial Signaling and Protection from Leprosy Reversal Reaction. *PLoS Negl Trop Dis* 2:e231.

243. Wille-Reece, U., B. J. Flynn, K. Lore, R. A. Koup, A. P. Miles, A. Saul, R. M. Kedl, J. J. Mattapallil, W. R. Weiss, M. Roederer, and R. A. Seder. 2006. Toll-like receptor agonists influence the magnitude and quality of memory T cell responses after prime-boost immunization in nonhuman primates. *J Exp Med* 203:1249-1258.

244. van Duin, D., R. Medzhitov, and A. C. Shaw. 2006. Triggering TLR signaling in vaccination. *Trends Immunol* 27:49-55.

245. Weeratna, R. D., S. R. Makinen, M. J. McCluskie, and H. L. Davis. 2005. TLR agonists as vaccine adjuvants: comparison of CpG ODN and Resiquimod (R-848). *Vaccine* 23:5263-5270.

246. Jahrsdorfer, B., J. E. Wooldridge, S. E. Blackwell, C. M. Taylor, T. S. Griffith, B. K. Link, and G. J. Weiner. 2005. Immunostimulatory oligodeoxynucleotides induce apoptosis of B cell chronic lymphocytic leukemia cells. *J Leukoc Biol* 77:378-387.

247. VanOosten, R. L., and T. S. Griffith. 2007. Activation of tumor-specific CD8+ T Cells after intratumoral Ad5-TRAIL/CpG oligodeoxynucleotide combination therapy. *Cancer Res* 67:11980-11990.

248. Seya, T., T. Akazawa, J. Uehori, M. Matsumoto, I. Azuma, and K. Toyoshima. 2003. Role of toll-like receptors and their adaptors in adjuvant immunotherapy for cancer. *Anticancer Res* 23:4369-4376.

249. Prins, R. M., N. Craft, K. W. Bruhn, H. Khan-Farooqi, R. C. Koya, R. Stripecke, J. F. Miller, and L. M. Liau. 2006. The TLR-7 agonist, imiquimod, enhances dendritic cell survival and promotes tumor antigen-specific T cell priming: relation to central nervous system antitumor immunity. *J Immunol* 176:157-164.

250. Janssen, E. M., N. M. Droin, E. E. Lemmens, M. J. Pinkoski, S. J. Bensinger, B. D. Ehst, T. S. Griffith, D. R. Green, and S. P. Schoenberger. 2005. CD4+ T-cell help controls CD8+ T-cell memory via TRAIL-mediated activation-induced cell death. *Nature* 434:88-93.

251. Robertson, N. M., J. G. Zangrilli, A. Steplewski, A. Hastie, R. G. Lindemeyer, M. A. Planeta, M. K. Smith, N. Innocent, A. Musani, R. Pascual, S. Peters, and G. Litwack. 2002. Differential expression of TRAIL and TRAIL receptors in allergic asthmatics following segmental antigen challenge: evidence for a role of TRAIL in eosinophil survival. *J Immunol* 169:5986-5996.

252. Beaulieu, S., M. Lafontaine, M. Richer, I. Courchesne, E. A. Cohen, and D. Bergeron. 1998. Characterization of the cytotoxic factor(s) released from thymic dendritic cells upon human immunodeficiency virus type 1 infection. *Virology* 241:285-297.

253. Hansjee, N., G. R. Kaufmann, C. Strub, R. Weber, M. Battegay, and P. Erb. 2004. Persistent apoptosis in HIV-1-infected individuals receiving potent antiretroviral therapy is associated with poor recovery of CD4 T lymphocytes. *J Acquir Immune Defic Syndr* 36:671-677.

254. Mundt, B., F. Kuhnel, L. Zender, Y. Paul, H. Tillmann, C. Trautwein, M. P. Manns, and S. Kubicka. 2003. Involvement of TRAIL and its receptors in viral hepatitis. *Faseb J* 17:94-96.

255. Park, S. M., R. Schickel, and M. E. Peter. 2005. Nonapoptotic functions of FADD-binding death receptors and their signaling molecules. *Curr Opin Cell Biol* 17:610-616.

256. Bosque, A., J. I. Aguilo, M. A. Alava, E. Paz-Artal, J. Naval, L. M. Allende, and A. Anel. 2007. The induction of Bim expression in human T-cell blasts is dependent on nonapoptotic Fas/CD95 signaling. *Blood* 109:1627-1635.

257. Strasser, A., P. J. Jost, and S. Nagata. 2009. The many roles of FAS receptor signaling in the immune system. *Immunity* 30:180-192.

258. Jenkins, M. R., J. A. Trapani, P. C. Doherty, and S. J. Turner. 2008. Granzyme K expressing cytotoxic T lymphocytes protects against influenza virus in granzyme AB-/- mice. *Viral Immunol* 21:341-346.

259. Moffat, J. M., T. Gebhardt, P. C. Doherty, S. J. Turner, and J. D. Mintern. 2009. Granzyme A expression reveals distinct cytolytic CTL subsets following influenza A virus infection. *Eur J Immunol* 39:1203-1210.

260. Somersalo, K., N. Anikeeva, T. N. Sims, V. K. Thomas, R. K. Strong, T. Spies, T. Lebedeva, Y. Sykulev, and M. L. Dustin. 2004. Cytotoxic T lymphocytes form an antigen-independent ring junction. *J Clin Invest* 113:49-57.

261. Crawford, A., and E. J. Wherry. 2007. Inhibitory receptors: whose side are they on? *Nat Immunol* 8:1201-1203.

262. McKinstry, K. K., T. M. Strutt, A. Buck, J. D. Curtis, J. P. Dibble, G. Huston, M. Tighe, H. Hamada, S. Sell, R. W. Dutton, and S. L. Swain. 2009. IL-10 deficiency unleashes an influenza-specific Th17 response and enhances survival against high-dose challenge. *J Immunol* 182:7353-7363.

263. Sun, J., R. Madan, C. L. Karp, and T. J. Braciale. 2009. Effector T cells control lung inflammation during acute influenza virus infection by producing IL-10. *Nat Med* 15:277-284.

264. Lightfield, K. L., J. Persson, S. W. Brubaker, C. E. Witte, J. von Moltke, E. A. Dunipace, T. Henry, Y. H. Sun, D. Cado, W. F. Dietrich, D. M. Monack, R. M. Tsolis, and R. E. Vance. 2008. Critical function for Naip5 in inflammasome activation by a conserved carboxy-terminal domain of flagellin. *Nat Immunol* 9:1171-1178.

265. Morioka, S., E. Omori, T. Kajino, R. Kajino-Sakamoto, K. Matsumoto, and J. Ninomiya-Tsuji. 2009. TAK1 kinase determines TRAIL sensitivity by modulating reactive oxygen species and cIAP. *Oncogene* 28:2257-2265.

266. Calkins, C. M., D. D. Bensard, B. D. Shames, E. J. Pulido, E. Abraham, N. Fernandez, X. Meng, C. A. Dinarello, and R. C. McIntyre, Jr. 2002. IL-1 regulates in vivo C-X-C chemokine induction and neutrophil sequestration following endotoxemia. *J Endotoxin Res* 8:59-67.

267. Fadel, S. A., S. K. Bromley, B. D. Medoff, and A. D. Luster. 2008. CXCR3-deficiency protects influenza-infected CCR5-deficient mice from mortality. *Eur J Immunol* 38:3376-3387.

268. Kummer, J. A., R. Broekhuizen, H. Everett, L. Agostini, L. Kuijk, F. Martinon, R. van Bruggen, and J. Tschopp. 2007. Inflammasome components NALP 1 and 3 show distinct but separate expression profiles in human tissues suggesting a site-specific role in the inflammatory response. *J Histochem Cytochem* 55:443-452.

269. Fukuyama, S., T. Nagatake, D. Y. Kim, K. Takamura, E. J. Park, T. Kaisho, N. Tanaka, Y. Kurono, and H. Kiyono. 2006. Cutting edge: Uniqueness of lymphoid chemokine requirement for the initiation and maturation of nasopharynx-associated lymphoid tissue organogenesis. *J Immunol* 177:4276-4280.

270. Rangel-Moreno, J., J. Moyron-Quiroz, K. Kusser, L. Hartson, H. Nakano, and T. D. Randall. 2005. Role of CXC chemokine ligand 13, CC chemokine ligand (CCL) 19, and CCL21 in the organization and function of nasal-associated lymphoid tissue. *J Immunol* 175:4904-4913.

271. Warnock, R. A., J. J. Campbell, M. E. Dorf, A. Matsuzawa, L. M. McEvoy, and E. C. Butcher. 2000. The role of chemokines in the microenvironmental control of T versus B cell arrest in Peyer's patch high endothelial venules. *J Exp Med* 191:77-88.

272. Chou, A. H., H. F. Tsai, L. L. Lin, S. L. Hsieh, P. I. Hsu, and P. N. Hsu. 2001. Enhanced proliferation and increased IFN-gamma production in T cells by signal transduced through TNF-related apoptosis-inducing ligand. *J Immunol* 167:1347-1352.

273. Tsai, H. F., J. J. Lai, A. H. Chou, T. F. Wang, C. S. Wu, and P. N. Hsu. 2004. Induction of costimulation of human CD4 T cells by tumor necrosis factor-related apoptosis-inducing ligand: possible role in T cell activation in systemic lupus erythematosus. *Arthritis Rheum* 50:629-639.